URANIUM AND URANIUM COMPOUNDS

1. Introduction

Uranium [7440-61-1] is a naturally occurring radioactive element with atomic number 92 and atomic mass 238.03. Uranium was discovered in a pitchblende [1317-75-5] specimen in 1789 by M. H. Klaproth (1) who named the element *Uranit* after the planet Uranus, which had been recently discovered. For 50 years, the material discovered by Klaproth was thought to be metallic uranium. Péligot showed that the Uranit discovered by Klaproth was really UO_2 [1344-57-6] and obtained the true elemental uranium as a black powder in 1841 by reduction of UCl_4 [10026-10-5] with potassium (2).

In 1896, Becquerel discovered that uranium was radioactive (3). Becquerel was studying the fluorescence behavior of potassium uranyl sulfate and observed that a photographic plate had been darkened by exposure to the uranyl salt. Further investigation showed that all uranium minerals and metallic uranium behaved in this same manner, suggesting that this new radioactivity was a property of uranium itself. In 1934, Fermi and co-workers bombarded uranium with neutrons to produce new radioactive elements (4).

Prior to 1939, uranium played no significant role in technical processes and was only used as a pigment in glass and ceramics. In 1939, Hahn and Strassman reported their seminal discovery of nuclear fission, which announced the dawn of the nuclear age (5). After this seminal report, uranium gained importance as fuel for nuclear reactors and as starting material for the synthesis of plutonium. There are 24 isotopes of uranium with masses 217–219, 222–240, and 242 and radioactive half-lives ranging from 1 μs (^{222}U) to 4.468×10^9 y, the latter for the main naturally occurring (99.27%) uranium isotope, ^{238}U (1,6).

Uranium is the fourth element of the actinide (5f) series (see ACTINIDES AND TRANSACTINIDES). In the actinide series, the 5f electrons are less effectively shielded by the 7s and 7p electrons relative to the 4f electrons (shielded by 6s, 6p) in the lanthanide (4f) series. Thus, there is a greater spatial extension of 5f orbitals for actinides than of 4f orbitals for lanthanides. This results in a small energy difference between $5f^n7s^2$ and $5f^{n-1}6d7s^2$ electronic configurations, and a wider range of oxidation states is therefore accessible to the early members of the actinide series (U - Am). Uranium has four common oxidation states: III, IV, V, and VI.

Of the four oxidation states, III, IV, V, and VI, only the IV and VI states are stable enough to be of general importance. Aqueous solutions of uranium(III) may be prepared, but they are readily oxidized to the IV state with evolution of hydrogen; and the V state disproportionates into the IV and VI states in the presence of water or hydrolytic compounds. The ease of alternation between IV and VI states has economic significance. The highly stable and disseminated grains of uraninite in igneous rock formations are in the IV state, but when altered to the VI state, they are soluble enough to dissolve in circulating groundwater. The solubility of uranium in the VI state accounts for its wide distribution in seawater, fresh water, and hydrothermal deposits. In aqueous media, the VI state predominates.

2. Isotopes

Natural uranium is a mixture of three alpha-emitting isotopes: ^{238}U (99.274%, half-life $= 4.47 \times 10^9$ years, 4.15 MeV α), ^{235}U (0.7202%, half-life $= 7.08 \times 10^8$ years, 4.29 MeV α), and ^{234}U (0.0057%, half-life of 2.45×10^5 years, 4.78 MeV α) (7). Uranium is the progenitor of two naturally occurring decay series, ^{238}U $(4n + 2)$, shown in Fig. 1, and ^{235}U $(4n + 3)$, which terminates at stable ^{207}Pb. The man-made neptunium series that ends in ^{209}Bi also includes ^{233}U (1). Two isotopes of the ^{238}U $(4n + 2)$ chain, ^{226}Ra and ^{222}Rn, have significant historical and radiological implications. Natural uranium is not highly radioactive in a

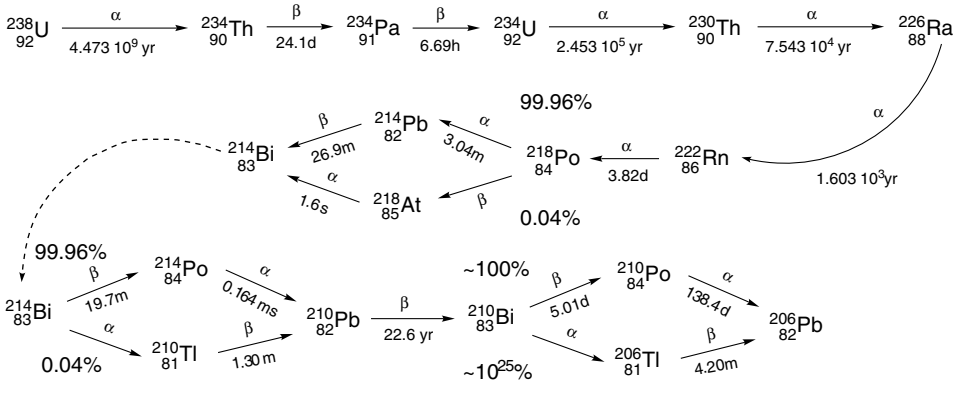

Fig. 1. Uranium decay series.

Table 1. **Radioactive Decay Properties of Selected Uranium Isotopes**[a]

Mass number	Half-life	Mode of decay	Main radiations (MeV)	Method of production
232	68.9 yr	α	α 5.320 (68.6%)	^{232}Th(α,4n)
	$\sim 8 \times 10^{13}$ yr	SF[b]	5.264 (31.2%)	
			γ 0.058	
233	1.592×10^{5} yr	α	α 4.824 (82.7%)	^{233}Pa daughter
	1.2×10^{17} yr	SF	4.783 (14.9%)	
			γ 0.097	
234	2.455×10^{5} yr	α	α 4.777 (72%)	nature
	2×10^{16} yr	SF	4.723 (28%)	
235	7.038×10^{8} yr	α	α 4.397 (57%)	nature
	3.5×10^{17} yr	SF	4.367 (18%)	
			γ 0.186	
235m	25 min	IT		^{239}Pu daughter
236	2.3415×10^{7} yr	α	α 4.494 (74%)	^{235}U(n, γ)
	2.43×10^{16} yr	SF	4.445 (26%)	
237	6.75 d	β^-	β^- 0.519	^{236}U(n, γ)
			γ 0.60	^{241}Pu daughter
238	4.468×10^{9} yr	α	α 4.196 (77%)	nature
	8.30×10^{15} yr	SF	4.149 (23%)	
239	23.45 min	β^-	β^- 1.29	^{238}U(n, γ)

[a]Ref. 1.
[b]SF = spontaneous fission.

relative sense; for example, 2800 kg of natural uranium have a radioactivity equivalent to that of approximately 1 g of ^{226}Ra (8).

Uranium isotopes and their radioactive decay products, from thorium to lead, are used extensively in determining the geochronology and geochemistry of a wide variety of minerals, rocks, and geologic formations. The radioactive decay properties of selected isotopes are shown in Table 1. In the uranium decay series (^{238}U parent), eight alpha particles are emitted in the decay from ^{238}U to ^{206}Pb. One can thus date a mineral once the concentration ratios of ^{238}U and He are known. Another common method of dating U-minerals is based on considering the distribution of lead isotopes. Lead has four stable isotopes, of which three are end products of radioactive decay series. The fourth isotope, ^{204}Pb, is found in lead minerals in about 1.4% isotopic abundance and has no radiogenic origin (9).

The U/Pb decay schemes have been used to date the oldest known terrestrial rocks (10). The types of samples studied using these methods are extensive, including but not limited to, archeological deposits, carbonates and other sediments, pebble conglomerates, zircons, volcanic and pyroclastic rocks, granites, basalts, and uranium ores (11–16). For example, uranium-bearing quartz-pebble conglomerates have been used to study uranium ore mineralization (14). The Greenbushes pegmatite is a giant Archean pegmatite dike with substantial Li-Sn-Ta mineralization, including half the world's Ta resource, and was dated using imprecise whole-rock Pb-Pb and precise U-Pb zircon techniques (15). Uranium oxide ages have been used to study ore formations and uranium mineralization (12,13).

Ratios of ^{234}U and ^{238}U to ^{230}Th and ^{226}Ra daughters, combined with differences in chemical reactivity, have been used to investigate the formation and weathering of limestone in karst soils of the Jura Mountains, and of the mountains in the central part of Switzerland. Uranium contained within calcite is released during weathering, and it migrates as stable uranyl(VI) carbonato complexes through the soil. In contrast, the uranium decay products, thorium and radium, hydrolyze and are strongly sorbed to soil particles and/or form insoluble compounds that become more and more enriched in the soil as a function of time (17). It is interesting to note that the ratios of ^{234}U and ^{238}U provide information on weathering, because ^{234}U, as the product of a lattice damaging α-decay of ^{238}U, is preferentially leached (18).

In addition, uranium and lead transport mechanisms in radioactive minerals have been studied to evaluate the suitability of mineral phases as hosts for radioactive wastes. Zircon is one of the most commonly used geochronometers, as well as a proposed nuclear waste matrix material, and there are many mechanisms by which uranium and lead can migrate through its structure (19).

3. Atomic Properties

Uranium, like all of the heaviest elements, has a very complex electronic structure. The complexity of the electronic structure is apparent in the spectral properties, such as x-ray absorption and emission spectra, and arc, spark, and discharge emission spectra. The uranium-free atom (U^0, denoted UI) has 92 electrons, of which 86 electrons are in filled shells as found in the radon atom. It is customary in discussing the actinide series to only list the electrons in shells outside the radon core. The outermost electrons of the free actinide atoms and ions outside the radon core are found in the 7s, 7p, 6d, and 5f shells. For example, the ground-state (lowest energy) configuration for UI is $5f^36d7s^2$. Identified excited configurations of UI within the first 3 eV ($\sim$24,000 cm^{-1}) of the ground state include $5f^36d^27s$, $5f^47s^2$, $5f^26d^27s^2$, $5f^37s^27p$, $5f^36d7s7p$, $5f^46d7s$, $5f^47s7p$, and $5f^36d^3$. The emission spectrum of neutral (U I), singly ionized (U^+, or U II) [15721-70-7], doubly ionized (U^{2+}, or U III) [15721-72-9] and higher spectra of uranium have been extensively studied. In the free atoms and ions, many low-lying configurations interact strongly with each other, giving rise to a large number of electronic states and tens of thousands of spectral lines. A detailed discussion and review of the spectra of actinide-free atoms and ions can be found in recent reviews (20,21).

4. Occurrence in Nature

Uranium is widely distributed in nature (22–24). It is found in significant concentrations in rocks, oceans, lunar rocks, and meteorites. Estimates of the concentrations of uranium in various geological matrices are given in Table 2. It can be seen (Table 2) that uranium is present at about 2–3 ppm in the Earth's crust,

Table 2. **Occurrence of Uranium in Nature**

Location	U concentration (ppm)
igneous rocks	
basalts	0.6
granites (normal)	4.8
ultrabasic rocks	0.03
sandstones, shales, limestones	1.2–1.3
Earth's crust	2.1
oceanic	0.64
continental	2.8
Earth's mantle	≈ 0.01
sea water	0.002–0.003
meteorites	0.05
chondrites	0.011
uraniferous materials	
high-grade veins	$(3–8.5) \times 10^5$
vein ores	$(2–10) \times 10^3$
sandstone ores	$(0.5–4) \times 10^3$
gold ores (South Africa)	150–600
uraniferous phosphates	50–300
uraniferous granites	15–100
Chattanooga shale (USA)	60

and it is thus more abundant than many other common elements, such as Cd, Ag, and Hg. In general, igneous rocks with a high silicate content, such as granite, contain an above-average uranium concentration, whereas basic rocks, such as basalts, contain a below-average uranium content. Sedimentary rocks also generally contain below-average uranium concentrations. Despite this low uranium content, sedimentary rocks like sandstones and conglomerates contain approximately 90% of the world's uranium resources.

Uranium resources (see NUCLEAR FUEL RESERVES) can be assigned on the basis of their geological setting to 15 main categories of uranium ore deposit types arranged according to their approximate economic significance. The 15 deposit types are as follows: (*1*) unconformity-related deposits; (*2*) sandstone deposits; (*3*) quartz-pebble conglomerate deposits; (*4*) vein deposits; (*5*) breccia complex deposits; (*6*) intrusive deposits; (*7*) phosphorite deposits; (*8*) collapse breccia pipe deposits; (*9*) volcanic deposits; (*10*) surficial deposits; (*11*) metasomatite deposits; (*12*) metamorphite deposits; (*13*) lignite; (*14*) black shale deposits; and (*15*) other deposits (25).

Unconformity-related deposits are found near major unconformities. Examples include the ore bodies at Cluff Lake, Key Lake, and Rabbit Lake in northern Saskatchewan, Canada, and in the Alligator Rivers area in northern Australia. Sandstone deposits are contained in rocks that were deposited under fluvial or marginal marine conditions. The host rocks nearly always contain pyrite and organic plant matter. The sediments are commonly associated with tuffs. Unoxidized deposits of this type consist of pitchblende and coffinite in arkasoic and quartzitic sandstones. Upon weathering, secondary minerals such as carnotite, tuyamunite and uranophane are formed. For more information on these and

Table 3. **Selected Uranium Minerals**[a]

Name	Chemical composition
	Oxides
uraninite	UO_2–$UO_{2.67}$ [1317-99-3]
schoepite	$UO_3 \cdot 2\,H_2O$ [22972-07-2]
becquerelite	$[(UO_2)_8O_2(OH)_{12}]\,(H_2O)_{12}$ [12378-67-5]
	Phosphates
autunite	$Ca(UO_2)_2(PO_4)_2 \cdot 10$–$12\,H_2O$ [16390-74-2]
torbernite	$Cu(UO_2)_2(PO_4)_2 \cdot 12\,H_2O$ [26283-21-6]
natroautunite	$Na_2(UO_2)_2(PO_4)_2 \cdot 8\,H_2O$ [161334-19-6]
meta-ankoleite	$K_2(UO_2)_2(PO_4)_2 \cdot 6\,H_2O$ [12169-00-5]
parsonsite	$Pb_2(UO_2)(PO_4)_2$ [12137-57-4]
	Carbonates
andersonite	$Na_2Ca(UO_2)(CO_3)_3 \cdot 6\,H_2O$ [12202-87-8]
liebigite	$Ca_2(UO_2)(CO_3)_3 \cdot 10\,H_2O$ [14831-68-6]
bayleyite	$Mg_2(UO_2)(CO_3)_3 \cdot 18\,H_2O$ [19530-04-2]
rutherfordine	UO_2CO_3 [12202-79-8]
	Vanadates
carnotite	$K_2(UO_2)_2(VO_4)_2 \cdot 1$–$3\,H_2O$ [60182-49-2]
tyuyamunite	$Ca(UO_2)_2(VO_4)_2 \cdot 5$–$8\,H_2O$ [12196-95-1]
	Silicates
uranophane	$Ca(UO_2)_2(Si_2O_7) \cdot 6\,H_2O$ [12195-76-5]
coffinite	$U(SiO_4)_{1-x}(OH)_{4x}$ [14485-40-6]
soddyite	$(UO_2)_5(SiO_4)_4(OH)_2 \cdot 5\,H_2O$ [12196-99-5]
	Arsenates
abernathyite	$K_2(UO_2)_2(AsO_4)_2 \cdot 6\,H_2O$ [12005-93-5]
metakahlerite	$Fe(UO_2)_2(AsO_4)_2 \cdot 8\,H_2O$ [12255-22-0]
novacekite	$Mg(UO_2)_2(AsO_4)_2 \cdot 8$–$10\,H_2O$ [12255-29-1]
	Molybdates
cousinite	$MgO \cdot 2\,MoO_3 \cdot UO_2 \cdot 6\,H_2O$
wulfenite	$Pb(Mo,U)O_4$ [14913-82-7]
irginite	$UO_3 \cdot 2MoO_3 \cdot 3\,H_2O$

[a]Compiled from Frondel and co-workers (27). For a more comprehensive listing, see Burns (22) and Finch and Murakami (23).

other uranium deposit types, the reader is referred to the description in Uranium 2003 (26).

Approximately 200 minerals are known that contain uranium as an important, or major, constituent, with another 60 that contain minor amounts of uranium, or that contain uranium as an impurity (22–24,27). A listing of several representative uranium minerals is given in Table 3. Uranium minerals can be divided into two mineral classes, primary and secondary. Primary uranium minerals are those that formed during the last stages of magma crystallization and are rich in silicates such as quartz, and feldspar. Primary uranium minerals include uraninite [1317-99-3], pitchblende [1317-75-5] and a large number of complex multiple oxides such as uranium-containing lanthanide niobates, tantalates, and titanates (28). Uraninite and pitchblende are very important uranium

minerals with a composition that varies from UO_2 to $UO_{2.67}$ and are found in veins, pegmatites, and unweathered portions of conglomerate and sandstone ores that contain the bulk of the world's economic uranium deposits. Secondary uranium minerals are produced by hydration, metathesis, oxidation, or possibly transport and redeposition. Primary minerals are generally black and contain uranium in an average oxidation state less than VI, whereas secondary minerals are generally yellow, green, or orange and contain uranium in the hexavalent state. Uraninite can be considered both a primary and a secondary mineral, and there are a wide variety of theories regarding the mechanism of formation of uraninite veins (29–31).

There is an extensive literature regarding all aspects of uranium geology, mineralogy, and mining. There are comprehensive descriptions of uranium minerals, including elemental compositions (23,27,32), mineralogical properties (32), ore distributions (24,33,34), crystal structures (22), and typical uranium contents (34). A 1970 symposium discussed the geology of known uranium deposits, theories of the genesis of ore deposits and uranium mineralization, and means of predicting where further deposits may be found (35). Excellent reviews of these data have been provided by Grenthe et al. (1), Burns (22), Finch and Murakami (23), Plant and co-workers (24), and DeVito and co-workers (36). The most comprehensive coverage of the literature of ore deposits, mineralogy, and geochemistry is still the Gmelin Handbook (37).

4.1. The Oklo Phenomenon. Naturally occurring uranium consists mainly of ^{238}U and fissionable ^{235}U. The isotopic ratio can be calculated from the relative decay rates of the two isotopes. As ^{235}U decays faster than ^{238}U, the isotopic ratio decreases with time. Currently, the isotopic abundance of ^{235}U in natural uranium is $0.7202 \pm 0.006\%$. In 1972, uranium samples from the Oklo open-pit uranium mine in southeastern Gabon Republic were found to be depleted in ^{235}U, relative to the expected "natural" isotopic composition. The levels of ^{235}U depletion were inhomogeneous throughout the ore body, with the lowest isotopic ratio being 0.296%. After much study, it was determined that the uranium ore deposit at Oklo was the site of at least six natural nuclear reactors (38,39). Geochemical reactions (weathering) and geological changes created different regions enriched and depleted in uranium, and at that time in geologic history, the ^{235}U enrichment was estimated to be approximately 3%, the same as used in commercial nuclear reactors. Under these conditions, a critical mass could be attained and a nuclear fission reaction initiated with groundwater or water in the clays as a neutron moderator. The chain reaction is thought to have cycled. As the reaction heated up, water would be driven away, thereby slowing the reaction. As the reaction cooled, water could return, thereby slowing the neutrons and starting the chain reaction all over again. The identification of fission products in the proper ratios, and differing from that expected for natural occurrence, gave unequivocal evidence that a nuclear chain reaction had taken place (40,41). In addition to the purely scientific interest, the Oklo phenomenon has also lead to a better understanding of environmental migration of radioactive materials (42). As such, the information attained at Oklo is of great importance in understanding the aqueous transport and redistribution of uranium as it pertains to the safe disposal of radioactive waste (39,43,44).

5. Resources

Resource estimates are divided into separate categories reflecting different levels of confidence in the quantities reported and further separated into categories based on the cost of production. A listing of uranium resources by country as of January 2003 is given in Table 4.

Reasonably assured resources (RAR) refers to uranium in known mineral deposits of size, grade, and configuration such that recovery is within the given production cost ranges with currently proven mining and processing technology. The majority of these resources are found in Australia, Brazil, Canada, Kazakhstan, Namibia, Niger, Russian Federation, South Africa, and the United States (Table 4).

Estimated additional resources (EAR) is a term that applies to resources that are inferred to occur as extensions of well-explored deposits, little-explored deposits, or undiscovered deposits believed to exist along a well-defined geological continuity with known deposits. There are two types of EAR: EAR-I and EAR-II, which are inferred based on direct or indirect evidence of existence, respectively.

In January 2003, RAR recoverable at costs of $130/kg U or less, for selected countries, were estimated at 3.169 million tons of uranium (26). Estimates of total RAR recoverable at costs between $80 and $130/kg U accounted for 661,900 tons. Total RAR recoverable at costs of $80/kg U or less were estimated at 2.458 million tons uranium (26), and RAR at costs below $40/kg were estimated at 1.730 million tons. This represents an increase from the 2001 values and is related to increases in Australia (Olympic Dam) and Niger, resulting from the discovery of additional resources and the transfer of higher cost resources into a lower cost category.

Uranium exploration is geographically imbalanced. Seventeen countries reported exploration expenditures in 2002, although only nine countries, Australia, Canada, China, Egypt, India, Kazakhstan, Niger, Russia and Uzbekistan accounted for about 96% of total domestic exploration expenditures. Canada continues to be the world's leader in domestic exploration spending with an annual expenditure of about $22.9 million in 2002 (26). A listing of total uranium production by country in 2002 is given in Table 5. In 2002, production of 36,042 tons of uranium accounted for only 54% of world reactor requirements of 66,815 tons. It is anticipated that world reactor requirements will reach 73,495 to 86,070 tons by the year 2020 (26). The shortfall between fresh production and reactor requirement is expected to be filled by several sources, including stocks of civilian and military inventories of natural and enriched uranium, nuclear fuel produced by reprocessing of spent reactor fuels and from surplus military uranium production by re-enrichment of depleted uranium tails.

A major source of secondary supply could be derived from civilian and military stockpiles. The actual inventories available from civilian stockpiles are difficult to estimate, due to commercial confidentiality concerns. Large stocks of uranium, previously dedicated to military applications in both the United States and the Russian Federation have become available for commercial use. In 1993 these countries signed an agreement to blend down 500 metric tons of highly enriched uranium (HEU) to low-enriched uranium (LEU) for peaceful use in

Table 4. **Uranium Resources by Country as of January 2003 (units of 1000 metric tons)**[a]

	Reasonably Assured Resources			Estimated Additional Resources		
Country	$80/kg	$80–$130/kg	$130/kg	$80/kg	$80–$130/kg	$130/kg
Algeria	19500	0	19500			
Argentina	4880	2200	7080			
Australia	702000	33000	735000	287000	36000	323000
Brazil	86190	0	86190	57140	0	57140
Bulgaria	5870	0	5870	6300	0	6300
Canada	333834	0	333834	104710	0	104710
Central African Rep.	6000	6000	12000			
Chile	NA	NA	560	NA	NA	885
China	35060	0	35060	14690	0	14690
Congo	1350	0	1350	1275	0	1275
Czech Republic	830	0	830	90	0	90
Denmark	0	20250	20250	0	12000	12000
Finland	0	1125	1125			
France				0	9510	9510
Gabon	0	4830	4830	0	1000	1000
Germany	0	3000	3000	0	4000	4000
Greece	1000	0	1000	6000	0	6000
Hungary				0	13800	13800
India	NA	NA	40980	NA	NA	18935
Indonesia	320	4300	4620	0	1155	1155
Iran	0	370	370	0	700	700
Italy	4800	0	4800	0	1300	1300
Japan	NA	NA	6600			
Kazakhstan	384625	145835	530460	237780	79380	317160
Malawi	8775	0	8775			
Mexico	0	1275	1275	0	525	525
Mongolia	46200	0	46200	15750	0	15750
Namibia	139297	31235	170532	73560	13525	87085
Niger	102227	0	102227	125377	0	125377
Peru	1215	0	1215	1265	0	1265
Portugal	7470	0	7470	1450	0	1450
Romania	0	3325	3325	0	3608	3608
Russian Federation	124050	18970	143020	34260	86960	121220
Solvenia	2200	0	2200	5000	5000	10000
Somalia	0	4950	4950	0	2550	2550
South Africa	231664	83666	315330	66940	13400	80340
Spain	2460	2465	4925	0	6380	6380
Sweden	0	4000	4000	0	6000	6000
Thailand	0	5	5	0	5	5
Turkey	6845	0	6845			
Ukraine	34630	30030	64660	4735	6675	11410
United States	102000	243000	345000			
Uzbekistan	61510	18110	79620	31760	7080	38840
Vietnam	NA	NA	1005	820	4615	5435
Zimbabwe	1350	0	1350			
Totals	2458152	661941	3169238	1078762	320868	1419450

[a]Data compiled from the OECD Nuclear Energy Agency and the IAEA (26).

Table 5. **World Uranium Production by Country in 2002 (tons of U)**[a]

Australia	6,854	Namibia	2,333
Brazil	272	Niger	3,080
Canada	11,607	Pakistan	38[b]
China	730[b]	Romania	90[b]
Czech Republic	465	Russia	2,850
France	18	South Africa	824
Germany	221	Spain	37
Hungary	10	Ukraine	800[b]
India	230	United States	902
Kazakhstan	2,822	Uzbekistan	1,859

[a]Data compiled from Uranium 2003 (26), totals = 36,042.
[b]OECD estimate.

commercial reactors over a 20-year period. This represents approximately 153,000 metric tons of uranium. As of September 2003, over 193 metric tons of HEU have been down-blended and 5,705 metric tons of LEU fuel have been delivered in the United States for use in commercial reactors and represents the dismantlement of 7,733 nuclear warheads.

Spent fuel from nuclear power plants represents a potentially substantial source of fissile material that could displace primary uranium production. Spent reactor fuel from commercial reactors contains approximately 96% of the original fissionable material, along with plutonium created during the fission process. The recycled plutonium can be used as mixed-oxide (MOX) fuel. The use of MOX has not yet significantly altered world uranium demand because only a relatively small number of reactors are using this fuel. As of January 2001, over 250,000 metric tons of heavy metal have been discharged from power reactors, with about 12,000 metric tons of heavy metal in spent fuel discharged annually. In September 2000, the United States and Russia entered into an agreement to each dispose of 34 metric tons of surplus weapon-grade plutonium over the next 25 years. Both countries agreed to dispose of surplus plutonium by fabricating it into MOX fuel for irradiation in existing commercial reactors.

Depleted uranium stocks represent a major uranium reserve, but re-enrichment of depleted uranium is limited as a fuel source because it is only economic in centrifuge enrichment plants that have spare capacity. As of 2000, it was estimated that the depleted uranium inventory was approximately 1.2 million tons, equivalent to 452,000 tons natural uranium.

The demand for uranium in the commercial sector is primarily determined by the consumption and inventory requirements of nuclear power reactors. In January 2003, 441 nuclear power plants were operating worldwide with a combined capacity of about 364 GWe (net gigawatts electric) (26). Current projections show a steady growth in nuclear capacity to 418–483 GWe by the year 2020.

6. Recovery from Ores

The extractive metallurgy of uranium has been discussed in detail in various older books (33,34,45–47) and in several more recent papers (48–53). A

comprehensive discussion and overview is provided in the *Gmelin Handbook of Inorganic Chemistry* (54). The extraction of uranium from ores varies widely and depends on the nature of the ore involved. The ore may vary from hard, igneous rock to soft, weakly cemented sedimentary rock. The principal gangue mineral may be quartz, which is chemically inactive, or an acid-consuming mineral, such as calcite. Some ores are highly refractory and require intensive processing, whereas others break down between the mine and the mill. To recover the uranium from ores, a series of steps is often required, including crushing and concentrating by conventional physical means, roasting and leaching the ore with acid in the presence of an oxidant to ensure conversion to UO_2^{2+}, recovery of the uranium from the leach solution, and refining to a high-purity product.

6.1. Preconcentration. Preconcentration enriches low-grade ores to the point where they can be processed economically. In general, conventional ore-dressing techniques have not been successful in the preconcentration of uranium minerals. However, it is usually possible to obtain acceptable concentration ratios. Where the uranium values occur as masses in pegmatitic rock with large areas of unmineralized pegmatite separating the ore minerals, they are preconcentrated by electronic sorting devices. Gravity separations are sometimes possible due to the high density of uranium minerals relative to most gangue components. However, uranium minerals tend to concentrate with the fines in the grinding and crushing process of some ores. Electrostatic methods generally give low recoveries at low concentrations. Magnetic gangue minerals, eg, magnetite, ilmenite, and garnet, may be separated by magnetic methods, which do not affect the nonmagnetic uranium component. Jaw crushers are employed for coarse crushing; smaller jaw crushers, gyratories, or hammer mills are used for secondary crushing. Rod mills, ball mills, and hammer mills are used for grinding. Uranium is concentrated in the cementing material and in the coating of the sand grains that are separated from the barren sand during the grinding action. In many cases, the ore is so poorly consolidated that there is no need to close the grinding circuit with screens or classifiers.

6.2. Roasting or Calcining. It is usually desirable to subject the ores to a high-temperature calcination prior to leaching. Carbonaceous material can be removed by an oxidizing roast, which at the same time converts the uranium to a soluble form. An oxidizing roast converts sulfides or other sulfur compounds to sulfates, in order to avoid poisoning of ion-exchange resins in subsequent treatments, and removes other reductants that might interfere in the leaching step. Roasting also improves the characteristics of many ores. Clays of the montmorillonite type, for instance, cause thixotropic slurries and thus interfere with leaching, settling, and filtering. Vanadium-containing ores are roasted with sodium chloride to convert vanadium into a soluble sodium vanadate, which in turn is believed to form soluble uranyl vanadates (34). Sodium chloride roasting also converts silver to silver chloride, rendering the silver insoluble for easier separation.

6.3. Leaching. Treatment with suitable solvents (acids or alkalis) converts uranium contained in the ore to water-soluble species. The uranium is separated by chemical processing, including at least one digestion step with acid or alkaline solution. Most mills use acid leaching, which completely extracts uranium. Because of its low cost, sulfuric acid is preferred; however, the more

corrosive hydrochloric acid is used where it is a byproduct of salt roasting. As a general rule, only uranium(VI) compounds dissolve readily in H_2SO_4, whereas minerals, such as uraninite [1317-99-3], pitchblende [1317-75-5], or others in which the uranium has a lower valence, do not. For minerals containing uranium in the lower oxidation state, oxidizing conditions must be provided by the addition of suitable oxidants, such as manganese dioxide or sodium chlorate. Iron must be present in solution as a catalyst for either reaction to be effective. Typical leach reactions are listed in equations 1–5:

$$2\,H_2SO_4 + MnO_2 + UO_2 \longrightarrow UO_2SO_4 + MnSO_4 + 2\,H_2O \quad (1)$$

$$3\,H_2SO_4 + NaClO_3 + 3\,UO_2 \longrightarrow 3\,UO_2SO_4 + NaCl + 3\,H_2O \quad (2)$$

$$UO_2 + 2\,Fe^{3+} \longrightarrow UO_2^{2+} + 2\,Fe^{2+} \quad (3)$$

$$2\,Fe^{2+} + MnO_2 + 4\,H^+ \longrightarrow 2\,Fe^{3+} + Mn^{2+} + 2\,H_2O \quad (4)$$

$$6\,Fe^{2+} + ClO_3^- + 6\,H^+ \longrightarrow 6\,Fe^{3+} + Cl^- + 3\,H_2O \quad (5)$$

In most ores, sufficient Fe^{3+} is already present. For some ores, it is necessary to add metallic iron. In practice, the oxidation potential of the solution can be monitored and controlled using the Fe^{2+}/Fe^{3+} ratio. Very high leaching efficiencies with H_2SO_4 are common, eg, 95–98% dissolution yield of uranium (46). If acid consumption exceeds 68 kg/ton of ore treated, alkaline leaching is preferred. The comparative costs of acid, sodium hydroxide, and sodium carbonate differ widely in different areas and are the determining factor.

Carbonate leaching is usually carried out using sodium carbonate. The utility of the carbonate process arises due to the high thermodynamic stability and solubility of the $UO_2(CO_3)_3^{4-}$ [24646-13-1] ion in aqueous media at low hydroxide ion concentration. This method takes advantage of the fact that U(VI) is very soluble in carbonate solution, unlike the majority of other metal ions that form insoluble carbonates and hydroxides under similar solution conditions. The sodium carbonate leach is therefore inherently more selective than the sulfuric acid leach process. Minerals containing U(IV) require the addition of an oxidant to generate the more soluble VI state. Oxygen (as air) or permanganate is typically used to provide the needed oxygen, and the dissolution of simple uranium oxide follows the reactions shown in equations 6–8. Bicarbonate is typically employed to keep the hydroxide concentration low and avoid precipitation of uranates according to equation 9. Under proper oxidizing conditions, carbonate extractions yield 90–95% of the uranium (34). For this process, fine ores are required, as follows:

$$2\,UO_2 + O_2 \longrightarrow 2\,UO_3 \quad (6)$$

$$UO_3 + 3\,CO_3^{2-} + H_2O \longrightarrow UO_2(CO_3)_3^{4-} + 2\,OH^- \quad (7)$$

$$OH^- + 2\,HCO_3^- \longrightarrow CO_3^{2-} + H_2O \quad (8)$$

$$2\,UO_2(CO_3)_3^{4-} + 6\,OH^- + 2\,Na^+ \longrightarrow Na_2U_2O_7 + 6\,CO_3^{2-} + 3\,H_2O \quad (9)$$

Carbonate leaching under ambient conditions is extremely slow with poor recoveries. Therefore, the ore is typically leached in an autoclave, with air

providing most of the needed oxygen. The leach liquor is separated from the solid in a countercurrent-decantation system of thickeners, and the uranium is precipitated from the clarified sodium carbonate solution with the addition of sodium hydroxide (equation 9) (46).

6.4. Recovery of Uranium from Leach Solutions. The uranium can be recovered from leach solutions using a variety of approaches, including ion exchange, solvent extraction, and chemical precipitation. The most common methods in practice are ion exchange and solvent extraction to purify and concentrate the uranium prior to final product precipitation.

6.5. Ion Exchange. The recovery of uranium from leach solutions using ion exchange is a very important process (48). The uranium(VI) is selectively adsorbed to an anion exchange resin as either the anionic sulfato or the carbonato complexes. In carbonate solutions, the uranyl species is thought to be the *tris*-carbonato complex, $UO_2(CO_3)_3^{4-}$ [24646-13-7], and from sulfate solutions the anion is likely to be $UO_2(SO_4)_n^{2-2n}$, where n is 3 [56959-61-6] or 2 [27190-85-8]. The uranium is eluted from the resin with a salt or acid solution of 1M MCl or MNO_3 ($M = H^+$, Na^+, NH_4^+). The sulfate solution is acidified, and the carbonate solution is kept slightly basic with addition of bicarbonate (34). From this solution, the uranium is precipitated and recovered as a fairly pure uranium concentrate. The uranium ion exchange process has been extensively reviewed, and specific flow sheets, processing rates, recycle methods for reagent conservation, and process equipment are available elsewhere (34,46,48).

6.6. Solvent Extraction. Solvent extraction has widespread application for uranium recovery from ores. In contrast to ion exchange, which is a batch process, solvent extraction can be operated in a continuous countercurrent-flow manner. Solvent extraction has a large disadvantage however, due to incomplete phase separation because of solubility and the formation of emulsions. These effects as well as solvent losses result in financial losses and a potential pollution problem inherent in the disposal of spent leach solutions. For leach solutions with a concentration greater than 1 g U/L, solvent extraction is preferred. For low-grade solutions with <1 g U/L and carbonate leach solutions, ion exchange is preferred (34). Solvent extraction has not been proven to be economically useful for carbonate solutions.

For extraction of uranium from sulfate leach liquors, alkyl phosphoric acids, alkyl phosphates, and secondary and tertiary alkyl amines are used in an inert diluent such as kerosene. The formation of a third phase is suppressed by the addition of modifiers such as long-chain alcohols or neutral phosphate esters. Such compounds also increase the solubility of the amine salt in the diluent and improve phase separation.

Amine extraction from sulfate solutions is mechanistically similar to anion-exchange separation of uranium from uranyl sulfate solution. Uranyl(VI) sulfato complexes are extracted by the alkyl ammonium cations at pH 1–2, and the $UO_2(SO_4)_3^{4-}$ [56959-61-6] complex is the predominant solution species extracted. The amine structure also affects selectivity and affinity. Other anions, such as nitrate or chloride, may interfere with the uranium extraction. Nitrate interferes with secondary amines and chloride with tertiary amines. The choice of suitable stripping agents depends on such factors, as does the recycling of solutions. Molybdenum (present in the ore) is extracted more readily than uranium. It

builds up as a poison in the amine, and it inhibits the process by precipitation at the aqueous–organic interface. The problem may be solved by including one or more specific molybdenum stripping steps in the process (34). Vanadium is also extracted to some extent. Various other ions function as salting-out agents for uranium, which is stripped from the organic solvent in their presence. The affinity of nitrate to the amine is so high that the latter has to be scrubbed by means of a hydroxide or carbonate wash before it can be recycled to another extraction run. Chloride does not give this complication, except with secondary amines, which have a high chloride affinity.

Monoalkyl phosphate extractants exhibit good efficiency in the presence of dilute nitrate, sulfate, or chloride and cause fewer phase-separation problems. However, they are less selective, and other cations present in the leach liquor are co-extracted with the uranium from which they must be separated. The most widely used extractants are di(2-ethylhexyl) phosphate (D2EHPA) and dodecylphosphate (DDPA). The selectivity for uranium is about equal. Fe(III) interferes and has to be quantitatively reduced to Fe(II) in the feed liquor prior to extraction. DPPA has substantially higher solubility losses than D2EHPA, and strong acids are required for backextraction from DPPA. For D2EHPA, sodium carbonate solution is used as the stripping agent; for DPPA, hydrochloric or hydrofluoric acids are used. The D2EHPA solvent extraction process is generally referred to the DAPEX process (dialkyl phosphate extraction).

6.7. Chemical Precipitation. The product of the extraction processes, whether derived from acid or carbonate leach, is a purified uranium solution that may or may not have been upgraded by ion-exchange or solvent extraction. The uranium in such a solution is concentrated by precipitation and must be dried before shipment. Solutions resulting from carbonate leaching are usually precipitated directly from clarified leach liquors with caustic soda without a concentration step, as shown in equation 9.

Losses are kept to a minimum by carbonation of the mother liquor with CO_2 and recycle of the carbonated product back to the leach system. From acid solutions, uranium is usually precipitated by neutralization with sodium hydroxide, ammonia, or magnesia or the precipitation of the peroxide $UO_2(O_2) \cdot n\,H_2O$ in the pH range 2.5–4.0 using hydrogen peroxide. Ammonia gives an acceptable precipitate, for which compositions such as $(NH_4)_2(UO_2)_2SO_4(OH)_4 \cdot n\,H_2O$ were calculated. The ammonium salt is preferred if the product is to be used in the manufacture of fuel-element material.

A higher uranium content can be obtained by precipitation with magnesia (MgO) to yield "yellow-cake." The magnesium sulfate formed is water-soluble, and the uranium compound can be separated by filtration. Yellow-cake consists of either ammonium diuranate [7783-22-4] or magnesium diuranate [13568-61-1]. The ammonium diuranate in yellow-cake is not a stoichiometric compound but a mixture of compounds ranging in composition from $(NH_4)_2UO_4$ [13597-77-8] to $(NH_4)_2U_8O_{25}$ and having the approximate composition $(NH_4)_2U_2O_7$ (55). Sodium uranate [13721-31-4] may be the product from carbonate leach plants.

6.8. Refining to a High-Purity Product. The normal yellow-cake product of uranium milling operations is not generally pure enough for use in most nuclear applications. Many additional methods have been used to refine the

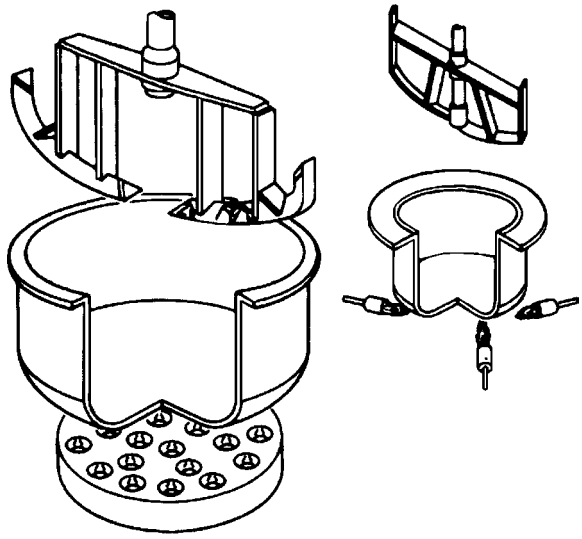

Fig. 2. Gas-fired denitration pots for denitration of $UO_2(NO_3)_2 \cdot 6\,H_2O$. The large pot(1.68 M id, 0.81 m height) is heated by three concentric rings of small radiant gas burners. The small pot (76 cm id, 46 cm height) is heated by four gas burners inside a ceramic furnace (47).

yellow-cake into a product of sufficient purity for use in the nuclear industry. The two most common methods for refining uranium to a high-purity product are tributyl phosphate (TBP) extraction from HNO_3 solutions, or distillation of UF_6, because this is the feedstock for uranium enrichment plants (see ISOTOPE SEPARATION).

In TBP extraction, the yellow-cake is dissolved in nitric acid and extracted with tributyl phosphate in a kerosene or hexane diluent. The uranyl ion forms the mixed complex $UO_2(NO_3)_2(TBP)_2$, which is extracted into the diluent. The purified uranium is then backextracted into nitric acid or water and concentrated. The uranyl nitrate solution is evaporated to uranyl nitrate hexahydrate, $UO_2(NO_3)_2 \cdot 6\,H_2O$ [13520-83-7]. The uranyl nitrate hexahydrate is dehydrated and denitrated during a pyrolysis step to form UO_3 [1344-58-7] as shown in equation 10. The pyrolysis is most often carried out in either a batch reactor (Fig. 2) or a fluidized bed denitrator (Fig. 3). The UO_3 is reduced with hydrogen to UO_2 [1344-57-6] (equation 11) and converted to UF_4 [10049-14-6] with HF at elevated temperatures (equation 12). The UF_4 can be either reduced to uranium metal or fluorinated to UF_6 [7783-81-5] for isotope enrichment. The chemistry and operating conditions of the TBP refining process and conversion to UO_3, UO_2, and ultimately UF_4 have been discussed in detail (47).

$$UO_2(NO_3)_2 \cdot 6\,H_2O \longrightarrow UO_3 + 2\,NO_2 + 1/2\,O_2 + 6\,H_2O \quad (10)$$

$$UO_3 + H_2 \longrightarrow UO_2 + H_2O \quad (11)$$

$$UO_2 + 4\,HF \longrightarrow UF_4 + 2\,H_2O \quad (12)$$

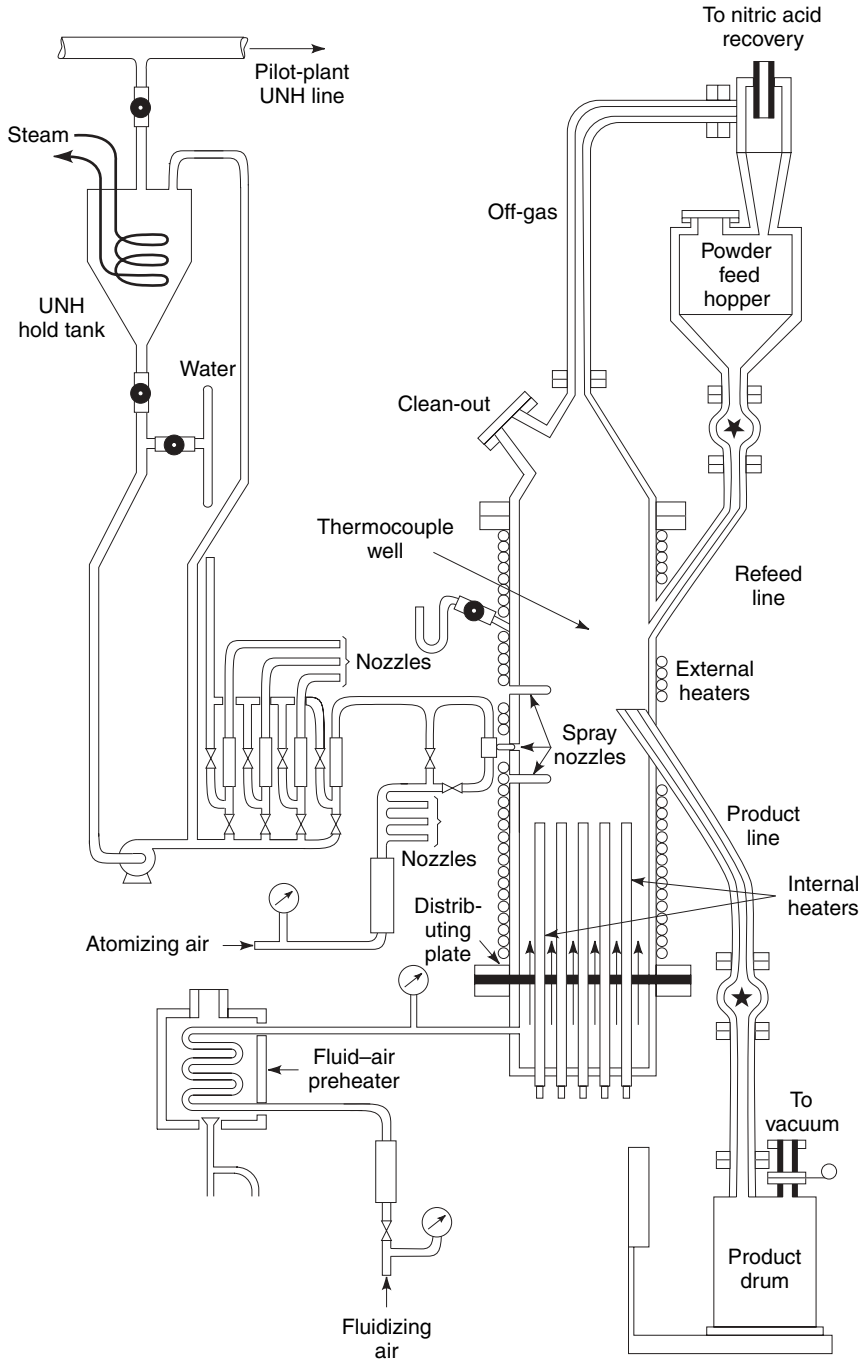

Fig. 3. Pilot-plant fluidized bed denitrator for denitration of $UO_2(NO_3)_2 \cdot 6\,H_2O$ (47).

7. Uranium Metal

7.1. Preparation. Uranium is a highly electropositive element and extremely difficult to reduce. As such, elemental uranium cannot be prepared by reduction with hydrogen. Instead, uranium metal must be prepared using several forcing conditions. Uranium metal can be prepared by reduction of uranium oxides (UO_2 [1344-59-8] or UO_3 [1344-58-7]) with strongly electropositive elements (Ca, Mg, Na), reduction of uranium halides (UCl_3 [10025-93-1], UCl_4 [10026-10-5], UF_4 [10049-14-6]) with electropositive metals (Li, Na, Mg, Ca, Ba), electrodeposition from molten salt baths, and decomposition of uranium halides (the van Arkel–de Boer method). There are several comprehensive treatments of developments in this field (32,56). Typical reaction stoichiometries are given in equations 13–18 as follows:

$$UO_3 + 6\,Na^0 \longrightarrow U^0 + 3\,Na_2O \quad (13)$$

$$UO_3 + 3\,Mg^0 \longrightarrow U^0 + 3\,MgO \quad (14)$$

$$UO_2 + 2\,Ca^0 \longrightarrow U^0 + 2\,CaO \quad (15)$$

$$UO_2 + 4\,Na^0 \longrightarrow U^0 + 2\,Na_2O \quad (16)$$

$$UCl_4 + 2\,Ca^0 \longrightarrow U^0 + 2\,CaCl_2 \quad (17)$$

$$UF_4 + 2\,Ca^0 \longrightarrow U^0 + 2\,CaF_2 \quad (18)$$

A combination of technical considerations makes the reduction of UF_4 by Mg or Ca the preferred method for the preparation of uranium metal. Most important is that the reaction mixture must be fluid for the molten uranium metal to collect into an ingot at the bottom of the reaction vessel. This is an important safety consideration because finely divided uranium metal is pyrophoric. As MgF_2 and CaF_2 have low melting points relative to MgO and CaO, the reduction of uranium halides generates low-melting reaction products, and therefore, Mg or Ca reduction of a uranium fluoride is preferred. The availability of large quantities of magnesium in high purity make it the reagent of choice for most applications. In addition, UF_4 is the starting material of choice due to its greater air and moisture stability.

In practice, uranium ore concentrates are first purified by solvent extraction with tributyl phosphate in kerosene to give uranyl nitrate hexahydrate (see REFINING TO A HIGH PURITY PRODUCT). The purified uranyl nitrate is then decomposed thermally to UO_3 (equation 10), which is reduced with H_2 to UO_2 (equation 11), which in turn is converted to UF_4 by high-temperature hydrofluorination (equation 12). The UF_4 is then converted to uranium metal with Mg (equation 19):

$$UF_4 + 2Mg^0 \longrightarrow U^0 + 2\,MgF_2 \quad (19)$$

Reduction of uranium tetrafluoride by magnesium metal has been described in detail (47,56). It is often referred to as the Ames process, because it was demonstrated at the Ames Laboratory in early 1942. The reaction is very exothermic, and the reduction process is carried out in a sealed bomb due to volatility at the

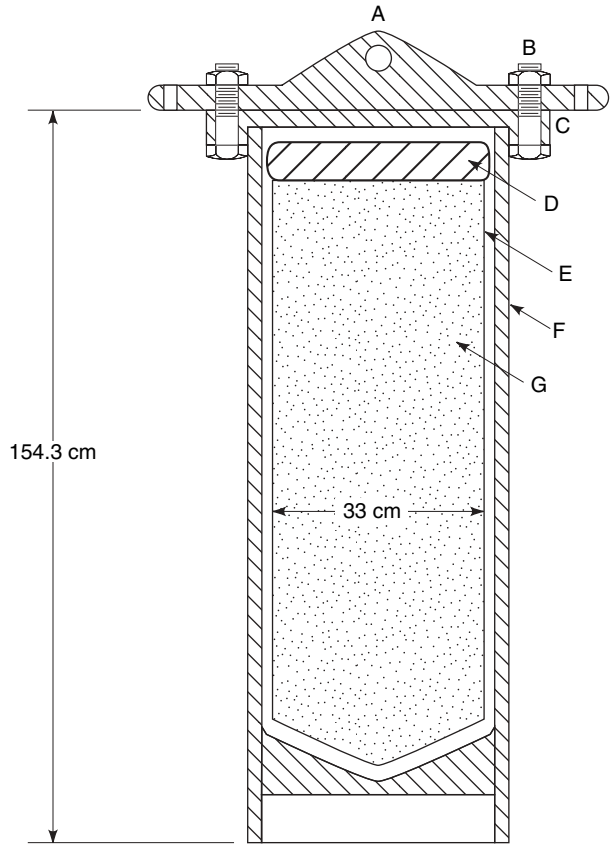

Fig. 4. Reduction bomb reactor for the reduction of UF_4 with Mg by the Ames process. Capacity 144.2-kg uranium metal. (A) Steel cover flange with lifting eye; (B) bolt and nut; (C) top flange of bomb; (D) graphite cover; (E) liner of fused dolomitic oxide; (F) stell bomb; and (G) charge.

temperatures reached in the reaction (Fig. 4). To avoid reaction between molten uranium and the steel container, and to prevent undue heat loss from the bomb, a refractory liner of CaO or MgO is placed inside the reactor. The reactor is then lined with MgF_2 and filled with a thoroughly mixed charge of anhydrous UF_4 powder and Mg chips. A typical reaction would employ 202 kg UF_4 and 32.1 kg of Mg chips. The charge is covered with MgF_2 powder, and the bomb is sealed.

The heat produced by the reaction is not sufficient to maintain a temperature high enough to ensure the fluidity of the mixture. Therefore, the bomb is typically heated to 700°C to provide sufficient heat to completely liquefy the reaction mixture. Alternatively, another oxidant or reaction "booster" can be added to the reaction mixture. During the reaction, uranium settles to the bottom of the bomb to form a metal "button" or ingot, which can be recast into a shape suitable for machining and fuel element fabrication. The average reaction time for a bomb containing a charge of the size given above is approximately 4.5 hours,

depending on the purity of UF_4. If 98% UF_4 is used, the yield may be 97% pure metal, which corresponds to 140 kg of uranium for the reaction size given above.

A direct ingot (dingot) method has been applied to charges of uranium up to 1540 kg of metal (47). The liquid uranium generated in the reduction collects as a pool in the bottom of the bomb and solidifies to an ingot with a diameter of about 25 cm and a height of 25 cm. Dingot metal is of high quality and can be fed directly to a milling machine or to an extrusion press without intermediate recasting. Magnesium is used as the reductant around 1900°C.

A unique problem arises when reducing the fissile isotope ^{235}U. The amount of ^{235}U that can be reduced is limited by its critical mass. In these cases, where the charge must be kept relatively small, calcium becomes the preferred reductant and iodine is often used as a reaction booster. This method was introduced by Baker et al. in 1946 (57). Researchers at Los Alamos National Laboratory have introduced a laser-initiated modification to this reduction process that offers several advantages (58). A carbon dioxide laser is used to initiate the reaction between UF_4 and calcium metal. This new method does not require induction heating in a closed bomb, nor does it use iodine as a booster. This promising technology has been demonstrated on a 200-g scale.

7.2. Properties. Uranium metal is a dense, bright silvery, ductile, and malleable metal. Uranium is highly electropositive, resembling magnesium, and tarnishes rapidly on exposure to air. Even a polished surface becomes coated with a dark-colored oxide/nitride layer in a very short time upon exposure to air. At elevated temperatures, uranium metal reacts with most common metals and refractories. Finely divided uranium reacts, even at room temperature, with all components of the atmosphere except the noble gases. The silvery luster of freshly cleaned uranium metal is rapidly converted first to a golden yellow and then to a black oxide/nitride film within three to four days. Powdered uranium is usually pyrophoric, an important safety consideration in the machining of uranium parts. Thorough reviews are available on the solid state (59), thermodynamic (60), and corrosion properties (32,61).

Uranium metal exhibits three crystalline forms before finally melting at (1134.8 ± 2.0)°C (Fig. 5). The transformation temperatures, enthalpies,

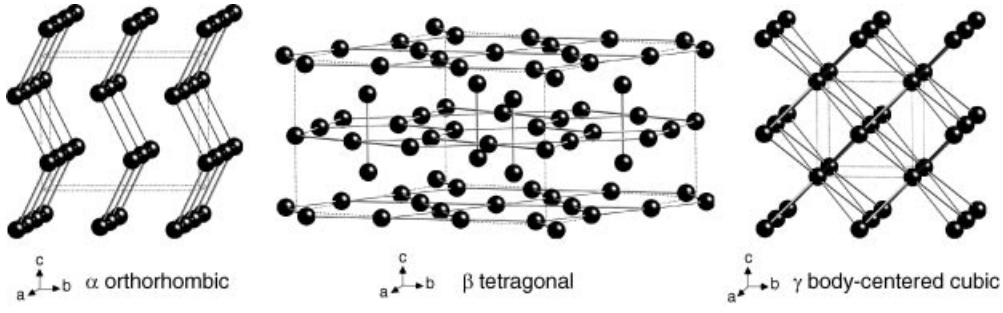

Fig. 5. Crystal structures of elemental uranium. The orthorhombic α-uranium structure consists of puckered layers within the ac plane with U–U distances of 2.80(5) Å within the layers and 3.26 Å between layers. The unusual tetragonal β-uranium structure has 30 atoms in the unit cell, whereas the γ-uranium structure is a more common body-centered cubic.

Table 6. **Some Physical Properties of Uranium Metal**[a]

crystallographic properties	
α, orthorhombic, 298°C	a = 2.8537Å
	b = 5.8695
	c = 4.9584
density	19.04 g cm^{-3}
atoms per unit cell (Z)	4
β, tetragonal, 757°C	a = 10.7766Å
	c = 5.6609
density	18.11 g cm^{-3}
Atoms per unit cell (Z)	30
γ, body centered cubic (bcc), 805°C	a = 3.524Å
density	18.06 g cm^{-3}
atoms per unit cell (Z)	2
melting point, °C	1134.8 ± 2.0°C
enthalpy of vaporization (25°C)	446.7 kJ mol^{-1}
enthalpy of fusion	19.7 kJ mol^{-1}
enthalpy of sublimation	487.9 kJ mol^{-1}
vapor pressure (1720–2340 K)	$\log (p/\text{atm}) = -(26{,}210 \pm 270)\,(\text{T})^{-1} + (5.920 \pm 0.135)$
(1480–2420 K)	$\log (p/\text{atm}) = -(25{,}230 \pm 370)\,(\text{T})^{-1} + (5.71 \pm 0.17)$
phase transformation temperature	
α → β	667.8 ± 1.3°C
β → γ	774.9 ± 1.6°C
γ → liquid	1134.8 ± 2.0°C
enthalpy of phase transformation	
$\Delta H_L(\alpha \rightarrow \beta)$	2.791 kJ mol^{-1}
$\Delta H_L(\beta \rightarrow \gamma)$	4.757 kJ mol^{-1}
$\Delta H_L(\gamma \rightarrow \text{liquid})$	9.142 kJ mol^{-1}
thermal conductivity (100°C)	0.263 W cm^{-1} K^{-1}
elastic constants	
elastic modulus	1758×10^6 kPa
shear modulus	73.1×10^6 kPa
bulk modulus	97.9×10^6 kPa
Poisson's ratio	0.20

[a]Data compiled from Oetting and co-workers (60).

crystallographic, and other parameters have been determined by various workers, and the relevant values are listed in Table 6. The room temperature α-phase adopts an orthorhombic structure and consists of corrugated sheets of uranium atoms (62). The β-phase exists between 668°C and 775°C and has a complex tetragonal structure with six crystallographically independent atom types and 30 atoms in the unit cell (63). The tetragonal lattice is a stacked layered structure with layers parallel to the ab-plane of the unit cell at 1/4c, 1/2c and 3/4c, with a stacking arrangement AB AC AB AC, etc (Fig. 5). The γ-phase is formed at temperatures above 775°C and has a body-centered cubic structure.

The mechanical properties of uranium metal are strongly dependent on purity, fabrication history, and crystal structure. An important property is its plastic deformation character (Table 6), which allows for extrusion. When

α-uranium is deformed at room temperature, the predominant deformation mechanism is twinning. As the temperature increases, deformation by slip becomes more important. Uranium is a relatively weak and extremely reactive metal, and alloys provide improved strength and corrosion resistance. A comprehensive listing and description of uranium alloys, including phase diagrams is given by Wilkinson (32).

Uranium metal is weakly paramagnetic and exhibits almost temperature-independent paramagentism at room temperature with a magnetic susceptibility of 1.740×10^{-5} A/g at 20°C and 1.804×10^{-5} A/g (A = 10 emu) at 350°C (64). Uranium is a relatively poor electrical conductor. Superconductivity has been observed in α-uranium, with the value of the superconducting temperature (T_c) being pressure-dependent. This was shown to be a result of the fact that there are actually three "transformations" within α-uranium (65,66).

Other Physical Properties. Alloys and Phase Transformations. As α- and β-uranium have unusual crystal structures, uranium shows only limited solid solubility with other elements. Intermetallic compounds are formed with several elements such as Al, As, Au, B, Bi, Cd, Co, Cu, Fe, Ga, Ge, Hg, Ir, Mn, Ni, Os, Pb, Pd, Pt, Rh, Ru, Sb, and Sn (32). Uranium alloys that have significant usage include those with Al, Fe, Mo, Nb, Ti, and Zr. The utility of these alloys includes the fact that pure uranium is structurally a weak metal, and alloying confers superior mechanical properties; that some of the alloys show superior corrosion resistance; and that lower melting intermetallics are a convenient form in which to collect uranium from metallothermic or electrochemical reduction operations (32). Binary phase diagrams of uranium with other elements have been summarized (67). Uranium alloys are of interest for many reasons (see USES).

The α- to β-uranium transformation occurring during slow cooling at or near the equilibrium temperature is controlled by diffusion, nucleation, and growth. When pure β-uranium is rapidly cooled, α-uranium forms by diffusionless shear transformation at a temperature about 50°C below the equilibrium temperature, but the β-to-α transformation cannot be avoided even with extremely rapid cooling rates. In contrast, alloyed β-uranium can be retained metastably at temperatures several hundred degrees below the equilibrium temperature by rapid cooling. In the γ-to-β transformation, nucleation and growth are generally observed.

Storage and Handling. Reviews on storage and handling are available (68,69). Corrosion of uranium metal during storage is concern for two reasons: (*1*) The resulting oxide surface layer can become airborne under unfavorable circumstances, resulting in loss of fissile material and an inhalation hazard; and (*2*) the resulting hydrogen evolution could cause a container pressurization and poses a fire and explosion hazard. For HEU, there are additional concerns regarding criticality safety.

Chemical Properties of Uranium Metal. Uranium metal is highly reactive and can react with practically every element in the Periodic Table except the noble gases. The most important reactions of elemental uranium are with oxygen, nitrogen, and water. When uranium metal is exposed to air, it undergoes reaction even at room temperature (61). The sliver luster of clean uranium metal is rapidly converted to a golden yellow and ultimately to a black oxide/nitride

film within three or four days. The mechanisms of corrosion have been discussed in some detail (32,61).

Uranium in finely divided form is readily ignitable, and uranium scrap from machining operations is subject to spontaneous ignition. This reaction can usually be avoided by storage under dry (without moisture) oil. Grinding dust has been known to ignite even under water, and fires have occurred spontaneously in drums of coarser scrap after prolonged exposure to moist air. Because of uranium's thermal conductivity, larger pieces generally have to be heated entirely to their ignition temperature before igniting. Moist dust, turnings, and chips react slowly with water to form hydrogen. Uranium surfaces treated with concentrated nitric acid are subject to explosion or spontaneous ignition in air.

Uranium dissolves rapidly in hydrochloric acid and dissolves at a more moderate rate in nitric acid. Particle size and surface area clearly important, as finely divided uranium can dissolve in nitric acid with explosive violence. Nonoxidizing acids such as sulfuric, phosphoric, and hydrofluoric acids react only very slowly. Uranium metal is inert to alkaline solutions, but the addition of oxidants such as peroxide to a sodium hydroxide solution will lead to dissolution, although the products are not well characterized.

Irradiation Effects. When uranium metal fuels are irradiated in a nuclear reactor, the metal undergoes substantial dimensional and structural changes in addition void swelling (70).

8. Isotope Enrichment

8.1. Uranium-235 Enrichment. The separation of isotopes is an important process in nuclear technology and is generally employed to achieve enrichment in the amount of ^{235}U in samples. The enrichment of uranium is expressed as the weight percent of ^{235}U in uranium. For natural uranium the enrichment level is 0.72% (see ISOTOPE SEPARATION), whereas the rest of the material is predominantly ^{238}U, which cannot sustain a nuclear chain reaction. Nuclear applications, such as nuclear reactor fuel, require enrichment levels above 0.72% (71). Normally for light water nuclear reactors (LWRs), the 0.72% natural abundance of ^{235}U is enriched to 2–5% (26,72). There are special cases like materials-testing reactors, high-flux isotope reactors, compact naval reactors, or nuclear weapons, where ^{235}U enrichment of 96–97% is used. Uranium enriched to 20% or more ^{235}U is called high enriched uranium (HEU), whereas uranium enriched above natural abundance, but below 20% is called low enriched uranium (LEU).

The separation of isotopes of uranium is an extremely difficult task. Uranium isotope enrichment can be achieved in several ways, including gaseous diffusion, gaseous centrifugation, electromagnetic separation, chemical exchange, laser photoionization and photodissociation, separation nozzle, and cyclotron resonance isotope separation. Most of these processes are of historical significance and have been described by Villani (71). The gaseous diffusion and centrifugation processes (GDP and GCP) are the only methods currently employed on an industrial scale.

8.2. Gaseous-Diffusion Process. This process is used for the separation of ^{235}U and ^{238}U on an industrial scale (73–77). It is based on the fact that

molecular transport through small pores takes place via Knudsen diffusion, where the speed of transport is inversely proportional to the square root of the mass of the molecules (78). Highly purified gaseous UF_6 is pumped through a barrier tube with porous walls. $^{235}UF_6$ and $^{238}UF_6$ diffuse through the barrier tubes at slightly different rates, based on the mass difference between $^{235}UF_6$ and $^{238}UF_6$ molecules. The separation efficiency for this process is very small because of the small mass difference (theoretical separation factor of 1.0043) between these uranium isotopes. To obtain an enrichment of the natural ^{235}U from 0.72% to 3% necessary for power generation, more than 1000 separation steps are needed. For many applications, the process must be repeated hundreds of thousands of times to obtain high enrichments of ^{235}U. This is accomplished by coupling many diffuser units in a series referred to as a cascade or stage (Fig. 6). Approximately 12 stages make up a larger unit known as a cell, and several cells make up a single GDP unit. Gaseous diffusion plants are enormous in size, often covering hundreds of acres, and requiring huge amounts of electric power to operate. Gaseous diffusion plants are known to exist in Argentina, China, France, Russia, and the United States.

8.3. Gas Centrifugation. The high capital cost and large power requirements of gaseous-diffusion plants led to an extensive investigation into centrifugal separation of ^{235}U and ^{238}U by several countries (79). The advantage of centrifugal separation over gaseous diffusion is that the separation factor is not proportional to the square root of the ratio of the masses of ^{235}U and ^{238}U but instead to the mass difference of isotopes. Therefore, centrifugal separation is more efficient than gaseous diffusion.

In the gas centrifuge uranium-enrichment process, gaseous UF_6 is fed into a spinning centrifuge near the center of a cylindrical rotor that spins at high speed inside an evacuated casing (Fig. 7). The UF_6 gas is acted on by two fields: the centrugal field induced by the high-speed rotation of the rotor and an internal countercurrent circulation. The centrifugal force causes the heavier $^{238}UF_6$ molecules to move closer to the wall than the lighter $^{235}UF_6$ molecules, thus partially separating the uranium isotopes. The radial separation factor is proportional to the absolute mass difference between the two isotopes. In addition to isotopic separation along the radial dimension, there is also separation along the vertical axis due to countercurrent circulation flow induced by an axial thermal gradient along the length of the rotor. The relatively slow axial countercurrent flow of gas within the centrifuge concentrates enriched gas at one end and depleted gas at the other. This flow can be driven mechanically by scoops and baffles or thermally by heating one end cap (79).

The separation factors obtainable from a centrifuge are large (1.01 to 1.10) compared with gaseous diffusion (1.004); several cascade stages are still required to produce even LEU material. However, power requirements are significantly less than that of a diffusion plant. Large cascades of gas centrifuges are operated by Brazil, France, Germany, the United Kingdom, India, Japan, Iran, Pakistan, Russia, and China to produce enriched uranium both for domestic use and for export, and by Japan for domestic use. A demonstration gas centrifuge plant was built at Piketon, Ohio in the United States by the United States Enrichment Corporation (USEC) for operation in 2006, and a full-size plant is planned for operation in 2010. The Pakistan nuclear program deployed new centrifuges

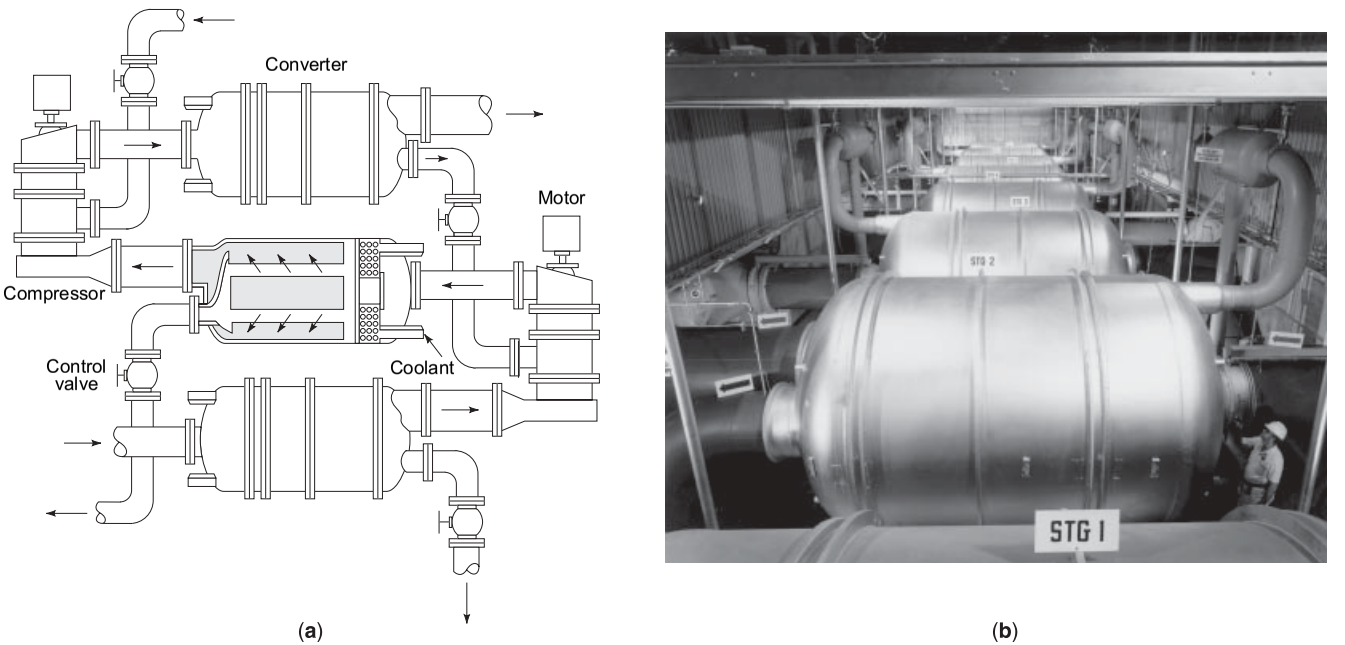

Fig. 6. (**a**) A gaseous-diffusion stage schematic showing a single converter in center. (**b**) Photo of gaseous-diffusion stage (photo courtesy of DOE).

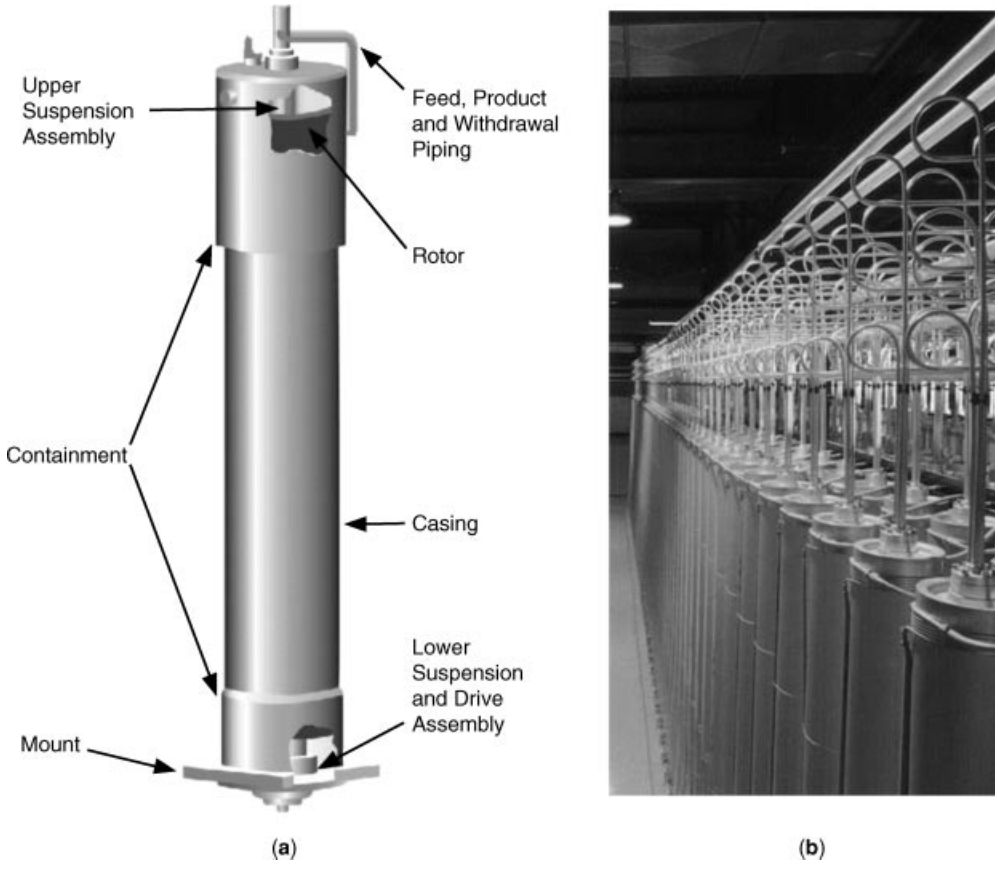

Fig. 7. (**a**) Generic schematic of a gas centrifuge, and (**b**) photo of a gas centrifuge cascade (photo courtesy of USEC).

in large numbers. Recently, Iran enriched uranium to 4.8% using a centrifuge cascade.

8.4. Electromagnetic Separation. The electromagnetic separation method was developed at the University of California Radiation Laboratory and employed on an industrial scale in the electromagnetic separation plant at Oak Ridge (80–82). Because the prototype machines were tested in the Berkeley cyclotron magnets, the Oak Ridge separators were called calutrons (California University Cyclotron). A comprehensive description of the calutron process has been given (83). A calutron separator is essentially a 180° mass spectrograph designed for a large throughput of ions. The uranium to be separated is converted to the tetrachloride and loaded into the charge bottle of the calutron, or it is generated in the charge bottle from UO_2 [1344-57-6] and CCl_4 vapor. The ions generated from the UCl_4 vapor in the ion source are accelerated into the magnetic field and deflected through an angle of 180°. The radius of curvature of the heavy beam (^{238}U) is larger than that of the light beam (^{235}U). Thus, the two beams are focused on two different locations on the receiver. The receiver, built of graphite, is equipped with pockets in which the beams of the two isotopes

are collected. After each run, the receiver is dismantled, and the individual isotopes are worked up separately. Electromagnetic separation is therefore an incredibly labor-intensive process.

The electromagnetic separation plant built during World War II at Oak Ridge involved two types of calutrons, alpha and beta. The larger alpha calutrons were used for the enrichment of natural uranium, and the beta calutrons were used for the final separation of ^{235}U from the pre-enriched alpha product. The calutron technique has been used to separate pure samples of ^{234}U, ^{236}U, and stable isotopes of many other elements. The Y-12 calutron plant at Oak Ridge was shut down in 1999. Electromagnetic separation is used in Russia to produce small quantities of research grade isotopes of extremely high purity (84,85), and the International Atomic Energy Agency (IAEA) found evidence that the Iraqi government was using electromagnetic separation of uranium prior to the 1991 Gulf War (86).

8.5. Laser Isotope Separation. Atomic and molecular laser isotope separation techniques use lasers to selectively excite atoms or molecules containing one isotope of uranium so they can be preferentially recovered. The science is promising and has been extensively evaluated for the production of fuel and moderators for nuclear power generation in several countries. Although the technology has been proven, it has been extremely difficult to master.

Atomic Vapor Laser Isotope Separation. In the atomic vapor laser isotope-separation (AVLIS) process, vibrationally cooled ^{235}U metal atoms are selectively ionized by means of high-power (1–2-kW) tunable copper vapor or dye laser operated at high (kHz) repetition rates (64,87,88). In the AVLIS process, an electron beam gun produces high-energy electrons that melt and vaporize the uranium metal feed. The electron beam is focused on the uranium melt using magnetic fields. The uranium melt is contained in a water-cooled copper crucible, and uranium feed is introduced into the melt in the form of a bar. The uranium atomic vapor produced by e-beam melting expands into a vacuum and becomes collimated upon cooling. Adiabatic cooling puts most of the uranium atoms in the ground electronic state. At this point, a high-power laser is tuned to selectively ionize ^{235}U atoms, leaving the ^{238}U atoms unaffected. An electromagnetic field is used to strip the ^{235}U ions from the vapor stream, and the unionized ^{238}U atomic vapor stream flows to the roof of the chamber (65). In 1999, the United States Enrichment Corporation (USEC) decided that AVLIS technology would never be profitable and made the decision to abandon AVLIS technology.

Molecular Laser Isotope Separation. In the molecular laser isotope (MLIS) process, UF_6 is irradiated by an infrared laser operating near the 16-μm wavelength, which selectively excites $^{235}UF_6$, leaving $^{238}UF_6$ relatively unperturbed. In a second step, a second laser system preferentially photodissociates $^{235}UF_6$ into $^{235}UF_5$ and free fluorine atoms. The $^{235}UF_5$ precipitates from the gas as a powder that can be filtered from the gas stream. The MLIS process has many complex hurdles to overcome, and most programs have been terminated. However, a variation of MLIS technology known as Separation of Isotopes by Laser Excitation (SILEX) has continued with development work in Australia. In May 2000, a U.S.–Australian Agreement for Cooperation for the development of SILEX technology was approved by President Clinton and the U.S. Congress.

In June 2001, the SILEX technology was officially classified by the U.S. and Australian governments, bringing the project formally under the security and regulatory protocols of each country.

8.6. Other Isotope Separation Methods. Several other methods for separating uranium isotopes have been developed, but none of these has been advanced beyond the pilot-plant stage, and many have received little attention due to the improved economics of gaseous diffusion, centrifugation, and SILEX. The liquid thermal-diffusion process was installed in a pilot plant in Oak Ridge at the time of the Manhattan Engineering District Project (89). Uranium hexafluoride, kept liquid at temperatures above its triple point, is subjected to diffusion in a thermal-diffusion column, the center of which is kept at 188–286°C, whereas the wall is maintained at 65°C. By thermal diffusion, the ^{235}U is enriched at the top, whereas ^{238}U migrates to the bottom of the column. The S-50 plant provided slightly enriched feed material for the calutron plant at Y-12. The S-50 operations were terminated in September 1945, when the K-25 gaseous-diffusion plant went into operation. In the separation-nozzle method, UF_6 [7783-81-5] vapor is effused out of a nozzle (90). During the effusion, the light isotope is enriched in certain parts of the gas jet and may be enriched by stripping those parts away from the other parts of the jet. The gas is an H_2-UF_6 mixture containing 5% UF_6. The process has been demonstrated on the pilot-plant scale at the Nuclear Engineering Institute of the Karlsruhe Nuclear Research Center in Germany.

9. Analytical Methods for Uranium Determination

The analytical determination of uranium can be accomplished through a variety of wet chemical, nuclear, and spectroscopic techniques. The majority of these methods rely on sample preparation and subsequent quantitative analysis of aqueous solutions containing dissolved uranium. Most solid uranium-containing compounds and alloys can be dissolved with mineral acids (HNO_3, H_2SO_4, and HCl) (91), although dissolution in HCl usually leaves a black residue (1). Open-vessel digestion in mineral acids will dissolve many U-containing minerals, such as autunite, uranophane, or urananite. Uranium can then be separated from solution and concentrated by (co-)precipitation, liquid–liquid extraction, ion exchange, evaporation, or electrochemical methods.

Coprecipitation of uranium occurs with Fe(III), Al(III), Ca, and ammonium hydroxides in the absence of carbonate or with $(NH_4)_2S$ or $(NH_4)_2CO_3$ (1). Precipitation of uranium can also be accomplished with organic or inorganic precipitants (such as Na_2CO_3 or K_2CO_3) and selectively precipitated from acidic solutions as a peroxide or oxalate.

Alcohols, ethers, esters, ketones, organic acids, and phosphoric acid derivatives are used for the liquid–liquid extraction of uranium from aqueous solution (92). The addition of nitrate salts can enhance the extraction of uranium (93). As an example, methylisobutyl ketone has been applied for large-scale uranium separation. Oxidation-state selective extraction of U(IV) occurs from an acidic solution pretreated with $Al(NO_3)_3$ using ethylacetate, whereas U(VI) can be extracted with 25% TBP in toluene.

Cation exchange resins generally have low selectivity for UO_2^{2+} over other metal cations; however, UO_2^{2+} chloride or sulfate complexes can be easily separated by anion exchange.

Uranium can be separated electrochemically via electrolysis with a mercury cathode and deposition on various solid metal electrodes (94). A thin sample of uranium for high-resolution alpha-spectrometric analysis is generally prepared by electrolytic deposition under acidic conditions [(95) and ASTM C1284-05].

Volumetric, gravimetric, and coulometric methods have been widely used for classic wet chemical uranium analysis to determine larger amounts of uranium. The most common volumetric method is a redox titration involving the reduction of U(VI) followed by oxidation to U(VI) with Ce(IV) or $KMnO_4$ (96). A highly accurate redox titration method has been developed using Fe(II) to reduce U(VI) in phosphoric acid solutions, followed by oxidation of U(IV) with Cr(VI) with potentiometric determination of the endpoint (ASTM 1994, C1267-94). Additional methods have been developed for both constant current and controlled potential coulometric titrations. Gravimetric methods are limited in use due to the difficulty of selectively precipitating uranium from solutions containing mixed metal cations. The most common method for gravimetric determination of uranium is by sulfide-carbonate–hydroxide precipitation and the gravimetric determination as U_3O_8.

Nuclear techniques have been developed to take advantage of the radioactivity of naturally occurring isotopes of uranium. High-resolution alpha spectrometry can give isotopic analysis for ^{238}U, ^{235}U, and ^{234}U, whereas high-resolution gamma spectroscopy with germanium detectors is used for analysis of ^{234}Th, the daughter of ^{238}U. Electrochemical deposition of uranium on metal planchets at pH 3.5 is commonly used for the preparation of thin samples for high-resolution alpha and gamma spectroscopy. Activation analysis, whereby the sample is irradiated with neutrons to increase the number of radioisotopes, followed by gamma spectroscopy is a highly specific technique for uranium, and is often used in analysis or uranium ores. Liquid scintillation counting is also used to determine uranium concentrations, and a standard method has been developed for analysis in aqueous solutions (ASTM 1998, D6239-98).

Spectroscopic methods used for uranium analysis can be categorized as x-ray-based techniques (absorbance, diffraction, fluorescence, etc), optical spectroscopy (ft-ir, uv-vis, Raman, etc), and miscellaneous techniques (mass spectroscopy, nuclear magnetic resonance, etc). Table 7 summarizes the key characteristics of the major methods, including the physical state of the sample, obtained information, and known detection limits. Mass spectroscopy gives the lowest detection limit, followed by luminescence spectroscopy. Fluorescence spectroscopy is particularly adaptable to uranium detection because it is one of the few elements that will fluoresce naturally eliminating the need to add a chelating agent to solution. Recently, techniques such as x-ray photoelectron spectroscopy and x-ray absorption near-edge structure (XANES) spectroscopy have gained popularity as a way to characterize the oxidation state and bonding characteristics of uranium in solids and solutions. This technique has been used to show that U(VI) was reduced to U(IV) by bacteria in uranium wastes (97), to determine the uranium speciation in soils from former US DOE uranium processing facilities and the mode of U(VI) binding to montmorillonite

Table 7. **Characteristics of Major Spectroscopic Techniques for Uranium Analysis**

Method	ASTM standard	Sample state[a]	Information	Detection limit
X-ray photoelectron spectroscopy (XPS)		S	coordination, oxidation state	
X-ray diffraction (XRD)		S	solid phase characterization	
X-ray absorption spectroscopy (XAS)		S, L	coordination, oxidation state	
X-ray fluorescence (XRF)	C1255-93 C1254-05 C1118-02 C1343-02 C1416-04 C1456-00	S, L	coordination, oxidation state	20 μg/mL
energy dispersive X-ray scanning electron microscopy (EDX-SEM)		S	element distribution	
uv-vis absorbance		S, L	concentration, speciation, oxidation state	
vibrational (IR, Raman)	C1441-04	S, L	concentration, coordination	
atomic absorption spectroscopy (AAS)		S, L	concentration	40 μg/mL (faas)[c] 30 ng/mL (gfaas)[d]
atomic emission spectroscopy (AES)	C1109-04 C1111-04	S, L	concentration	20 ng/mL (icpaes)[e] 250 ng/mL (icpase)
luminescence spectroscopy	D2907-91[b] D5174-91(02)	S, L	concentration, speciation	5 ng/mL fluorometric 50 pg/mL phosphorometric
mass spectrometry (MS)	C1344-97 (03) C1413-99 (05) C1310-01 C1345-01 C1379-04 C1428-05 C1429-04 C1474-00 C1477-00	S, L	concentration, speciation, isotopics	100 fg/mL (icpms) 1 fg/mL (HR-icpms)[f] (Brenner 1998)
^{235}U nuclear magnetic resonance (NMR)		S, L	coordination	

[a] S = solid, L = liquid.
[b] This ASTM standard is retired.
[c] Flame source atomic absorption spectroscopy (faas).
[d] Graphite furnace source atomic absorption spectroscopy (gfaas).
[e] Inductively coupled plasma (ICP).
[f] High resolution (HR).

clays (98,99). Currently, no ASTM standards have been developed for these methods.

10. Uses and Economic Aspects

Uranium is a synthetic precursor of transuranium elements and the source of the light isotope, ^{235}U. The primary use of ^{235}U, as a source of nuclear energy for nuclear power generators and nuclear weapons, is well known. The thermal energy generated by fission of 1 g of ^{235}U is equivalent to that released by burning 2200 L of crude oil or 2.7 tons of coal. The predominate species used as nuclear fuel in power stations is UO_2. The mixed uranium–plutonium oxide (MOX) system, $(U,Pu)O_2$, with the PuO_2 fraction varying between 2% and 35% finds increasing application as nuclear reactor fuel. The percentage of plutonium in the MOX fuel greatly alters its use and behavior. MOX fuel that contains only a small percentage (2–6%) of PuO_2 behaves like UO_2 and is used in light water reactors (LWRs); fuels for fast breeder reactors contain a significantly higher percentage (15–35%) of PuO_2 and behave very differently (100). MOX provides about 2% of the new fuel used today with over 30 reactors in Europe using MOX fuel. Japan aims to use MOX in around one third of its reactors by 2010. Only four plants in France (2), Belgium, and the United Kingdom currently produce commercial quantities of MOX fuel with a production capacity of about 300 tons per year. Over the last 50 years, used nuclear fuel has been reprocessed in some countries to recover fissile materials for recycling and to reduce the volume of high-level wastes. The current main method used in commercial reprocessing plants is the well-established hydrometallurgical PUREX (Plutonium URanium EXtraction) process (see PLUTONIUM AND PLUTONIUM COMPOUNDS). This process is based on the dissolution of spent nuclear fuel in nitric acid and subsequent separation of uranium and plutonium by solvent extraction. A variation of PUREX is the UREX (URanium EXtraction) process, which separates the uranium, and leaves the plutonium with other transuranics providing a greater proliferation resistance than PUREX. About 99.9% of Uranium and >95% of technetium can be separated from other fission products. The addition of acetohydroxamic acid to the extraction and scrub sections of the process greatly diminishes the extractability of neptunium and plutonium by the reduction and subsequent complexation of dissolved plutonium and neptunium species (101).

Among the three isotopes suitable for nuclear reactor fuel, ^{233}U, ^{235}U, and ^{239}Pu, ^{233}U is superior due to its higher neutron yield per neutron absorbed. The Thorium fuel cycle (102–105) uses ^{232}Th as a fertile isotope that absorbs neutrons to form ^{233}Th, ^{233}Pa, and ultimately ^{233}U, which can be extracted and then used as nuclear fuel in any reactor type forming a closed fuel cycle. One challenge for implementing the thorium fuel cycle is the presence of hard gamma-emitting radionuclides among the descendents of ^{232}Th and impurities associated with ^{233}U, ie, ^{232}U. Some reactor prototypes were built and tested in the late 1960s; however, interest in the thorium fuel cycle decreased around 1980 in part due to the technical difficulties and costs associated with the fabrication of ^{233}U fuel (see THORIUM AND THORIUM COMPOUNDS).

Other uranium compounds/alloys are also being considered for use as nuclear fuels in alternative reactors. Uranium carbide (UC) has been used in sodium or lead-cooled reactors (see Section 11.1), whereas uranium silicides have been proposed as a fuel source in light-water reactors. Uranium–zirconium and uranium–aluminum alloys are used in materials and research testing reactors. Uranium–zirconium alloys are also widely used in marine reactors, whereas the hydrogenated U-Zr alloys ($UZrH_x$) are fuels for spacecraft reactors. The full details of the role of uranium in the nuclear fuel cycle have been presented in previous editions of this encyclopedia and the Gmelin Handbook (37).

Depleted uranium (^{238}U), which is about 0.2% ^{235}U, has a density more than twice that of steel. This property has been used for military purposes in the production of armor and armor-piercing projectiles, also known as kinetic energy penetrators (106). Depleted uranium and uranium alloys such as $UTi_{0.75}$ [39460-95-2] are very useful as armor piercing projectiles (107), and the penetration mechanism has been determined (108). The superior penetration behavior of depleted uranium penetrators is presently attributed to the ability to self-sharpen during armor penetration via failure along adiabatic shear bands. This is in contrast to conventional tungsten heavy alloy (WHA) penetrators that form a "mushroom" head, which decreases the energy delivered to the target. The radiological hazard of depleted uranium combined with chemical corrosion during storage has resulted in significant research into improving the penetration behavior of tungsten alloys (109,110).

The high density of uranium makes it attractive for flywheels, whereas its density and effectiveness at absorbing gamma rays also suggests a possible use for shielding of spent nuclear fuels. Two types of storage canister have been proposed: one made of metallic uranium and one made of UO_2-containing concrete. One of the difficulties in designing metallic uranium shields is the tendency for corrosion in air, forming oxide surfaces. A corrosion-resistant material can be obtained by alloying uranium with 2–8 wt% molybdenum and, therefore, can be used in medical radiation equipment shielding and in aircraft trimming weights.

11. Uranium Compounds

11.1. Materials. *Oxides.* Oxides of uranium are some of the most prevalent and technologically important binary uranium compounds known. Numerous oxide phases have been observed and characterized, including UO [12035-97-1], UO_2 [1344-57-6], U_4O_9 [12037-15-9], U_3O_7 [1203-04-6], U_3O_8 [1344-59-8], UO_3 [1344-58-7], anionic uranates including $[U_2O_7]^{2-}$ [85096-44-2] and $[U_4O_{13}]^{2-}$ [128085-85-8], and hydrated species such as $UO_3 \cdot x\,H_2O$ and the peroxo complex $UO_4 \cdot x\,H_2O$. The crystal structures of UO_2 and polymorphs of U_4O_9 and U_3O_7 are closely related to the fluorite structure, whereas the higher oxides, eg, U_3O_8, and most UO_3 polymorphs exhibit layered structures with linear UO_2^{2+} groups perpendicular to the plane of the layers. Of these oxide phases, UO_2, U_3O_8, and UO_3 are extremely important both industrially and in the nuclear energy cycle. The preparation of some of these most important oxides

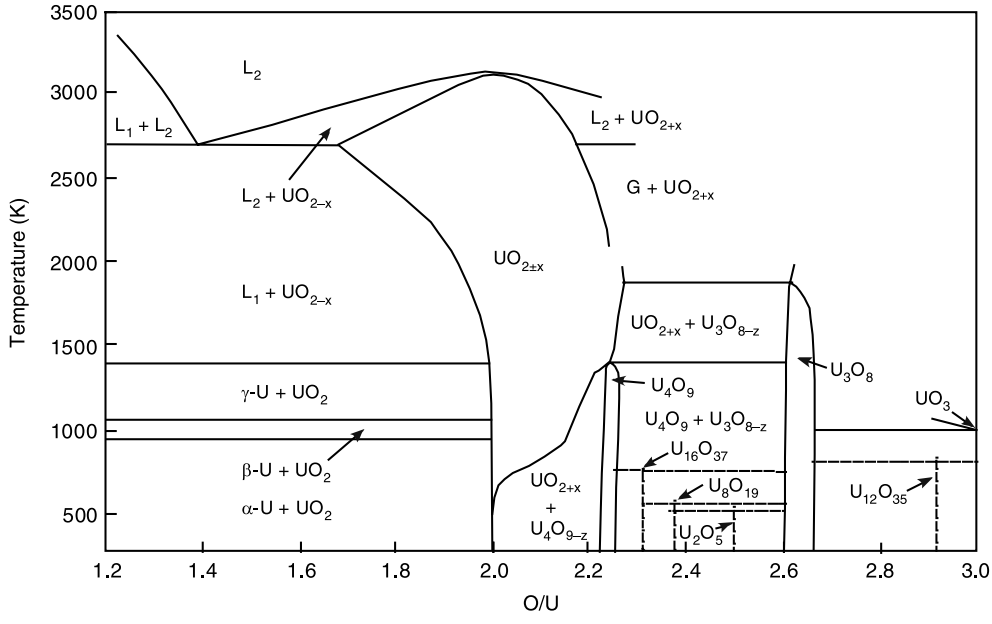

Fig. 8. The uranium oxygen phase diagram, developed from data in Ref. 1.

is given in equations 20–26. The phase diagram of uranium oxide phases as a function of the O/U ratio is shown in Figure 8 (1).

$$UO_3 + H_2 \xrightarrow{700^\circ C} UO_2 + H_2O \quad (20)$$

$$UO_3 + CO \xrightarrow{350^\circ C} UO_2 + CO_2 \quad (21)$$

$$3\,UO_2 + O_2 \xrightarrow{600^\circ C} U_3O_8 \quad (22)$$

$$3\,UO_3 \xrightarrow{700^\circ C} U_3O_8 + 1/2\,O_2 \quad (23)$$

$$U_3O_8 + 5\,UO_2 \xrightarrow{\text{sealed tube}} 2\,U_4O_9 \quad (24)$$

$$4\,UO_2 + 1/2\,O_2 \xrightarrow[900^\circ C]{0.1\text{ mm air}} U_4O_9 \quad (25)$$

$$3\,UO_2 + 1/2\,O_2 \xrightarrow{<200^\circ C} U_3O_7 \quad (26)$$

Uranium dioxide, UO_2 [1344-57-6], is found in nature as the mineral pitchblende and as a component in uraninite. The crystalline solid melts at 2878°C and is paramagnetic with a room temperature magnetic moment of $3.2\mu_B$. The density has been found to range from 10.79 to 10.95 g/cm^3, with lower values being observed for hyper-stoichiometric complexes, UO_{2+x}. UO_2 is prepared by reducing higher uranium oxides, ie, UO_3 or U_3O_8, with hydrogen between 700°C and 1100°C (111,112). Oxygen impurities in the hydrogen gas induce formation of hyperstoichiometric UO_{2+x}, which forms on cooling below 300°C. Industrially, UO_2 is prepared by the decomposition of ammonium uranyl carbonate on the scale of 10 kg/d, using a fluidized-bed furnace (113). In addition to the

industrial process, pure UO_2 has been synthesized via (*1*) oxidation of uranium metal, (*2*) reduction of higher valent oxides, (*3*) thermal decomposition of uranyl uranates, (*4*) oxidation or reduction of uranium halides, (*5*) decarboxylation of uranium compounds of carbonic acids, (*6*) hydrometallurgical preparation, and (*7*) electrolysis of uranium halides. Starting materials for commercial UO_2 synthesis are ammonium salts, ie, $(NH_4)_2U_2O_7$ and $(NH_4)_4UO_2(CO_3)_3$, or the peroxide $UO_4 \cdot 2\,H_2O$.

Single crystals of UO_2 have been grown by a variety of techniques, including vapor or electrolytic deposition from salt melts or vapor deposition on ionic substrates. Electrolysis of uranyl chloride in fused alkali chloride melts produced single crystals of 3 mm length (114). The x-ray analysis of the stoichiometric complex reveals a face-centered cubic CaF_2 type structure, with the uranium atoms occupying the face-centered sites. Hyper- and hypo-stoichiometric, UO_{2+x} and UO_{2-x} (respectively), are also known and have been analyzed by x-ray crystallography. In the case of the UO_{2+x}, extra oxygen atoms occupy central lattice vacancies in the normal UO_2 structure though this view has recently been challenged. For the hypo-stoichiometric complex, the structure indicates the presence of layers of UO_2 and UO.

The main technological uses for UO_2 are found in the nuclear fuel cycle as the principal component for light and heavy water reactor fuels. Uranium dioxide is also a starting material for the synthesis of UF_4 [10049-14-6], UF_6 [7783-81-5] (both critical for the production of pure uranium metal and isotopic enrichment), UCl_4 [10026-10-5], and $UO_2(NO_3)_2 \cdot 6\,H_2O$ [10102-06-4]. To be useful as a nuclear fuel, the material must have certain physical and chemical properties in the reactor temperature range, ie, small coefficients of linear and volume expansion, reasonable heat conductivity, and chemical stability. Uranium dioxide has been found to exhibit most of these desirable properties with an average thermal coefficient of expansion of 10.8×10^{-6} (20–946°C), specific heat from 0.237 to 0.338 J/gK (300–1773°C), and a thermal conductivity of 8.281 to 2.353 W/mK (300–1773°C) at 0 at.% burnup UO_2. The sintered complex has also been found to be chemically stable toward air and H_2O up to 300°C. The thermodynamic and transport properties of UO_2, including hypo/hyper-stoichiometric as well as doped species under reactor conditions, are under investigation (115–122).

For most nuclear applications, UO_2 must be produced as uniform spheres and pellets. Three techniques used for microsphere fabrication are sol-gel, gel-precipitation, and plasma spheroidization (123). Details on the sol-gel and gel-purification processes, the two most popular, can be obtained from the Gmelin Handbook (37). The common method for producing UO_2 pellets consists of pressing granules in the presence of binding agents and lubricants with a subsequent sintering, after the organics have been removed. Recently, high-density spheres without open porosity have been fabricated from soft UO_2 microspheres, using a gel pelletization technique (124).

The ternary plutonium–uranium–oxygen system is probably one of the best-understood plutonium–actinide oxide systems due to its application as MOX fuel for nuclear reactors. Up to 1000°C mixed uranium–plutonium oxides with stoichiometric compositions form a continuous solid solution from UO_2 to PuO_2, and the lattice parameters follow Vegard's law (125,126). The

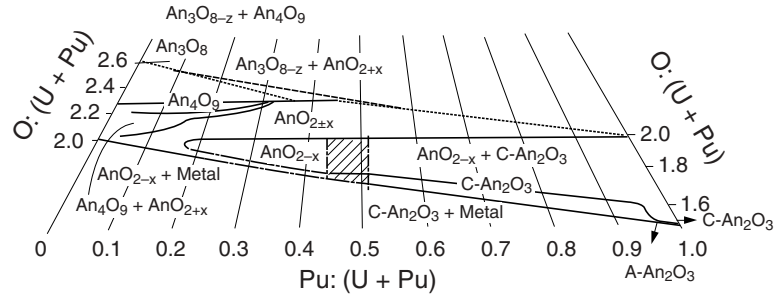

Fig. 9. The phase diagram for the ternary U-Pu-O system in the composition range $(U,Pu)O_2$–$(U,Pu)O_{2.67}$ at room temperature (127).

room-temperature phase diagram of the ternary U-Pu-O system (Fig. 9) is characterized by four single-phase regions (126–129): orthorhombic U_3O_8; a cubic fluorite phase, AnO_{2+x}, which occupies the largest area of the single-phase region; a cubic superstructure, An_4O_9; and a face-centered cubic C-An_2O_3 phase. The maximum amount of plutonium in the U_3O_8 phase corresponds to a Pu:(U + Pu) ratio of 0.06 at 1000°C and 0.02 at 1400°C. The fluorite phase $(U,Pu)O_{2\mp x}$ may be hyperstoichiometric, stoichiometric, or substoichiometric with regard to the O:(U + Pu) ratio. Oxidation of $(U,Pu)O_2$ mixtures yields one- or two-phase products, depending on conditions (130). In the hyperstoichiometric fluorite phase $(U,Pu)O_{2+x}$, only U is oxidized to U(>IV). At room temperature, for a ratio Pu:(U + Pu) $\leq$0.30 and for O:(U + Pu) $\leq$2.20, a two-phase region $An_4O_9 + AnO_{2+x}$ is observed. The An_4O_9 phase exists in the range 2.20 $\leq$O: (U + Pu) $\leq$2.27. The oxidation of $(U,Pu)O_2$ at 600°C yields a metastable U_3O_7 type phase for Pu:(U + Pu) $<$0.25 and O:(U + Pu) = 2.28.

The thermophysical properties of mixed uranium–plutonium oxide phases have been studied in some detail. The data available in the open literature have been critically reviewed by Fink (131), and by Carbajo et al. (132). The density of $(U,Pu)O_2$ is slightly higher than of UO_2 and decreases with temperature due to thermal expansion. At low burnup, the density increases by densification, and at higher burnup, the density decreases due to swelling (132). The thermal conductivity of MOX fuels decreases with temperature up to approximately 2000 K and then increases with temperature. The addition of PuO_2 to the fuel, increasing porosities, and burnup also reduce the thermal conductivity. The melting point of $(U,Pu)O_2$ solid solution is found at temperatures between that of pure UO_2 (2730–2876°C) and pure PuO_2 (2238–2445°C) depending on the content of plutonium. In MOX fuel, the actual melting temperature decreases with increasing PuO_2 content of the fuel and with burnup (132).

The major technical challenge in preparing $(U,Pu)O_2$ fuels is to produce a product with the maximum degree of homogeneity. Hundreds of tons of MOX fuel have been produced using two main routes: (*1*) comilling of UO_2 and PuO_2 and (*2*) coprecipitation of UO_2 and PuO_2. Once the $(U,Pu)O_2$ material is formed, both processes entail mixing, pressing, sintering, and grinding operations (100, 133–135). Comilling generally involves mechanical grinding of UO_2 and PuO_2 powders followed by a granulation step before pressing into pellets. This process

has been employed extensively at the CEA (Commissariat à l'Energie Atomique) plant in Cadarache, France. An alternative comilling approach practiced at the French MELOX plant is referred to as the micronized master blend (MIMAS) process. In this process, plutonium and uranium oxides are mixed into a master blend that is 30% PuO_2, homogenized, micronized in a dry ball mill, then blended with free-flowing UO_2 powder to achieve the desired plutonium enrichment, and then pellitized (100,133,134). The main precipitation process is the ammonium–uranyl–plutonyl–carbonate process (AUPuC), in which a mixed uranyl/plutonyl nitrate solution (<40% Pu) is dosed into an aqueous solution along with gaseous NH_3 and CO_2 to generate an ammonium–uranyl–plutonyl–carbonate salt (AUPuC) of formula $[NH_4]_4[(U,Pu)O_2(CO_3)_3]$. The AUPuC precipitates as a coarse green crystalline product. These crystals are calcined into a $(U,Pu)O_2$ powder by firing at 800°C under a reducing atmosphere of N_2/H_2. The resulting $(U,Pu)O_2$ shows good flowability and sinterability (100).

Triuranium octaoxide, U_3O_8 [1344-59-8], is a greenish black material that is also a constituent of pitchblende. This complex has been identified with several different oxygen deficiencies, depending mostly on the temperature and partial pressure of O_2 used in the preparation. From 900°C to 1500°C, the oxide decomposes prior to melting or subliming to form gaseous UO_3. The material is paramagnetic and EPR-active with a room temperature μ_{eff} of $1.32\mu_B$. XPS studies of U_3O_8 have indicated the presence of two valences, U(IV) and U(VI), in a 1:2 ratio (136). The density of the stoichiometric complex has been found to range from 8.16 to 8.41 g/cm^3. This density for U_3O_8 is significantly smaller than that of UO_2, a property that is problematic for nuclear fuel cells (*vide infra*). The preparation of U_3O_8 has been accomplished by a variety of means, including thermal decomposition of $(NH_4)_2U_4O_{13}$ [129002-73-9], $UO_4 \cdot x\,H_2O$ [12036-71-4], and $UO_2(NO_3)_2 \cdot 6\,H_2O$ [10102-06-4] at 600°C, the oxidation of UO_2 under streaming O_2 at 600°C (eq. 22), and the reduction of UO_3 at high temperatures (600–800°C) under streaming oxygen (eq. 23). Oxidation of UO_2 at 800°C in air leads to the α-form, which converts to β-U_3O_8 at 1350°C in air or oxygen followed by slow cooling to room temperature. One problem associated with synthesizing stoichiometric U_3O_8 is the propensity of oxygen loss at elevated temperatures (500–700°C), producing oxygen-deficient complexes U_3O_{8-x}. Depending on the partial pressure of O_2, the oxygen deficiency can go as low as $UO_{2.62}$. In addition to the different U/O ratios, U_3O_8 has been found to exist in at least five different crystalline modifications. In the α-form (orthorhombic, *C2mm*), the uranium atom displays a pentagonal biypyramidal coordination geometry, whereas β-U_3O_8 (orthorhombic, *Cmcm*) has two different coordination environments, one pseudo-octahedral and one pentagonal biypyramidal. A full description of the anionic sheets has been reported in Refs. 137 and 138.

Industrially, U_3O_8 has been shown to be active in the decomposition of organics, including benzene and butanes (139,140), and as supports for methane steam-reforming catalysts (141). In the nuclear fuel industry, U_3O_8 is an oxidation product of UO_2 and, thus, a major component of spent fuel rods (142,143). As mentioned, U_3O_8 is less dense than UO_2, and as a result, the production of U_3O_8 in nuclear fuel can lead to the destruction of the UO_2 pellet by pulverization. It is for this reason that many studies of the formation kinetics (142) and the thermal and mechanical properties of U_3O_8 have been reported. Triuranium octaoxide is

not always a destructive force in the fuel cycle, and it is actually useful in the initial production of UO_2 pellets for fuel (144), of MOX pellets (145), as well as of dispersive nuclear fuel itself (146).

Uranium trioxide, UO_3 [1344-58-7], is a versatile solid, which also has important applications in the nuclear fuel cycle. The trioxide has been isolated in six well-defined stoichiometric modifications as well as a hypo-stoichiometric modification, $UO_{2.9}$. Similar to U_3O_8, the trioxide decomposes into lower oxides prior to melting or subliming. Even though UO_3 is formally U(VI), a small temperature-dependent paramagnetism exists with molar magnetic susceptibility values ranging from 128 to 157×10^{-6} cm^3/mol. A general trend has been observed for the densities of uranium oxides: an inverse proportionality between the O/U ratio and the density of the material. The trioxide does not deviate from this trend with density values ranging from 6.99 to 8.54 g/cm^3, depending on the modification. The preparation of UO_3 has been accomplished by a variety of means. Industrially, the complex is prepared by three main routes: thermal decomposition of $UO_4 \cdot x\,H_2O$ [12036-71-4], $(NH_4)_2U_4O_{13}$ [128085-85-8], or $UO_2(NO_3)_2 \cdot 6\,H_2O$ [10102-06-4] in air or O_2 at temperatures between 400°C and 550°C. For the latter complex, the techniques used to accomplish the decomposition include batch decomposition, continuous stirred-bed, fluidized bed, and spray decomposition. The trioxide can also be synthesized by the oxidation of lower oxides, UI_3 [13775-18-3] (low temp), UI_4 [13470-22-9] (low temp) (147), UC [12070-09-6], or UN [25658-43-9] (148) with O_2 and by the calcination of $(NH_4)_4UO_2(CO_3)_3$ [17872-00-3] (149,150). At 650°C and 40 atm O_2, all phases of UO_3 convert to the γ-phase.

As mentioned, uranium trioxide exists in six well-defined modifications with colors ranging from yellow to brick-red. They are, α-brown, hexagonal; β-orange, monoclinic; γ-yellow, rhombic; δ-red, cubic; ε-brick red, triclinic; and η-rhombic. Of these phases, the γ-phase has been found to be the most stable; however, other phases, especially α and β, are also frequently used and studied. The structure of the α-modification is based on sheets of hexagons, whereas the β-, γ-, and δ-modifications contain an infinite framework. All of these topologies have been fully described (137,138). The most characteristic feature of solid U(VI) oxides is the presence of the linear UO_2^{2+} groups that contain strong covalent bonds with short distances of 1.7–1.9 Å. For comparison, U–O bond distances in the equatorial plane around the U atom are between 2.1 and 2.5 Å.

The most important role of UO_3 is in the production of UF_4 [10049-14-6] and UF_6 [7783-81-5], which is used in the isotopic enrichment of uranium for use in nuclear fuels (151–153). The trioxide also plays a part in the production of UO_2 for fuel pellets (154). In addition to these important synthetic applications, microspheres of UO_3 can themselves be used as nuclear fuel. Fabrication of UO_3 microspheres has been accomplished using sol-gel or internal gelation processes (19,155–157). Finally, UO_3 is also a support for destructive oxidation catalysts of organics (158,159).

Nitrides. Uranium nitrides are well known and have applicability in the nuclear fuel cycle. There are three well-characterized nitrides of exact stoichiometry, UN [25658-43-9], U_2N_3 [12033-85-1], and U_4N_7 [12266-20-5], although UN_2 [12033-89-9] has also been reported. In addition to these, the nonstoichiometric complexes, U_2N_{3+x}, where the N/U ratio ranges from 1.64 to 1.84 have

been identified (160). The brown mononitride, which is the only nitride complex stable above 1300°C, melts at 2600°C. Uranium mononitride shows the highest density of the nitrides with a density of 14.31 g/cm^3. The magnetic properties of the nitrides are extremely dependent on the phase and stoichiometry of the complex. The mononitride, α-U_2N_3, and β-U_2N_3 are paramagnetic at room temperature, with the former two becoming anti-ferromagnetic and the latter becoming ferromagnetic at low temperatures. Classically, the different nitrides have been prepared from direct interaction of the elements under the appropriate conditions. Recently, several alternatives to this preparation have been investigated, including uranium metal under static NH_3 at 300–350°C to yield U_2N_3 (161,162) uranium metal or uranium carbides with NH_3 or N_2 at 600–900°C to produce U_2N_{3+x} (163,164), uranium carbide fuels reacted with N_2/H_2 to form UN (165), and a self-propagating metathetical reaction, thermolysis at 500°C of UCl_4 [10026-10-5] with Li_3N, yielding UN and U_2N_3 (166,167). The structures of some nitrides have been determined. The mononitride has a face-centered cubic NaCl-type structure. The sesquinitride complex has two modifications: The α-phase is found with a body-centered cubic Mn_2O_3-type structure (160), whereas the high-temperature β-phase crystallizes in a hexagonal Mn_2O_3-type structure. The substoichiometric nitride complex, $UN_{1.9}$, crystallizes in the CaF_2-type lattice.

Uranium and mixed uranium–plutonium nitrides have a potential use as nuclear fuels for lead cooled fast reactors (168–171). Reactors of this type have been proposed for use in deep sea research vehicles (168). However, similar to the oxides, for these materials to be useful as fuels, the nitrides must have an appropriate size and shape, ie, spheres. Microspheres of uranium nitrides have been recently fabricated by internal gelation and carbothermic reduction (172,173). Another use for uranium nitrides is as a catalyst for the cracking of NH_3 at 550°C, which results in high yields of H_2 (174).

Carbides. Uranium carbides, UC [12070-09-6], U_2C_3 [12076-62-9], and UC_2 [12071-33-9] are all dark gray solids with a metallic luster. In addition to these binary materials, numerous mixed uranium–plutonium and uranium–transition metal carbides have been prepared and are mainly used in nuclear fuel. The melting points of UC and U_2C_3 are 2400°C and 2417°C, respectively, and the dicarbide melts at 2475°C and boils at 4370°C (760 mm Hg). The monocarbide is the most dense of the carbide series, with a room temperature density of 13.60 g/cm^3, whereas U_2C_3 and UC_2 have densities of 12.85 g/cm^3 and 11.69 g/cm^3, respectively. The magnetic properties of the carbides are extremely composition dependent. All three materials are paramagnetic at room temperature, with U_2C_3 becoming antiferromagnetic at low temperatures. The typical techniques involved in the synthesis of the carbides include the reaction of carbon or hydrocarbons with uranium metal or UH_3 [13598-56-6] at elevated temperature, precipitation from metal melts, and reduction of uranium halides. Recent techniques for the synthesis include the carbothermic reduction of UO_2 (175) and the direct interaction of uranium and carbon under highly exothermic conditions (176). The crystal structure of UC is a face-centered cubic NaCl-type lattice, identical to that of UN [25658-43-9]. The sesquicarbide crystallized with a body-centered cubic Pu_2C_3 type structure, whereas two modifications exist for UC_2. The α-phase of UC_2 is a body-centered tetragonal CaC_2-type structure and the β-phase crystallizes in a face-centered cubic KCN-type lattice. It should

also be noted that the α-modification undergoes a phase transition from a tetragonal to a hexagonal lattice under increased pressure, ie, 17.6 GPa.

As stated, uranium carbides are used as nuclear fuel (177). Two of the typical reactors fueled by uranium and mixed-metal carbides are thermionic, which are continually being developed for space power and propulsion systems, and high-temperature gas cooled reactors (178,179). To be used as nuclear fuel, carbide microspheres are required. These microspheres have been fabricated by a carbothermic reduction of UO_3 and elemental carbon to form UC (180,181). In addition to these uses, the carbides are also precursors for uranium nitride based fuels (see Nitrides in Section 11.1).

Oxo Ion Salts. Salts of oxo anions, such as nitrate, sulfate, perchlorate, iodate, hydroxide, carbonate, phosphate, and oxalate, are very important for the separation and reprocessing of uranium, and hydroxide, carbonate, and phosphate ions are important for the chemical behavior of uranium in the environment (182–184). For detailed information on the formation and stability of uranium complexes in solution and solid phase we refer to the extensive reviews and compilations in Refs. 1, 185, and 186.

Nitrate complexes are very weak, and the determination of the formation constants for aqueous nitrate solution species is extremely difficult. There seems to be reliable thermodynamic data only for the formation of $UO_2(NO_3)^+$ (1,185). Although the determination of the formation constants is complicated, there is little doubt that under high nitric acid conditions, $UO_2(NO_3)_2$ and, perhaps, $UO_2(NO_3)_3^-$ are formed, at least to some extent. Solid uranyl nitrate, $UO_2(NO_3)_2 \cdot x\,H_2O$ [10102-06-4], is obtained as the orthorhombic hexahydrate from dilute nitric acid solutions and as the trihydrate from concentrated acid. The melting point of the hexahydrate is at 118°C. Uranyl nitrate plays an important role in the reprocessing of uranium in spent fuel and in uranium extraction from aqueous solutions. The preparation of the anhydrous uranyl nitrate by dehydration is extremely difficult. Several molecular structures of uranyl nitrate complexes have been reported, and all show the common formula unit of $UO_2(NO_3)_2(OH_2)_2$ with a local hexagonal bipyramidal coordination about the central uranyl ion (**1**) (187,188). The technologically important $UO_2(NO_3)_2(TBP)_2$ complex also displays *trans*-nitrate ligands with the TBP ligands occupying the same coordination sides as H_2O in (**1**).

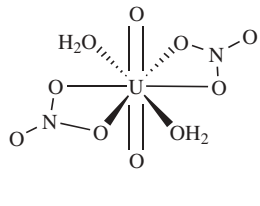

(**1**)

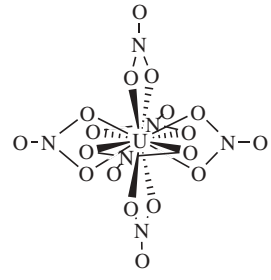

(**2**)

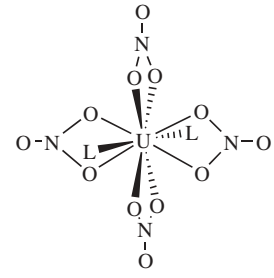

(**3**)

There is reasonable evidence for the formation of aqueous U(IV) nitrate complexes of general formula $U(NO_3)_n^{4-n}$, where $n = 1–4$. However, due to the inherent weakness of the complexes, quantitative data on the formation

constants is only available for $U(NO_3)^{3+}$ and $U(NO_3)_2{}^{2+}$ (189). No neutral U(IV) nitrates have been obtained from aqueous solution, but several anionic complexes of general formula $M_2[U(NO_3)_6]$, where M = NH_4, Rb, Cs, and $M[U(NO_3)_6]\cdot 8H_2O$, where M = Mg and Zn have been isolated and characterized. These solids contain the 12 coordinate anionic U(IV) center shown in **2** (190). Neutral, U(IV) nitrate complexes of formula $U(NO_3)_4L_2$ (**3**) [L = $OP(C_6H_5)_3$, $OP(NC_4H_8)_3$] have also been isolated and structurally characterized (191).

The aqueous uranyl sulfate system has been extensively studied, and complexes of formula $UO_2(SO_4)_n^{2n-2}$, where $n = 0$, 1, and 2, are likely to be formed in solution. Quantitative data only exist for the formation of complexes with $n = 0$ and 1 (189). $UO_2(SO_4)\cdot x\,H_2O$ ($x = 1$, 2, 2.5, 3, or 4) can be precipitated from aqueous solutions as the trihydrate. The monohydrate and the anhydrous salt can be obtained by dehydration of the trihydrate. The fluorosulfate, $UO_2(SO_3F)_2$ [75357-79-8], is obtained by treating $UO_2(MeCO_2)_2$ [541-09-3] with HSO_3F (192). Many ternary U(VI) sulfates of the general formula $(M)_k(UO_2)_m(SO_4)_n\cdot x\,H_2O$, where M = monovalent cation, ie, NH_4 or alkali metals, $M(UO_2)_m(SO_4)_n\cdot x\,H_2O$, where M = bivalent cation, such as alkaline earth or transition metals (Mn, Cd, Hg), have been reported. A layered structure is observed for $(NH_4)_2UO_2(SO_4)_2\cdot 2\,H_2O$ O [12357-71-0] with local pentagonal biypyramidal coordination around the U atom and bridging sulfate groups joining the uranyl polyhedra (193). In $K_4UO_2(SO_4)_3$ [69567-87-9], each uranium in the pentagonal bipyramid is coordinated to five oxygen atoms from four sulfate groups in the equatorial plane (194).

The U(IV) sulfate system has also been studied in strong acid solutions, and quantitative data are only available for $U(SO_4)^{2+}$ and $U(SO_4)_2$ (189). Solids of composition $U(SO_4)_2\cdot 8\,H_2O$ [14355-39-6] and $U(SO_4)_2\cdot 4\,H_2O$ can be precipitated from weakly and concentrated sulfuric acid solution, respectively. In neutral solution, the basic salt, $UOSO_4\cdot 2\,H_2O$ [18902-45-9], is formed. The octahydrate loses four hydration waters at 70°C, and the remaining four molecules of water can be removed at temperatures over 400°C. In $U(SO_4)_2\cdot 4\,H_2O$, the uranium atoms are surrounded by a square antiprism of O atoms, with each U bonded to four molecules of water and linked by bridging sulfate groups to other uranium atoms (195). Several U(IV) fluorosulfates have been obtained involving mono- and bidentate SO_3F^- groups as reported for $U(SO_3F)_4$ (192).

Crystals of uranyl perchlorate, $UO_2(ClO_4)_2\cdot x\,H_2O$ [13093-00-0], have been obtained with six and seven hydration water molecules. The uranyl ion is coordinated with five water molecules (**4**) in the equatorial plane with a U-O(aquo) distance of 2.45 Å. The perchlorate anion does not complex the uranyl center. The unit cells contain two $[ClO_4]^-$ and one or two molecules of hydration water linked by hydrogen bonding (196).

Peroxide complexes of actinides have been of great importance due to the multiple uses of peroxide as a precipitating agent and to adjust oxidation states. A crystalline uranyl peroxide, $UO_4\cdot 4H_2O$ (197), has been obtained. In the layered structure of $Na_4[UO_2(O_2)_3]\cdot 9\,H_2O$, three peroxo groups are coordinated in the equatorial plane to the U(VI) center (198), whereas bridging peroxo groups create a one-dimensional structure in the peroxide mineral, $[UO_2(O_2)(H_2O)_2](H_2O)_2$ (199). In the presence of carbonate, a molecular structure of a mixed U(VI) peroxo carbonate can be crystallized with tetraanionic, $UO_2(O_2)(CO_3)_2^{4-}$, units that contain one side-on coordinated peroxo group.

Hydroxides. The hydrolysis of uranium has been recently reviewed (1,186,189); yet as noted in these compilations, studies are ongoing to continue identifying all of the numerous solution species and solid phases. U(IV) and U(VI) are the most stable oxidation states of uranium under most conditions. The very "hard" uranium(IV) ion hydrolyzes even in fairly strong acid (~0.1 M), and the hydrolysis is complicated by the precipitation of insoluble hydroxides or oxides. There is reasonably good experimental evidence for the formation of the initial hydrolysis product, $U(OH)^{3+}$; however, there is no direct evidence for other hydrolysis products such as $U(OH)_2^{2+}$ or $U(OH)_3^+$. There is a substantial amount of data, particularly from solubility experiments, which is consistent with the neutral species $U(OH)_4$ (189). A recent study under reducing conditions in NaCl solution confirms its importance and reports that it is monomeric (200). Solubility studies indicate that the anionic species $U(OH)_5^-$, if it exists, is only of minor importance (201). There is limited evidence for polymeric species such as $U_6(OH)_{15}^{9+}$ (189).

The hydrolysis of the uranyl(VI) ion, UO_2^{2+}, has been studied extensively and begins at about pH = 3. In solutions containing less than 10^{-4} M uranium, the first hydrolysis product is the monomeric $UO_2(OH)^+$, as confirmed using time-resolved laser-induced fluorescence. At higher uranium concentrations, it is accepted that polymeric U(VI) species are predominant in solution, and the first hydrolysis product is then the dimer, $(UO_2)_2(OH)_2^{2+}$ (189,202). Further hydrolysis products include the trimeric uranyl hydroxide complexes $(UO_2)_3(OH)_4^{2+}$ and $(UO_2)_3(OH)_5^+$ (189). At higher pH, hydrous uranyl hydroxide precipitate is the stable species (203). In studying the sol-gel UO_2 ceramic fuel process, ^{17}O NMR was used to observe the formation of a trimeric hydrolysis product, $[(UO_2)_3(\mu_3\text{-}O)(\mu_2\text{-}OH)_3]^+$, which then condenses into polymeric UO_2O_6/3 layers of a gel based on the hexagonal structure of α-$UO_2(OH)_2$. In the same process, there is a second pathway where a uranyl derivative is treated with excess hydroxide in the absence of metal or H-bonding ammonium cations that form insoluble solid uranates. Condensation of the resulting solution of $UO_2(OH)_n^{2-n}$ anions can then lead to a similar UO_2O_6/3 gel (204,205).

A study performed in the nonstandard electrolyte, tetramethylammonium trifluoromethanesulfonate, provided data on additional species, $(UO_2)_3(OH)_7^-$, $(UO_2)_3(OH)_8^{2-}$, and $(UO_2)_3(OH)_{10}^{4-}$ (206). Solid-state structures of uranyl hydroxides are limited, but they are known for the important cations of formula $(UO_2)_2(OH)_2(OH_2)_6^{2+}$ (**5**) (207) and $(UO_2)_3O(OH)_3(OH_2)_6^+$ (**6**) (208).

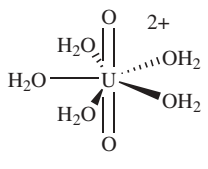

(**4**)

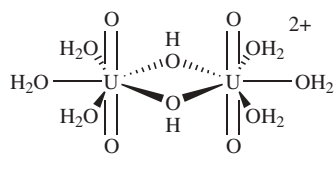

(**5**)

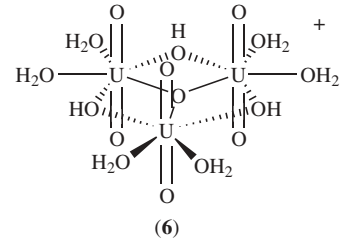

(**6**)

Carbonates. Actinide carbonate complexes are of interest not only because of their fundamental chemistry and environmental behavior (183) but

also because of extensive industrial applications, primarily in uranium recovery from ores (see RECOVERY FROM ORES, LEACHING) and nuclear fuel reprocessing.

The aqueous U(VI) carbonate system has been very thoroughly studied, and there is little doubt about the compositions of the three monomeric complexes $UO_2(CO_3)$, $UO_2(CO_3)_2^{2-}$, and $UO_2(CO_3)_3^{4-}$ present under the appropriate conditions (189). There is also a great deal of evidence from emf, solubility, and spectroscopic data supporting the existence of polymeric solution species of formulas $(UO_2)_3(CO_3)_6^{6-}$, $(UO_2)_2(CO_3)(OH)_3^-$, $(UO_2)_3O(OH)_2(HCO_3)^+$, and $(UO_2)_{11}(CO_3)_6(OH)_{12}^{2-}$, which form only under conditions of high metal ion concentration or high ionic strength (189,209). Determining the formation constant for the triscarbonato uranyl monomer, $UO_2(CO_3)_3^{4-}$, was complicated because at higher concentrations this species is in equilibrium with the hexakiscarbonato uranyl trimer, $(UO_2)_3(CO_3)_6^{6-}$ rather than the mononuclear $UO_2(CO_3)_2^{2-}$. Bidoglio et al. used thermal lensing spectroscopy (which is sensitive enough to allow the study of relatively dilute solutions where the trimer is not favored) to determine the equilibrium constant for the addition of one carbonate to $UO_2(CO_3)_2^{2-}$ to form $UO_2(CO_3)_3^{4-}$ and used this value to calculate the formation constant, β_{13} (210).

The trimetallic uranyl cluster $(UO_2)_3(CO_3)_6^{6-}$ has been the subject of a good deal of study, including nmr spectroscopy (211–213), solution x-ray diffraction (211), potentiometric titration (209,214,215), single-crystal x-ray diffraction (212), and exafs spectroscopy in both the solid and the solution states (212). The data in this area have consistently led to the proposal and recent verification of a trimeric $(UO_2)_3(CO_3)_6^{6-}$ cluster (**7**).

The known uranium(VI) carbonate solids have empirical formulas, $UO_2(CO_3)$, $M_2UO_2(CO_3)_2$, and $M_4UO_2(CO_3)_3$. The solid of composition $UO_2(CO_3)$ is a well-known mineral, rutherfordine, and its structure has been determined from crystals of both the natural mineral and the synthetic samples. Rutherfordine is a layered solid in which the local coordination environment of the uranyl ion consists of a hexagonal bipyramidal arrangement of oxygen atoms, with the uranyl units perpendicular to the orthorhombic plane. Each uranium atom forms six equatorial bonds with the oxygen atoms of four carbonate ligands, two in a bidentate manner and two in a monodentate manner.

Biscarbonato complexes of uranium(VI) are well established in solution (189), and there are many reports dating from the late 1940s through the 1960s of solid phases with the general stoichiometry $M_2UO_2(CO_3)_2$, where M is a monovalent cation (Na^+, K^+, Rb^+, Cs^+, NH_4^+, etc). A summary of the preparative details is given by Chernyaev et al. (216), and a listing of the compounds is given by Bagnall (217). A careful examination of the more recent literature and a detailed understanding of the solution chemistry suggests that the claims of some of these early reports on solid $M_2UO_2(CO_3)_2$ compounds should be reinterpreted. It is now known that solids of general composition $M_2UO_2(CO_3)_2$ form trimetallic clusters of molecular formula $M_6(UO_2)_3(CO_3)_6$. The trimetallic cluster forms in solution when high metal ion concentrations are present, and these solutions are relatively unstable unless the pH is kept near 6 and a CO_2 atmosphere is maintained over the solution. A recent single crystal x-ray diffraction study of $[C(NH_2)_3]_6[(UO_2)_3(CO_3)_6] \cdot 6.5\ H_2O$ revealed that the central $(UO_2)_3(CO_3)_6^{6-}$ anion (**7**) possesses a D_{3h} planar structure in which all six carbonate ligands and the three uranium atoms lie within the molecular plane (212). The

six uranyl oxygen atoms are perpendicular to the plane, with three above and three below the plane. The local coordination geometry about each uranium is hexagonal bipyramidal.

Without question, the triscarbonato solids, $M_4UO_2(CO_3)_3$ (M = monovalent cation), are the most thoroughly studied uranium(VI) carbonate solids. These solid phases are generally prepared by evaporation of an aqueous solution of the components or by precipitation of the UO_2^{2+} ion with an excess of carbonate. Some of these salts can be further purified by dissolution in water and recrystallization via evaporation. Single-crystal x-ray diffraction studies have been reported for many uranyl complexes. Detailed lists of complexes that have been characterized by x-ray diffraction are given by Bagnall (217) and Grenthe et al. (1). In the solid state, all monomeric $M_4AnO_2(CO_3)_3$ complexes show the same basic structural features: a hexagonal bipyramidal coordination geometry where three bidentate carbonate ligands lie in a hexagonal plane (**8**), and the *trans*-oxo ligands occupy coordination sites above and below the plane. Typical metrical parameters for these structures have An=O bond distances within the relatively narrow range of 1.7–1.9 Å and An–O bonds to the carbonate ligands in the range 2.4–2.6 Å.

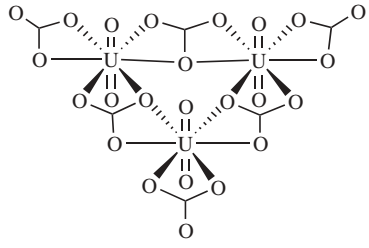

(**7**)

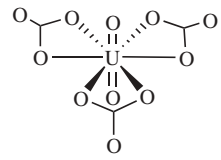

(**8**)

Although there is a great deal of qualitative information regarding anionic carbonato complexes of the tetravalent actinides, reliable quantitative data are rare (189). Quantitative data exist only for $U(CO_3)_5^{6-}$ and $U(CO_3)_4^{4-}$ (218,219). Tetracarbonato uranium salts of composition $[C(NH_2)_3]_4[U(CO_3)_4]$ and $[C(NH_2)_3]_3\cdot(NH_4)[U(CO_3)_4]$ have been reported (220). The pentacarbonato salts of formula $M_6U(CO_3)_5\cdot n\,H_2O$ ($M_6 = Na_6$, K_6, Tl_6, $[Co(NH_3)_6]_2$, $[C(NH_2)_3]_3[(NH_4)]_3$, $[C(NH_2)_3]_6$; $n = 4–12$) have all been reported (216,221,222). The sodium salt can be prepared by chemical or electrochemical reduction of $Na_4UO_2(CO_3)_3$, followed by the addition of Na_2CO_3 to form a precipitate. The potassium salt, $K_6U(CO_3)_5\cdot 6H_2O$ can be prepared by dissolution of freshly prepared U(IV) hydroxide in K_2CO_3 solution in the presence of CO_2; and the guanidinium salt can be prepared by the addition of guanidinium carbonate to a warm $U(SO_4)_2$ solution, followed by cooling (220).

Phosphates. Inorganic phosphate ligands are important with respect to the behavior of uranium in the environment and as potential waste forms. There have been several experimental studies to determine the equilibrium constants in the uranium–phosphoric acid system, but they have been complicated by the formation of relatively insoluble solid phases and the formation of ternary uranium complexes in solution (189). In acidic solution (hydrogen ion

concentration range 0.25–2.00M), H_3PO_4 and $H_2PO_4^-$ are potential ligands, whereas in neutral to basic solution, HPO_4^{2-} and PO_4^{3-} ligands are predominant. While numerous U(VI) phosphate complexes have been identified and their formation constants determined, relatively little thermodynamic data have been recommended with confidence. There is good evidence for the formation of $UO_2(PO_4)^-$, $UO_2(HPO_4)$, $UO_2(H_2PO_4)^+$, $UO_2(H_2PO_4)_2$, $UO_2(H_3PO_4)^{2+}$, and $UO_2(H_3PO_4)(H_2PO_4)^+$ complexes in solution. There are only a few studies on the U(IV) phosphate system, and recent reviews on the thermodynamics of uranium have not recommended any thermodynamic data for the U(IV) phosphate system (189).

Solid uranium phosphate complexes have been reported for the IV and VI oxidation states, as well as for compounds containing mixed oxidation states of U(IV) and U(VI). Only a few solid-state structures of U(IV) phosphates have been reported, including the metaphosphate $U(PO_3)_4$, the pyrophosphate $U(P_2O_7)$, and the orthophosphate, $CaU(PO_4)_2$. The crystal structure of orthorhombic $CaU(PO_4)_2$ is similar to anhydrite (223). Compounds of the general formula $MU_2(PO_4)_3$ have been reported for M = Li, Na, and K, but they could not be obtained with the larger Rb and Cs ions (224). In the solid state, uranium(IV) forms the triclinic metaphosphate, $U(PO_3)_4$. Each uranium atom is eight-coordinate with square antiprismatic UO_8 units bridged by $(P_4O_{12})^{4-}$ rings (225,226). The pyrophosphate of uranium(IV) belongs to the family of ZrP_2O_7-type structures (227). The dissolution of U chips in HCl and H_3PO_4 results in the formation of orthorhombic $U_2O(PO_4)_2$ (228). Each uranium atom is 7-coordinate, with a local edge-sharing pentagonal bipyramidal coordination geometry, and linear U-O-U and bridging bidentate phosphate units making up a three-dimensional structure. Pyrophosphates of composition $U_2O_3P_2O_7$ and $U_3O_5P_2O_7$ have been synthesized containing uranium in oxidation states IV and VI in a ratio 1:1 and 2:1, respectively. $U_2O_3P_2O_7$ melts at 1442°C, is stable under oxic conditions up to 1250°C, but it decomposes in nitrogen and argon at 950°C. $U_3O_5P_2O_7$ oxidizes in air above 500°C to form $(UO_2)_3(PO_4)_2$ at 950°C (229). $M_2UO_2P_2O_7$, with M = alkali, have been synthesized by heating uranyl nitrate in the presence of alkali metal pyrophosphates and ammonium dihydrogenphosphate. The new mixed valence $U(UO_2)(PO_4)_2$ has been synthesized and characterized spectroscopically showing the absence of pyrophosphate and the existence of the dioxo cation unit, UO_2^{2+}, as one of the two independent U atoms. Bidentate phosphates ligands connect the chains generating a three-dimensional network (230).

Uranium(VI) phosphates have been widely investigated and can be divided in several structure types: orthophosphates $M(UO_2)_n(PO_4)_m \cdot x\,H_2O$, hydrogenphosphates $M(UO_2)_n(H_kPO_4)_m \cdot x\,H_2O$, pyrophosphates $U_mO_nP_2O_7$, metaphosphates $(UO_2)_n(PO_3)_m \cdot x\,H_2O$, and poly phosphates $(UO_2)_n(P_aO_b)_m \cdot x\,H_2O$ (1).

A few uranyl metaphosphates have been described in the literature. $UO_2(PO_3)_2$ is formed in 85% H_3PO_4 at 300–350°C or by thermal decomposition of $UO_2(H_2PO_4)_2$ at 800 to 850°C. At 600–700°C, $UO_2(PO_3)_2$ forms uranium(IV) pyrophosphate, UP_2O_7. Uranium(VI) orthophosphates of the general formula $M(UO_2)_n(PO_4)_m \cdot xH_2O$, where $M = H^+$, M^+, or M^{2+}, are readily prepared by reaction of uranyl nitrates or perchlorates with phosphoric acid. Several hydrates are known for the uranyl phosphates. Hydrogen uranyl phosphates readily exchange

the hydrogen with alkali or alkaline earth metals. Some of the latter compounds are identical with natural minerals. The tetrahydrate, $H(UO_2)(PO_4) \cdot 4\,H_2O$, is reported to form three different polymorphic modifications at room temperature (231). The geometry about the uranyl ion in $K_4(UO_2)(PO_4)_2$ is tetragonal bipyramidal with four oxygen atoms in the equatorial plane from four tetrahedral phosphate groups, making up a $[UO_2(PO_4)_2]_n^{4n-}$ layer (232). The neutral compound, $(UO_2)_3(PO_4)_2 \cdot x\,H_2O$, has been synthesized as a mono-, tetra-, and hexahydrate. $(UO_2)_3(PO_4)_2 \cdot 4.8\,H_2O$ was prepared by addition of 0.5M uranyl nitrate to 0.36M H_3PO_4 at 60°C and pH 1. Orthorhombic crystals formed with lower symmetry than the natural analog troegerite (233). The anhydrous salt can be obtained from the hydrates upon heating to 250–500°C. The tetrahydrate is the stable form under normal conditions and precipitates at U:PO_4^{3-} ratios $\leq$1:3. The hexahydrate has been found to precipitate from a solution low in phosphate (<0.014M).

The trihydrate of uranyl dihydrogenphosphate, $UO_2(H_2PO_4)_2 \cdot 3\,H_2O$, has been obtained from a suspension of $HUO_2PO_4 \cdot 4\,H_2O$ in 85% phosphoric acid after stirring for several days. Uranium(VI) polyphosphates, $(UO_2)_2(P_3O_{10})_2 \cdot x\,H_2O$, were obtained by precipitation of a uranyl solution with $Na_5P_3O_{10}$. The dodecahydrate and the hydrate with 21 hydration water molecules were precipitated from a solution 0.06–0.02M and 0.15–0.25M, respectively, in uranyl ion. The U(VI) ultraphosphate, $(UO_2)_2(P_6O_{17})_2$, was obtained from a phosphate melt with a P:U = ratio of 8:1 at 400–420°C.

Recently, novel three-dimensional frameworks of uranyl(VI) phosphates have been synthesized. Diethylhydroxyamine was used to synthesize the first three-dimensional organically templated open framework, $[(C_2H_5)_2NH_2]_2(UO_2)_5(PO_4)_4]$, where six $[UO_7]$ and six $[PO_4]$ polyhedra are linked to form open channels along the crystallographic a and c axis (234). Mixed gallium uranyl phosphates, $[Cs_4[(UO_2)_2(GaOH)_2(PO_4)_4] \cdot H_2O$ and $Cs[UO_2Ga(PO_4)_2]$, incorporate octahedral $[GaO_6]$ or tetrahedral $[GaO_4]$ units linked with bridging $[PO_4]$ tetrahedra and $[UO_7]$ units to form three-dimensional structures with ion exchange properties (235).

12. Coordination Complexes

The coordination chemistry of uranium continues to be of great interest, and it has expanded greatly during the last decades (236–238). Considered "hard" metal ions, U(III to VI) have the greatest affinity for "hard" donor atoms such as N, O, and the light halides. Tetravalent and hexavalent uranium coordination complexes are the most common; however, trivalent and pentavalent complexes have been identified with increasing frequency. As with all actinides, the ionic radius of any uranium ion is significantly larger compared with a transition metal ion in an identical oxidation state. The result of this increased ionic radius is an expansion of the possible coordination environments (3 to 14 coordinate) and electron counts (up to 24 electrons). The following sections provide some specific examples of uranium coordination complexes and are organized by the ligand type and metal oxidation state.

12.1. Nitrogen Donors. Numerous N-donating ligands have been complexed with uranium. Classic examples range from neutral mono/bi/poly-dentate

ligands, ie, ammonia, primary, secondary, and tertiary amines, alkyl/aryldiamines (en = ethylenediamine, 1,4-diaminobenzene), N-heterocycles (py = pyridine, bipy = bipyridine, terp = terpyridyl), nitriles (MeCN), to anionic amides [NEt_2^-, $N(SiMe_3)_2^-$], thiocyanates, and polypyrazolyl-borates. A complete listing of ligands can be found in the general references, Gmelin handbook and Comprehensive Coordination Chemistry.

Very few U(III) coordination complexes with neutral N-donor ligands have been identified due in part to the ease of oxidation; examples include $UX_3(NH_3)_n$ ($X = Cl$, $n = 1, 3$; $X = Br$, $n = 3, 4, 6$), UI_3py_4, $UI_3(tmed)_2$, and $UCl_3(MeCN)$ [27459-32-1]. A *tris*-silylamido complex, $U[N(SiMe_3)_2]_3$ [110970-66-6], has also been synthesized and shown to be a very useful starting material for the synthesis of other trivalent uranium compounds (237). Poly-pyrazol-1yl-borates of the form $U(HBpz_3)_mI_{3-m}(THF)_n$ ($m = 1$, $n = 2$ [159438-24-1]; $m = 2$, $n = 0$ [159438-25-2]) have been synthesized, which are also becoming useful synthons for stabilizing U(III) organometallic complexes (239).

N-donor coordination complexes of U(IV) are numerous and have been well characterized. Adducts of UX_4 (X = halogen, alkoxide) have been isolated with all of the ligand types described above. The most common coordination environments for U(IV) is 8 to 12, as exemplified by UX_4L_n [X = Cl, L = NH_3 ($n = 1$–10), en ($n = 4$), bipy ($n = 2$); X = Br, I, L = NH_3 ($n = 4$–6), 1,4-diaminobenzene ($n = 4$); X = alkyl, L = MeCN ($x = 4$)]. Lower coordination environments can be obtained by increasing the steric bulk of the anionic ligand, ie, $U(OR)_4(NH_3)_n$ (R = alkyl, aryl; $n = 1, 2$). Amido complexes of U(IV) are important starting materials due to their highly reactive nature toward insertion reactions and protonation. For example, $[U(NR_2)_4]_n$ (R = alkyl, aryl) undergoes insertion reactions with CO_2, COS, CS_2, and CSe_2 to form carbamate complexes and reacts with alcohols to form alkoxide complexes. A tripodal amido complex has been synthesized, $[UCl(N(CH_2CH_2NSiMe_3)_3)]_2$ [157342-43-3], with which numerous metathetical reactions may be performed (240). Polypyrazol-1-yl-borate complexes of uranium are important in stabilizing inorganic and organometallic uranium complexes. Examples of these include UCl_2L_2 (L = $HBPz_3$ [55914-06-2], Ph_2BPz_2 [60459-89-4], BPz_4 [60459-92-9]), and UL_4 (L = H_2BPz_2 [55914-08-4], $HBPz_3$ [55914-07-3]). Another N-donor ligand set that has been complexed to U(IV) are porphyrins yielding bis-porphyrin complexes, $U(P)_2$ (P = octaethylporphyrin [149214-28-8], and tetra-*p*-tolylporphyrin [514923-00-6]). These complexes are useful for studying the electronic structure and activities of interacting porphyrins (241).

As in the case of U(III), the coordination chemistry of U(V) N-donor complexes is relatively unexplored due to disproportionation, which yields U(IV) and U(VI) complexes. Typically, ammonia, secondary amines, pyridines, pyrazines, and nitrile adducts of $U(OR)_5$ and UX_5 have been isolated with coordination numbers ranging from 6 to 8. Examples of these complexes are given by the following: $U(OCH_2CF_3)_5(NH_3)_n$ ($n = 6$–12), U(O*t*-Bu)$_5$(py) [104577-09-5], [UCl_4 (bipy)]Cl [30370-04-8], and $UBr_5(MeCN)_n$ ($n = 2, 3$). Structural details of these complexes are scarce.

The majority of U(VI) coordination chemistry has been explored with the *trans*-dioxo uranyl cation, UO_2^{2+}. The simplest complexes are ammonia adducts, of importance due to the ease of their synthesis and their versatility as starting

materials for other complexes. Many of the ligand types mentioned in Section 12.1 have been complexed with U(VI) and usually have coordination numbers of either 6 or 8 resulting in an octahedral or hexagonal bipyramidal coordination environment. Examples include $UO_2X_2L_n$ (X = halide, OR, NO_3, RCO_2, L = NH_3, primary, secondary, and tertiary amines, py; $n = 2-4$), $UO_2(NO_3)_2L_n$ (L = en, diaminobenzene; $n = 1, 2$). The use of thiocyanates has lead to the isolation of typically 6 or 8 coordinate neutral and anionic species; ie, $[UO_2(NCS)_x]^{2-x} \cdot y\,H_2O$ ($x = 2-5$).

12.2. Phosphorous Donors. Phosphine coordination complexes of uranium are rare due to the preference of uranium for "hard" donor atoms. Most of the stable uranium–phosphine coordination complexes contain the chelating ligand 1,2-(bis-dimethylphosphino)ethane (dmpe), ie, $U(BH_4)_3$(dmpe) and UX_4(dmpe)$_2$ (X = Cl [80290-55-7], Br [80290-57-9], Me [80290-60-4]); however, complexes with monodentate phosphines, ie, PMe_3, have been identified. Uranium(V) phosphine complexes have been synthesized, using amido ligands with a phosphine appendage, such as $UCl_2[N(CH_2CH_2PPri_2)_2]_3$ [158845-39-7] (242,243). One of the first actinide complexes containing exclusively metal-phosphorous bonds was the phosphido complex, $U(PPP)_4$ [165825-64-9] (PPP = $P(CH_2CH_2PMe_2)_2$) (244). Its X-ray structural analysis indicated a distorted bicapped triganol prism with 3-3-electron donor phosphides and 1-1-electron phosphide, suggesting a formally 24-electron complex. Similar to the amido system, this phosphido compound is also reactive toward insertion reactions, especially with CO (244).

12.3. Oxygen Donors. A wide variety of O-donors have been used to complex uranium. The predominate oxidation states are IV and VI; however, complexes with U(III) and U(V) are also known. Most complexes have coordination numbers of 6 to 12, depending mostly on the steric bulk of the ancillary ligands. Due to the prevalence of O-donating ligands in natural systems, ie, aquo, hydroxo, carbonate, phosphates, carboxylates, and catecholates, understanding the complexation of uranium with these ligands is very important to environmental, waste processing and storage, and bioinorganic chemistry. Some other O-donating ligands, which have been studied, are crown ethers (245), Schiff bases (246,247), polyglycols, and cryptands (248). These ligands have been proposed as actinide sequestering agents (249). A complete listing of the O-donating ligands complexed with uranium can be found in the general references, Gmelin handbook, and Comprehensive Coordination Chemistry.

Oxygen-containing Organics. Neutral and anionic oxygen-containing organic molecules form a wide variety of complexes with uranium. Much of the recent work has focused on alkoxides (250), aryloxides, and carboxylates; complexes with alcohols, ethers, esters, ketones, aldehydes, ketoenolates, and carbamates are also well known.

Alkoxides and Aryloxides. The studies of uranium complexation with alkoxide and aryloxide ligands have focused on determining which ligand systems yield crystalline compounds and provide useful starting materials. Oligomerization in uranium alkoxide complexes, as well as many of their solution properties, are highly dependent on the steric requirements of the alkoxide ligands. In the case of the sterically demanding ligand O-2,6-t-$Bu_2C_6H_3$, monomeric U(O-2,6-t-$Bu_2C_6H_3)_4$ can be readily isolated (251). As the steric bulk of the

alkoxide ligand decreases, dimers, $U_2(O\text{-}t\text{-}Bu)_8(HO\text{-}t\text{-}Bu)$, $U_2(O\text{-}i\text{-}Pr)_{10}$, and trimers, $U_3O(O\text{-}t\text{-}Bu)_{10}$ are usually observed (250).

13. Halides

Uranium halide complexes can be found in all four of the available uranium oxidation states: III, IV, V, and VI. In general, fluoride ligands tend to favor higher oxidation states, and iodide ligands tend to favor the lower oxidation states. As a result of the important industrial applications of binary fluorides and chlorides (vide infra), the majority of the halide discussion will focus on the binary systems. A selected listing of physical constants for the binary uranium halides is provided in Table 8. Halide complexes are extremely useful as starting materials for coordination and organometallic complexes, ie, hydrocarbon-soluble $UX_m(THF)_n$ ($m = 3, 4, 5$). The oxohalide complexes of the form, UOX_n ($n = 2, 3$) and $[UO_2X_n]^{4-n}$ ($n = 1$ to 4), have been isolated and fully characterized. The latter U(VI) dioxohalide complexes have usually been isolated with ancillary ligands, ie, H_2O, phosphine oxides when $x < 4$. Mixed halide systems are also known, ie, UClBrI [84370-90-1]. Ternary uranium halides are well known and are usually isolated with alkali or alkaline-earth metal ions. These halide complexes can be described by the general formulas, M_xUF_y ($x = 1$, $y = 5, 6, 7$; $x = 2$, $y = 6, 7, 8$; $x = 3$, $y = 7, 8, 9$; $x = 4$, $y = 8$), M_xUCl_y ($x = 1$, $y = 6$; $x = 2$, $y = 5, 6, 7$; $x = 3$, $y = 6, 7, 8$), M_xUBr_y ($x = 1, 2$; $y = 6$), and MUI_6.

13.1. Fluorides. Uranium fluorides play an important role in the nuclear fuel cycle as well as in the production of uranium metal. The dark-purple UF_3 [13775-06-9] has been prepared by two different methods: The first involves a direct reaction of UF_4 [10049-14-6] and uranium metal under elevated temperatures, whereas the second consists of the reduction of UF_4 [10049-14-6] by UH_3 [13598-56-6]. The local coordination environment of uranium in the trifluoride is penta-capped trigonal prismatic with an 11-coordinate uranium atom. The trifluoride is insoluble in H_2O but is soluble in strong acids, ie, nitric, hot sulfuric, and perchloric.

The tetrafluoride, UF_4 [10049-14-6], is a green solid, which can be isolated with high purity and has industrially important properties, ie, high stability and low volatility. As a result of these properties, UF_4 is widely used as a starting

Table 8. **Physical Constants for Selected Uranium Halides**

Compound	Density (g/mL)	Melting point (°C)	Boiling point (°C)
UF_6	4.68	64.5–64.8	56.2^{765}
UF_4	6.70	960	
UF_3		decom. above 1000	
UCl_5	3.81	decom. above 300	
UCl_4	4.87	590	792^{760}
UCl_3	5.44	842	
UBr_4	5.35	516	792^{760}
UBr_3	6.53	730	volatile
UI_4	5.6	506	759^{760}

material in uranium production processes. The solid-state structure of the tetrafluoride indicates halogen-bridged polymers with the metal center in a distorted square antiprismatic geometry. The preparation of UF_4 has been accomplished by reaction of HF with UO_2 [1344-57-6] at elevated temperatures (eq. 12) or by electrolytic reduction of uranyl fluoride in aqueous HF. The latter process leads to a hydrated species, which may be dehydrated by heating under reduced pressure or flowing N_2. Another preparation of UF_4 is the direct fluorination of β-UO_3 [1344-58-7] at 753 K by flowing Freon-12. It has been found that impurities of nitrates or ammonium ions facilitate the conversion to the tetrafluoride (152). UF_4 is insoluble in dilute acids and bases, soluble in strong acids and bases, and very slightly soluble in cold H_2O.

Uranium pentafluoride, UF_5 [13775-07-0], has been isolated and characterized in two different modifications, α and β. The former is a grayish-white solid, which is synthesized from the interaction of UF_6 [7783-81-5] and HBr or by heating UF_4 [10049-14-6] and UF_6 to 80–100°C. The yellowish-white β-modification is obtained by reacting UF_4 and UF_6 at higher temperatures (150–200°C). The α-form consists of infinite chains of octahedral UF_6 units. The β-form has eight coordinate uranium atoms with the fluorides in a geometry between dodecahedral and square anti-prismatic.

Uranium hexafluoride, UF_6 [7783-81-5], is an extremely corrosive, colorless, crystalline solid, which sublimes with ease at room temperature and atmospheric pressure. The complex can be obtained via multiple routes, ie, fluorination of UF_4 [10049-14-6] with F_2, oxidation of UF_4 with O_2 (152), or fluorination of UO_3 [1344-58-7] by F_2. The hexafluoride is monomeric in nature having an octahedral geometry. Although soluble in H_2O, CCl_4, and other chlorinated hydrocarbons, UF_6 is insoluble in CS_2 and decomposes in alcohols and ethers. The importance of UF_6 in isotopic enrichment and the subsequent applications of uranium metal has been discussed (see ^{235}U ENRICHMENT).

13.2. Chlorides. The olive-green trichloride, UCl_3 [10025-93-1], has been synthesized by chlorination of UH_3 [13598-56-6] with HCl. This reaction is driven by the formation of gaseous H_2 as a reaction byproduct. The structure of the trichloride has been determined, and the central uranium atom possesses a nine-coordinate tricapped trigonal prismatic coordination geometry. UCl_3 is soluble in H_2O, methanol, and glacial acetic acid, but it is insoluble in ethers.

Uranium tetrachloride, UCl_4 [10026-10-5], has been prepared by reduction/chlorination of UO_3 [1344-58-7] with boiling hexachloropropene or by heating UO_2 [1344-57-6] under flowing CCl_4 or $SOCl_2$. The structure of the dark-green tetrachloride is identical to that of Th, Pa, and Np, which all show a dodecahedral geometry of the chlorine atoms about a central actinide metal atom. The tetrachloride is soluble in H_2O, alcohol, and acetic acid and insoluble in ether and chloroform. Industrially, the tetrachloride has been used as a charge for calutrons.

The reddish-brown pentachloride, UCl_5 [13470-21-8], has been prepared in a similar fashion to UCl_4 [10026-10-5] by reduction/chlorination of UO_3 [1344-58-7] under flowing CCl_4, but at a lower temperature. Another synthetic approach that has been used is the oxidation of UCl_4 by Cl_2. The pentachloride has been structurally characterized and consists of an edge-sharing bioctahedral dimer, U_2Cl_{10}.

The pentachloride decomposes in H_2O and acid, is soluble in anhydrous alcohols, and is insoluble in benzene and ethers.

The hexachloride, UCl_6 [13763-23-0], is best prepared by chlorination of UCl_4 [10026-10-5] with $SbCl_5$. An alternative preparative approach is the disproportionation UCl_5 [13470-21-8] to UCl_4 and UCl_6 under reduced pressure. The obvious disadvantage of the second method is contamination by UCl_4; however, sublimation offers a possible purification technique. Isostructural with the hexafluoride, the hexachloride is monomeric with an octahedral arrangement of the chlorine atoms around the uranium center.

13.3. Bromides and Iodides. The red-brown tribromide, UBr_3 [13470-19-4], and the black triiodide, UI_3 [13775-18-3], may both be prepared by direct interaction of the elements, ie, uranium metal with X_2 (X = Br, I). The tribromide has also been prepared by interaction of UH_3 and HBr, producing H_2 as a reaction product. The tribromide and triiodide complexes are both polymeric solids with a local bicapped trigonal prismatic coordination geometry. The tribromide is soluble in H_2O and decomposes in alcohols.

The best synthetic approach to isolate UBr_4 [13470-20-7] and UI_4 [13470-22-9] is by direct interaction of the elements by heating uranium turnings under flowing nitrogen/halogen gas. The tetrabromide is dark brown and hygroscopic. The black tetraiodide is unstable, undergoing reduction to UI_3 [13775-18-3] and I_2. Structural details of the tetrabromide and the tetraiodide are not available. The tetrabromide is soluble in H_2O and liq. NH_3, but it decomposes in alcohols, whereas the tetraiodide is soluble in cold H_2O and acetonitrile and decomposes in hot H_2O.

Uranium pentabromide, UBr_5 [13775-16-1], is unstable toward reduction, and the pentaiodide is unknown. Two synthetic methods used for the production of UBr_5 involve the oxidation of UBr_4 [13470-20-7] by Br_2 or by bromination of uranium turnings with Br_2 in acetonitrile. The metastable pentabromide is isostructural with the pentachloride, being dimeric with edge-sharing octahedra U_2Br_{10}.

14. Organometallic Complexes

The organometallic chemistry of uranium has grown rapidly during the last four decades. Most organouranium complexes are found with U(IV) centers; however, some examples of higher and lower valent species are being isolated. Uranium organometallic compounds have potential uses in homogeneous and heterogeneous catalysis (237,238), with activities ranging from the hydrogenation and polymerization of olefins to the selective activation of alkanes (252). In addition, uranium complexes are also used as models for other more radioactive actinides. A wide range of organic molecules have been complexed with uranium, including hydrocarbyl, allyl, arene, cyclooctatetraenyl, and a host of cyclopentadienyl-based ligands. More detailed discussion, background material, and extensive references to the primary literature can be found in excellent reviews by Marks (253), Burns et al. (236–238), Takats (254), Santos et al. (255), Bursten and Strittmatter (256), and Ephritikhine (257).

14.1. Cyclopentadienyl and Substituted Cyclopentadienyl Complexes. Uranium complexes containing cyclopentadienyl rings, Cp ($C_5H_5^-$), and its modified analogs, Cp* ($C_5Me_5^-$), Cp† ($Me_3SiC_5H_4^-$), Cp‡ [$(Me_3Si)_2C_5H_3^-$], and Cp′ ($MeC_5H_4^-$), are among the most common organouranium complexes known. Electron-deficient mono ring U(IV) compounds of general formula (η-Ring)UX_3 (X = halogen) are unstable, but they can be isolated as Lewis base adducts of the general formula $CpUX_3L_n$ ($n = 2$, X = Cl, Br, L = THF, DME, amides, organonitriles, R_3PO; $n = 3$, X = NCS, L = R_3PO), or with the more sterically demanding permethylcyclopentadienyl ligand as in Cp*UX_3L_2 (X = Cl, Br; L = R_3PO, THF, and organonitriles). Borohydrides, which generally coordinate in a tripodal fashion, have also found utility in stabilizing monocyclopentadienyl-uranium systems, ie, (η-ring)$U(BH_4)_3$ (ring = Cp [103948-79-4], Cp′ [120628-95-7], $C_5H_4PPh_2$ [157620-00-3]) (258). Trivalent organouranium complexes are relatively rare; however, the trivalent species $CpU(BH_4)_3^-$, Cp*$U(BH_4)_3^-$, Cp*$UI_2(THF)_3$ [120410-81-3] have been isolated and fully characterized. A pseudo-octahedral coordination geometry was revealed for the latter compound with a *trans*-mer arrangement of iodide and THF ligands (237).

Both U(III) and U(IV) bis-Cp complexes have been isolated, with the former exhibiting slightly lower stabilities. Dimeric uranium(III) bis-ring complexes $[Cp^\ddagger{}_2UX]_2$ (X = Cl [109144-35-6], Br [109192-52-1], I [109168-46-9], aryloxide) are readily cleaved in THF solution to give $Cp^\ddagger{}_2UX(THF)$, further indicating the tendency for high coordination numbers to stabilize this oxidation state.

Although Cp_2MX_2 compounds are ubiquitous in early transition-metal organometallic chemistry, the uranium analogs are prone to ligand redistribution reactions. Thus, attempts to prepare Cp_2UCl_2 in dme solution actually provide a mixture of Cp_3UCl and $CpUCl_3$(dme). In some cases, these complexes have been successfully stabilized against ligand redistribution by adding chelating ancillary ligands, such as the chelating phosphate 1,2-bis(diphenylphosphineoxide)ethane to form $Cp_2UCl_2(Ph_2P(O)CH_2CH_2P(O)Ph_2)$ [67588-78-7]. High valent uranium organometallic complexes with organoimido and oxo groups have been synthesized, ie, [Cp*$_2$U(NR)$_x$Cl$_{2-x}$ (R = alkyl, $x = 1, 2$)] (259). Bis–Cp hydrides and borohydrides have also been stabilized, ie, (η-ring)$_2UH_2$ (ring = Cp, Cp*) and $Cp_2U(BH_4)_2$ [65888-45-1]. The hydrides behave like typical transition metal hydrides, inserting CO and catalyzing homogenous alkene hydrogenation.

Tris–Cp uranium complexes have been isolated with U(III, IV, V) metal centers. The (η-ring)$_3$U system has been studied with a variety of substituted ring systems. These complexes form 1:1 adducts with Lewis bases, ie, THF, nitriles, isonitriles, and phosphine oxides, all of which show a pseudo-tetrahedral geometry (**9**). The relatively high solubility of the THF adducts make these complexes excellent starting materials.

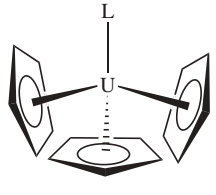

(**9**)

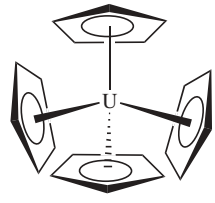

(**10**)

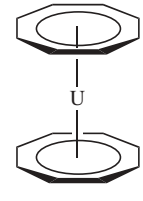

(**11**)

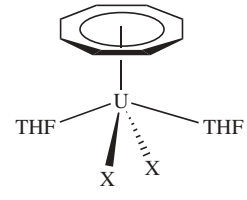

(**12**)

Uranium(IV) ring systems of general formula (η-ring)$_3$UX (X = halide, CN, PPh_2, NEt_2, BH_4, OR, SR, $C(CN)_3$, NO_3, ClO_4) are well known and have been prepared via metathesis with (η-ring)$_3$UCl. The crystal structure of $Cp_3U(SMe)$ [174576-68-2] has recently been determined, showing the common pseudotetrahedral geometry illustrated in (**9**) (260). Being highly Lewis acidic, these complexes tend to react with neutral ligands to afford adducts of the form, (η-ring)$_3$UXL (X = anionic ligand, L = neutral 2-electron donor).

Organometallic U(V) complexes are extremely rare. Two examples include $Cp'_3U(NR)$ (R = Ph [94161-46-3], $SiMe_3$ [94202-28-5]), and $Cp_3U[CHP(MePh_2)]$ [77357-86-9]. In both cases, multiple bonding characteristics have been found (U = NR, U = CHR), and they can be considered as U(V) members of the class of pseudotetrahedral Cp_3UX compounds.

Tetrakis–Cp uranium complexes are readily prepared via metathesis of UCl_4 and KCp in refluxing benzene. These complexes are a relatively rare example of a pseudo-tetrahedral complex with four η^5-Cp rings, (η-Ring)$_4$U (**10**). The Cp derivative has been shown to react with CO and CO_2 to give acyl and carboxylato complexes. This complex also reacts with alkyl halides to afford the U(IV) complex, Cp_3UX (X = halide).

14.2. Cyclooctatetraenyl Compounds. Sandwich-type complexes of uranium with the cyclo-octatetraenyl anion ($COT = C_8H_8^{2-}$) are significant in the history of organouranium chemistry with the synthesis of *uranocene*, $U(COT)_2$ being the first example of an organouranium bis-ring sandwich complex (**11**). Uranocene, $(COT)_2U$ [11079-26-8] (**11**), the simplest and most prominent of the COT derivatives, has been prepared by the interaction of UCl_4 [10026-10-5] with two equivalents of $K_2C_8H_8$. These compounds are thermally stable, but they are exceedingly by sensitive to oxygen.

Mono–COT compounds have been studied, which are usually stabilized by Lewis bases, ancillary ligands capable of π-bonding, or both. Examples include $(COT)UX_2(THF)_2$ (**12**) (X = Cl [117097-69-5], BH_4), $[(COT)U(NEt_2)_x]^{2-x}$ ($x = 2$ [152249-41-7], 3 [152249-43-9]), $(COT)U(CH_2SiMe_3)_2(HMPA)$ [136937-74-1], and $[(COT)U(CH_2SiMe_3)_3]^-$ [130950-94-6]. Cationic uranium COT species have also been generated by protonolysis of amides to form $[(COT)U(NEt_2)(THF_2)]BPh_4$ [152249-47-3] and $[Cp^*(COT)U(THF)_2]BPh_4$ [171975-76-1] (261). The only successful preparation of a mixed ring U(III) complex is illustrated by $[(Me_3Si)COT]UCp^*(THF)$ and the bipyridine analog, $(COT)UCp^*(4,4'\text{-}Me_2\text{-}2,2'\text{-bipy})$ (262).

14.3. Hydrocarbyl Complexes. Stable homoleptic and heteroleptic uranium hydrocarbyl complexes have been synthesized. Unlike the thorium analogs, uranium alkyl complexes are generally thermally unstable due to β-hydride elimination or reductive elimination processes. A rare example of a homoleptic uranium complex is $U(CH(SiMe_3)_2)_3$, the first stable U(III) homoleptic complex to have been isolated. A structural study indicated a triganol pyramidal geometry with stabilizing γ-agostic U–H interactions.

Heteroleptic complexes of uranium can be stabilized by the presence of the ancillary ligands; however, the chemistry is dominated by methyl and benzyl ligands. Examples of these materials include $UR_4(dmpe)$ (R = alkyl, benzyl) and $U(benzyl)_4MgCl_2$. The former compounds coordinate "soft" chelating phosphine ligands, a rarity for the "hard" U(IV) atom.

Another class of heteroleptic alkyl complexes contains π-donating ancillary ligands such as $RU[N(SiMe_3)_2]_3$ (R = Me, H, BH_4). The methyl compound has

exhibited insertion chemistry with small molecules, including aldehydes, ketones, nitriles, and isocyanides (257). Stable metallacycle compounds are also known, ie, $[(Me_3Si)_2N]_2U(CH_2Si(Me_2)N(SiMe_3))$. Generally, uranium metallacycles are quite reactive inserting a host of organics, ie, CO, secondary amines, nitriles, isonitriles, aldehydes, ketones, and alcohols.

14.4. Bimetallic Complexes. There are two types of bimetallic organometallic uranium complexes: those with and those without metal–metal interactions. Examples of species containing metal–metal bonds are complexes with Mo, W, Fe, or Ru carbonyl fragments. Examples of these include $(\eta\text{-ring})_3U(\mu\text{-OC})\{M(CO)_2(\eta\text{-ring})\}$ (M = Mo, W), $[N(SiMe_3)_2]_3U(\mu\text{-OC})\{M(CO)_2(\eta\text{-ring})\}$ (M = Mo, W), and $(\eta\text{-ring})_3U\{CpM(CO)_2\}$ (M = Fe, Ru).

The chemistry of non-metal–metal bonded species is more extensive. Diphenylphosphinocyclopentadienyl (CpP) complexes of uranium have been used to coordinate molybdenum carbonyl fragments, ie, $R_2U(\mu\text{-CpP})_2\{Mo(CO)_4\}$ (R = NEt_2, CpP). Hydrides have also been used as a bridging ligand to rhenium in $Cp_3UReH_6L_2$ (L = PPh_3, $P(C_6H_4F\text{-}p)$). In this case, the rhenium hydride acts like a borohydride coordinated in a tridentate fashion. The polyoxoanions are represented by $[N\text{-}n\text{-}Bu_4][Cp_3U(MW_5O_{19})_2]$ (M = Nb, Ta); compounds of this type are also known for thorium. All Cp ligands are bound in an η^5-fashion with two polyoxoanions in a *trans*-geometry bound through the oxygen atoms.

15. Health and Safety Factors

15.1. Exposure and Health Effects. Uranium is a general cellular poison, which can potentially affect any organs or tissues. Uranium and its compounds can be damaging due to chemical toxicity and by the injury caused by ionizing radiation. The chemical toxicity of uranium compounds depends on their solubility in biological media. Highly soluble and therefore highly transportable and toxic compounds include fluorides, chlorides, nitrates, and carbonates of uranium(VI); moderately transportable compounds include corresponding uranium(IV) compounds; and slightly transportable compounds include oxides, hydrides, and carbides. In experiments where uranium was administered to laboratory animals, the dose after which 50% of the animals died on days 14 to 21 (LD_{50}) were as follows: for uranyl fluoride, 2.5 mg/kg for male rats and 1 mg/kg for female rats; and for uranyl nitrate 2.0 mg/kg and 1.0 mg/kg for male and female rats, respectively (8).

Uranium can enter the human body orally, by inhalation, and through the skin and mucous membranes. Uranium compounds, both soluble and insoluble, are absorbed most readily from the lungs. In the blood of exposed animals, uranium occurs in two forms in equilibrium with each other: as a nondiffusible complex with plasma proteins and as a diffusible carbonate complex (263).

Studies show that the main sites of uranium deposition are the renal cortex and the liver. Uranium is also stored in bones; deposition in soft tissues is almost negligible. Uranium(VI) is deposited mostly in the kidneys and eliminated with the urine; however, tetravalent uranium is preferentially deposited in the liver and eliminated in the feces. The elimination of uranium absorbed into the blood

occurs via the kidneys in urine, and most, ~84%, of it is cleared within 4 to 24 hours (8).

The critical organs for the chemical toxicity of uranium and its soluble compounds are the kidney and the liver. In acute uranium poisoning, kidney lesions, renal hemorrhage, and liver-cell changes were observed. Occupational exposure to uranium usually involves inhalation of aerosols carrying particles varying in size and density and containing a mixture of uranium compounds with different solubilities. Insoluble particles are deposited in the lungs, retained there for a long time, and can cause radiation damage of varying degree or silicosis (8).

An accident in the 1940s involved acute uranium fluoride exposure. The accident was caused by the sudden rupture of a tank containing gaseous UF_6 and resulted in the death of 2 persons, the serious injury of 3 others, and minor injury (dispensary treatment) of 13 others. Health effects of the exposed personnel included renal lesions and diffuse inflammatory changes in the lungs and gastrointestinal tract effects. The renal damage was thought to be caused by absorbed uranium; skin, eye, and respiratory effects were presumed to be due to direct action of fluorine.

A study performed in the 1940s, where 31 workers were examined after year-long inhalation exposure to dusts of uranium(VI) oxide, uranium peroxide, and uranium chlorides (at concentrations that at times reached 155 mg/m^3 in terms of uranium), did not reveal any symptoms or signs of chronic poisoning (264).

However, examination of 237 uranium mine workers revealed anemia in 31% of them, marked leukopenia in 23%, and lymphocytosis in 14%. In another similar group of uranium workers employed for about 10 years, reduced body weight and pathological changes in the lungs, kidneys, and blood were observed and shown to have resulted from radiation exposure. On the other hand, none of the 100 individuals who had been exposed for 5 years to slightly soluble uranium compounds exhibited any signs of renal damage nor any pulmonary or blood changes (8).

In another study of workers exposed to UF_6, the review of two years of follow-up medical data on 31 workers who had been exposed to uranium(VI) fluoride and its hydrolysis products after the accidental rupture of a 14-ton shipping cylinder in early 1986 indicated that none of the 31 workers sustained any observable health effects from exposure to U, even though an exposure limit of 9.6 mg was exceeded by 8 of the workers (265).

Results of extensive studies have demonstrated that the consumption of drinking water containing uranium at elevated levels of 0.04 to 0.05 mg/L is not detrimental to human health (8).

15.2. Occupational Protection and Radiation Considerations. The major adverse factor during the mining and processing of uranium and uranium-containing minerals is airborne dust. Personal protection should include respirators, protective clothing, surgical gloves, suitable footwear, use of wet processes wherever possible, and in operations involving dust formation, face masks, constant ventilation, and glove boxes. Local exhaust ventilation is necessary—recall that one of the daughter products of U is radioactive radon. Environmental protection measures against radioactive contamination in the mining and processing of uranium ores has been described in detail by Andreyeva et al. (266). In

the United States, the hygienic standards for both soluble and insoluble compounds of natural uranium are, expressed as threshold limit values, 0.2 mg/m^3 for an 8-hour time-weighted average and 0.6 mg/m^3 for a short-term exposure (8). Finely divided uranium metal, some alloys, and uranium hydride are pyrophoric. Therefore, such materials should be handled in an inert atmosphere glovebox.

The toxicity of uranium caused by its radiation depends on the isotopes present. Natural uranium does not constitute an external radiation hazard because it emits mainly low-energy alpha radiation. It does, however, present an internal radiation hazard if it enters the body by inhalation or ingestion. The concentration of 1-mg U/g biological tissue corresponds to an absorbed dose of 0.006 Sv (Sievert) per year. Radiation exposure may occur in the mining of uranium ores, although the inhalation of particulates to which miners are exposed is a greater hazard (8). Isotopes such as ^{232}U, which emit fairly strong γ-radiation, should be handled in a hot cell; ^{233}U, ^{234}U, and ^{236}U should be handled in glove boxes; ^{235}U and ^{238}U, because of their soft radiation, can be handled on an open laboratory bench or in a fume hood. The laboratory should be equipped as an α-laboratory. In the handling of uranium, as in the case of all radionuclides, radioactivity due to the progeny, such as Th, Ra, and Rn, should be considered.

Large quantities of fissile isotopes, ^{233}U and ^{235}U, should be handled and stored appropriately to avoid a criticality hazard. Clear and relatively simple precautions, such as, dividing quantities so that the minimum critical mass is avoided, following administrative controls, using neutron poisons, and avoiding critical configurations (or shapes), must be followed to prevent an extremely treacherous explosion (267).

16. Acknowledgments

The authors acknowledge Los Alamos National Laboratory and the Division of Chemical Sciences, Geosciences, and Biosciences, Office of Basic Energy Sciences, U.S. Department of Energy, for their support of actinide chemistry research at Los Alamos National Laboratory.

BIBLIOGRAPHY

"Uranium and Uranium Compounds" in *ECT* 1st ed., Vol. 14, pp. 432–458, by J. J. Katz, Argonne National Laboratory; in *ECT* 2nd ed., Vol. 21, pp. 1–36, by V. L. Mattson, Kerr-McGee Corp.; in *ECT* 3rd ed., Vol. 23, pp. 502–547, by F. Weigel, University of Munich; "Uranium and Uranium Compounds," in *ECT* 4th ed., Vol. 24, pp. 638–694, David L. Clark, D. Webster Keogh, Mary P. Neu, Wolfgang Runde, Glenn T. Seaborg Institute for Transactinium Science, Los Alamos National Laboratory; "Uranium and Uranium Compounds" in *ECT* (online), posting date: December 4, 2000, by David L. Clark, D. Webster Keogh, Mary P. Neu, and Wolfgang Runde, Glenn T. Seaborg Institute for Transactinium Science, Los Alamos National Laboratory; "Uranium and Uranium Compounds" in *ECT* (online), posting date: June 4, 2001, by J. Whitlock, Atomic Energy of Canada Ltd.

CITED PUBLICATIONS

1. I. Grenthe, J. Droz˙ dz˙ yn′ski, T. Fujino, E. Buck, T. E. Albrecht-Schmitt, and S. S. Wolfa, in N. M. Edelstein, J. Fuger, and L. R. Morss, eds., *The Chemistry of the Actinide and Transactinide Elements*, Vol. 1, Springer, New York, 2006.
2. E. Péligot, *Compt. Rend.* **13**, 417 (1842).
3. A. H. Becquerel, *C. R. Acad. Sci.* **128**, 771 (1896).
4. E. Fermi, E. Amaldi, O. D'Agostino, R. Rasetti, and E. Segré, *Proc. R. Soc. London* **A146**, 483 (1934).
5. O. Hahn and F. Strassman, *Naturwissenschaften* **27**, 11 (1939).
6. N. E. Holden, in D. R. Lide, ed., *Handbook of Chemistry and Physics*, Chemical Rubber Publishing Company, Boca Raton, Fla., 1997.
7. R. B. Firestone, V. S. Shirley, C. M. Baglin, S. Y. F. Chu, and J. Zipkin, eds., *Table of Isotopes*, 8th ed., John Wiley & Sons, New York, 1998.
8. V. A. Filov and A. L. Ivin, in *Harmful Chemical Substances, Volume 1: Elements in Group I–IV of the Periodic Table and their Inorganic Compounds*, Ellis Horwood, New York, 1993, pp. 351–373.
9. G. Choppin, J. Rydberg, and J. O. Liljenzin, *Radiochemistry and Nuclear Chemistry*, Butterworth-Heinemann Ltd., Oxford, U.K., 1995.
10. S. Moorbath, P. N. Taylor, and N. W. Jones, *Chem. Geol.* **57**(1–2), 63–86 (1986).
11. *Proceedings of the Mineralogical Association of Canada Short Course on Radiogenic Isotope Systems to Problems in Geology*, Toronto, Canada, 1991.
12. K. Bell, *Can. Mineral. Mag.* **44**(336), 371–381 (1981).
13. D. S. Bhattacharyya, *Precambrian Res.* **58**(1–4), 71–83 (1992).
14. G. R. N. Das, R. V. Viswanath, and S. A. Pandit, *Mem. - Geol. Soc. India* **9**, 29–31 (1988).
15. G. A. Partington, N. J. McNaughton, and I. S. Williams, *Econ. Geol.* **90**(3), 616–635 (1995).
16. R. D. Tucker and W. S. McKerrow, *Can. J. Earth Sci.* **32**(4), 368–379 (1995).
17. H. R. von Gunten, H. Surbeck, and E. Roessler, *Environ. Sci. Technol.* **30**(4), 1268–1274 (1996).
18. G. Faure, *Principles of Isotope Geology*, John Wiley & Sons, New York, 1986.
19. J. K. W. Lee, *Australia. Dev. Petrol.* **14**, 423–446 (1993).
20. J. Blaise and J.-F. Wyart, *Energy Levels and Atomic Spectra of Actinides*, Tables Internationales de Constantes, Paris, France, 1992.
21. E. F. Worden, J. Blaise, M. Fred, N. Trautmann, and J.-F. Wyart, in L. R. Morss, N. M. Edelstein, and J. Fuger, eds., *The Chemistry of the Actinide and Transactinide Elements*, Springer, New York, 2006.
22. P. C. Burns, *Rev. Mineral.* **38**(Uranium), 23–90 (1999).
23. R. Finch and T. Murakami, *Rev. Mineral.* **38**(Uranium), 91–179 (1999).
24. J. A. Plant, P. R. Simpson, B. Smith, and B. F. Windley, *Rev. Mineral.* **38**(Uranium), 255–319 (1999).
25. *Uranium 2005. Resources, Production and Demand*, OECD, International Atomic Energy Agency (IAEA), 2005.
26. *Uranium 2003: Resources, Production and Demand*, Organisation for Economic Co-operation and Development, Nuclear Energy Agency, Paris, France, 2003.
27. J. W. Frondel, M. Fleischer, and R. S. Jones, *Glossary of Uranium and Thorium-Bearing Minerals*, U.S. Geological Survey Bulletin 1250, 1967.
28. C. Frondel, *Systematic Mineralogy of Uranium and Thorium*, U.S. Geological Survey Bulletin 1064, 1958.
29. S. H. U. Bowie, in *Uranium Exploration Geology*, IAEA, Vienna, STI/PUB/277, 1970, pp. 285–300.

30. J. W. Gabelman, in IAEA, Vienna, STI/PUB/277, 1970, pp. 315–330.
31. D. S. Robertson, in IAEA, Vienna, STI/PUB/277, 1970, pp. 267–284.
32. W. D. Wilkinson, *Uranium Metallurgy, vol I, Process Metallurgy, vol II, Uranium Corrosion and Alloys*, Wiley-Interscience, New York, 1962.
33. J. H. Gittus, *Uranium*, Butterworths, Washington, D.C., 1963.
34. R. C. Merritt, *The Extractive Metallurgy of Uranium*, Colorado School of Mines Research Institute and USAEC, Golden, Colo., 1971.
35. IAEA, *Uranium Exploration Geology*, Vienna, STI/PUB/277, 1970, pp. 285–300.
36. B. DeVito, F. Ippolitio, G. Capoldi, and P. R. Simpson, eds., *Uranium Geochemistry, Mineralogy, Geology, Exploration and Resources*, Institution of Mining and Metallurgy, London, 1984.
37. *Gmelin Handbook of Inorganic Chemistry*, Springer-Verlag, Berlin, 1988.
38. J. Janeczek, *Rev. Mineral.* **38**(Uranium), 321–392 (1999).
39. L. Zetterstrom, *Oklo—A Review and Critical Evaluation of Literature*, Lab. Isotope Geology, Swedish Musuem of Natural History, Report SKB TR-00-17, 2000, pp. 1–37.
40. G. A. Cowan, *Sci. Am.* **235**, 36 (1976).
41. R. West, *J. Chem. Ed.* **53**, 336 (1976).
42. A. Berzero and M. D'Alessandro, *The Oklo Phenomenon As an Analog of Radioactive Waste Disposal. A Review.*, Comm. Eur. Communities Eur., Report EUR 12941, 1990.
43. F. Gauthier-Lafay, P. Holliger, and P.-L. Blanc, *Geochim. Cosmochim. Acta* **60**(23), 4831–4851 (1996).
44. L. Raimbault, H. Peycelon, and P.-L. Blanc, *Radiochim. Acta* **74**, 283–287 (1996).
45. R. G. Bellamy and N. A. Hill, *The Extraction and Metallurgy of Uranium, Thorium, and Beryllium*, Pergamon Press, Oxford, U.K., 1963.
46. J. W. Clegg and D. D. Foley, *Uranium Ore Processing*, Addison-Wesley, Reading, Mass., 1958.
47. C. D. Harrington and A. E. Ruehle, *Uranium Production Technology*, Van Nostrand, Princeton, N.J., 1959.
48. J. P. Bibler, *Ion Exchange in the Nuclear Industry*, 2nd ed., Elsevier, London, U.K., 1990, pp. 121–133. Recent Dev. Exch. 2, [Proc. Int. Conf. Ion Exch. Processes], 2nd, Westinghouse Savannah River Co., Aiken, SC, 29808, USA, P. A. H. Williams, Michael James Eds., Elsevier, London, UK, (1990), 121–33.
49. S. J. Browning, *Aust. Mining* **64**, 48 (1972).
50. J. H. Cavendish, in W. W. Schulz and J. D. Navratil, eds., *Sci. Technol. Tributyl Phosphate*, Vol. 2, CRC Press, Boca Raton, Fla., 1987, Issue Pt. A, pp. 1–41.
51. J. G. H. Du Preez, *Radiat. Prot. Dosim.* **26**, 7 (1989).
52. N. Petrescu, S. G. Choi, and L. Ganovici, *Metalurgia* (*Bucharest*) **40**(2), 88–92 (1988).
53. D. R. Weir, *Can. Metall. Q.* **23**, 353 (1984).
54. *Gmelin Handbook of Inorganic Chemistry, Suppl. Ser., Uranium, vol. A3, Technology Uses*, Springer-Verlag, Berlin, 1981.
55. E. H. P. Cordfunke, *J. Inorg. Nucl. Chem.* **24**, 303 (1962).
56. J. C. Warner, *Metallurgy of Uranium*, Oak Ridge, Tenn., Report Natl. Nucl. En. Ser., Div. IV, USAEC Technical Information Service, 1953.
57. R. D. Baker, B. R. Hayward, C. Hull, H. Raich, and A. R. Weiss, *Preparation of Uranium Metal by the Bomb Method*, Los Alamos Scientific Laboratory, Report LA-472, 1946.
58. M. H. West, M. M. Martinez, J. B. Nielson, D. C. Court, and Q. D. Appert, *Synthesis of Uranium Metal Using Laser-Initiated Reduction of Uranium Tetrafluoride of Calcium Metal*, Los Alamos National Laboratory, Report LA-12996-MS, 1995.
59. G. H. Lander, E. S. Fisher, and S. D. Bader, *Adv. Phys.* **43**(1), 1–111 (1994).

60. F. L. Oetting, M. H. Rand, and R. J. Ackermann, *The Chemical Thermodynamics of Actinide Elements and Compounds, Part 1, The Actinide Elements*, IAEA, Vienna, STI/PUB/424/1, 1976.
61. J. M. Haschke, *J. Alloys Compounds* **278**(1–2), 149–160 (1998).
62. G. H. Lander and M. H. Mueller, *Acta Crystallographica, Section B: Structural Crystallography and Crystal Chemistry* **26**(Pt. 2), 129–136 (1970).
63. A. C. Lawson, C. E. Olsen, J. W. Richardson, Jr., M. H. Mueller, and G. H. Lander, *Acta Crystall. Section B: Structural Sci.* **B44**(2), 89–96 (1988).
64. R. H. Hackel and B. E. Warner, *Laser Isotope Separation, SPIE Proceedings Series*, Vol. 1859, Society of Photo-Optical Instrumentation Engineers, Bellingham, Wash., 1993.
65. T. M. Anklam, L. V. Berzins, K. G. Hagans, G. W. Kamin, M. A. McClelland, R. D. Scarpetti, and D. W. Shimer, *Laser Isotope Separation, SPIE proceedings series*, Vol. 1859, Society of Photo-Optical Instrumentation Engineers, Bellingham, Wash., 1993, p. 277.
66. S. Kidd, in T. Brewis, J. Chadwick, D. Clifford, R. Ellis, M. Forest, A. Kennedy, R. Morgan, G. Pearse, N. Rosin, and M. West, eds., *Metals and Minerals Annual Review*, Mining Journal LTD, London, U.K., 1996.
67. M. E. Kassner and D. E. Peterson, *Phase Diagrams of Binary Actinide Alloys*, ASM International, Materials Park, Ohio, 1995.
68. *Assessment of enriched uranium storage safety issues at the Oak Ridge Y-12 Plant*, Oak Ridge National Laboratory, Report Y/ES-104/R4, 1996.
69. P. D. Wilson, *The Nuclear Fuel Cycle: From Ore to Wastes*, Oxford Science Publications, Oxford, U.K., 1996.
70. G. L. Hofman, L. C. Walters, and T. H. Bauer, *Progr. Nucl. Energy* **31**(1/2), 83–110 (1996).
71. S. Villani, *Uranium Enrichment*, Springer-Verlag, New York, 1979.
72. G. Choppin, J. O. Liljenzin, and J. Rydberg, *Radiochemistry and Nuclear Chemistry*, Butterworth-Heinemann Ltd., Oxford, U.K., 2002.
73. National Research Council (U.S.), Committee on Decontamination and Decommissioning of Uranium Enrichment Facilities; *Affordable Cleanup? Opportunities for Cost Reduction in the Decontamination and Decommissioning of the Nation's Uranium Enrichment Facilities*, National Academy Press, Washington, D.C., 1996.
74. *Data on New Gaseous Diffusion Plants*, U.S. DOE Oak Ridge Operations Office, Report ORO-685, 1972.
75. D. Massignon, *Top. Appl. Phys.* **35** (Uranium Enrich.), 55 (1979).
76. E. Von Halle, *AIChE Symp. Ser.* **76**, 82 (1980).
77. J. F. Petit, *Bull. Inf. Sci. Tech., Commis. Energ. At.* (*Fr.*) **223**, 19 (1977).
78. K. Keizer and H. Verweij, *Chemtech*. 37 (1996).
79. R. Green, *Nuclear Eng. Int.* 36–39 (2003).
80. H. W. Savage, *Separation of Isotopes in Calutron Units*, Oak Ridge, Tenn., Report Natl. Nucl. En. Ser., Div. I, Vol. 6, TID-5218, USAEC Technical Information Service, 1951.
81. G. A. Akin, H. P. Kackenmaster, R. J. Schrader, J. W. Strohecker, and R. E. Tate, *Chemical Processing Equipment: Electromagnetic Separation Process*, Oak Ridge, Tenn., Report National Nuclear Energy Series Div. I, Vol. 12, TID-5232, USAEC Technical Information Service, 1951.
82. I. Alexeff, *Current Limitations in Calutrons*, Oak Ridge Natl. Lab., Oak Ridge, Tenn., Report ORNL-TM-3722, 10 pp. Avail.: Dep. NTIS, 1972.
83. Oak Ridge, Tenn., Report National Nuclear Energy Series Div. I, Volumes 1–13, McGraw-Hill Book Co., Inc., and USAEC Technical Information Service, 1949–1952.

84. S. P. Vesnovskii and V. N. Polynov, *Nucl. Instrum. Methods Phys. Res., Sect. B* **b70**, 9 (1992).
85. S. M. Abramychev, N. V. Balashov, S. P. Vesnovskii, V. N. Vyachin, V. G. Lapin, E. A. Nikitin, and V. N. Polynov, *Nucl. Instrum. Methods Phys. Res., Sect. B* **b70**, 5 (1992).
86. D. L. Donohue and R. Zeisler, *Anal. Chem.* **65**, 359A–360A, 364A–368A (1993).
87. N. Camarcat, A. Lafon, J. P. Pervés, A. Rosengard, and G. Sauzay, *Laser Isotope Separation, SPIE proceedings series*, Vol. 1859, Society of Photo-Optical Instrumentation Engineers, Bellingham, Wash., 1993.
88. N. Morioka, in *Laser Isotope Separation, SPIE Proceedings Series*, Vol. 1859, Society of Photo-Optical Instrumentation Engineers, Bellingham, Wash., 1993.
89. P. A. Abelson, N. Rosen, and J. I. Hoover, *Liquid Thermal Diffusion*, Oak Ridge, Tenn., Report Natl. Nucl. En. Ser., Div. IX, Vol. 1, TID-5229, USAEC Technical Information Service, 1951.
90. S. Villani, *Isotope Separation*, American Nuclear Society, La Grange Park, Ill., 1976.
91. L. Meites, *Handbook of Analytical Chemistry*, McGraw-Hill, New York, 1963.
92. A. E. Lally, in *Uranium Series Disequilibrium Applications to Earth, Marine, and Environmental Sciences*, Clarendon Press, Oxford, U.K., 1992, pp. 94–126.
93. G. E. Gindler, *Radiochemistry of Uranium*, Technical Information Center, USAEC, Report NAS-NS-3050, 1962.
94. C. C. Casto, in C. J. Rodden, ed., *Analytical Chemistry of the Manhatten Project*, McGraw-Hill, New York, 1950, pp. 511–536.
95. I. K. Kressin, *Anal. Chem.* **49**, 842–845 (1977).
96. J. A. Dean, *Analytical Chemistry Handbook*, McGraw-Hill, New York, 1995.
97. A. J. Francis, C. J. Dodge, F. Lu, G. P. Halada, and C. R. Clayton, *Environ. Sci. Technol.* **28**, 636 (1994).
98. C. Chisholm-Brause, S. D. Conradson, C. T. Buscher, P. G. Eller, and D. E. Morris, *Geochim. Cosmochim. Acta* **58**, 3625 (1994).
99. C. Chisholm-Brause, S. D. Conradson, P. G. Eller, and D. E. Morris, *Mat. Res. Soc., Sci. Basis for Nucl. Waste Management* **XV**, 315 (1992).
100. V. W. Schneider and H. Roepenack, in *Handbook on the Physics and Chemistry of Actinides*, Elsevier Science, New York, 1986, pp. 531–555.
101. C. Pereira, G. Vandegrift, M. Regalbuto, A. Bakel, and D. L. Bowers, *Lab-scale Demonstration of the UREX+ 1 Process Using Spent Nuclear Fuel*, 2005 AIChE Annual Meeting and Fall Showcase, Cincinnati, Ohio.
102. M. S. Kazimi, *Am. Scientist* **91**, 408–415 (2003).
103. J. Yu, K. Wang, S. You, B. Jia, S. Shen, and G. Shi, *Progr. Nucl. Energy* **45**(1), 71–84 (2004).
104. R. K. Sinha and A. Kakodkar, *Nucl. Eng. Design* **236**(7–8), 683–700 (2006).
105. M. Yamawaki, H. Yamana, H. Unesaki, and K. Fukuda, *J. Atom Energ. Soc. JPN* **47**(12), 802–821 (2005).
106. D. J. Sandstrom, *Los Alamos Sci.* **17**, 36–50 (1989).
107. J. W. Hopson, L. W. Hantel, and D. J. Sandstrom, *Evaluation of Depleted-Uranium Alloys for Use in Armor-Piercing Projectiles* (*U*), Los Alamos Scientific Laboratory, Report LA-5238, 1973.
108. P. S. Dunn and B. K. Damkroger, *Tungsten-Uranium Penetrator Target Interaction*, in A. Bose and R. J. Dowding, eds., Tungsten Refract. Met.–1994, Proc. Int. Conf., 2nd (1995), Meeting Date 1994, Metal Powder Industries Federation, Princeton, N.J., 1995.
109. A. Bose, J. Lankford, and H. Couque, *Development and Characterization of Adiabatic Shear Prone Tungsten Heavy Alloys*, Wyman-Gordon Co., Worcester, Mass., Report SWRI-06-4601, 1993.

110. S. Guha, C. Kyriacou, J. C. Withers, and R. O. Loutfy, *Development of a Tungsten Heavy Alloy that Falls by an Adiabatic Shear Mechanism*, *Phase 1.*, Mater. Electrochem. Res. Corp., Tucson, Az, Report ARL-LR-56, 1993.
111. J. J. Katz and E. Rabinowich, *The Chemistry of Uranium*, McGraw-Hill, New York, 1951.
112. H. Wedermeyer, in *Gmelin Handbuch der Anorganischen Chemie*, Suppl. Ser. Uranium, C4, 1984, pp. 1–64.
113. U. C. Gupta, M. Anuradha, and R. Meena, *Adv. Chem. Eng. Nucl. Process Ind.* (1994).
114. R. G. Robins, *J. Nucl. Mater.* **3**, 294–301 (1961).
115. M. Amaya, T. Kubo, and Y. Korei, *J. Nucl. Sci. Technol.* **33**(8), 636–640 (1996).
116. Y. Arita, S. Hamada, and T. Matsui, *Thermochim. Acta* **247**(2), 225–236 (1994).
117. Y. Arita and T. Matsui, *Thermochim. Acta* (1995).
118. J. K. Fink, *Tables of Thermodynamic and Transport Properties of Uranium Dioxide*, 1982.
119. M. Hoch, *J. Nucl. Mater.* **130**, 94–101 (1985).
120. P. G. Lucuta, H. J. Matzke, and R. A. Verrall, *J. Nucl. Mater.* **223**(1), 51–60 (1995).
121. S. Peng and G. Grimvall, *J. Nucl. Mater.* **210**(1–2), 115–122 (1994).
122. R. A. Verrall and P. G. Lucuta, *J. Nucl. Mater.* **228**(2), 251–253 (1996).
123. I. Amato, P. G. Cappelli, and M. Ravizza, *Metall. Ital.* **22**(5), 323–327 (1967).
124. S. Suryanarayana, N. Kumar, Y. R. Bamankar, V. N. Vaidya, and D. D. Sood, *J. Nucl. Mater.* **230**(2), 140–147 (1996).
125. F. Thuemmler, R. Theisen, and E. Patrussi, *Phase Relations, Production, and Characteristics of Substoichiometric Uranium and Plutonium Oxide Fuels* (UO_{2-x} *and* (*Uranium, Plutonium, Uranium*)O_{2-x}), Kernforschungszentrum, Karlsruhe, Germany, Report KFK-543, 1967.
126. T. L. Markin and R. S. Street, *J. Inorg. Nucl. Chem.* **29**(9), 2265–2280 (1967).
127. U. Benedict and C. Sari, *Ternary System Uranium Dioxide-Uranium Oxide* (U_3O_8)*-Plutonium Dioxide*, Transuranium Inst., Eur. At. Energy Community, Karlsruhe, Germany, Report EUR-4136, 1969.
128. IAEA, *The Plutonium-Oxygen and the Uranium-Plutonium-Oxygen Systems. A Thermochemical Assessment*, International Atomic Energy Agency, Report Tech. Rep Ser. No. 79, STI/DOC-10/79, 1967.
129. G. Koch, *Gmelin Handbook of Inorganic Chemistry*. Vol. 4: *Transuranium Elements, C*, Verlag Chemie, Weinheim, Germany, 1972.
130. N. H. Brett and A. C. Fox, *J. Inorg. Nucl. Chem.* **28**(5), 1191–1203 (1966).
131. J. K. Fink, *Int. J. Thermophys.* **3**(2), 165–200 (1982).
132. J. J. Carbajo, G. L. Yoder, S. G. Popov, and V. K. Ivanov, *J. Nucl. Mater.* **299**(3), 181–198 (2001).
133. H. Baily, H. Bernard, and B. Mansard, *Mater. Sci. Forum* **48–49**(Nucl. Fuel Fabr.), 175–183 (1989).
134. H. Bernard, *J. Nucl. Mater.* **166**(1–2), 105–111 (1989).
135. R. Güldner and H. Schmidt, *J. Nucl. Mater.* **178**(2–3), 152–157 (1991).
136. S. Liu, K. Guo, Y. Hu, Q. Wang, D. Gu, and Z. Shen, *Fenxi Huaxue* **22**(10), 984–988 (1994).
137. P. C. Burns, M. L. Miller, and R. C. Ewing, *The Canadian Mineralogist* **34**, 845–880 (1996).
138. M. L. Miller, R. J. Finch, P. C. Burns, and R. C. Ewing, *Mater. Res. Soc. Symp. Proc.* (1996).
139. G. J. Hutchings, C. S. Heneghan, I. D. Hudson, and S. H. Taylor, *Acs. Symp. Ser.* **638** (Heterogeneous Hydrocarbon Oxidation), 58–75 (1996).

140. S. H. Taylor, I. Hudson, and G. J. Hutchings, *Pct Int. Appl.*; WO 9630085 A1 961003 (U.S. Patent).
141. L. G. Gordeeva, Y. I. Aristov, E. M. Moroz, N. A. Rudina, V. I. Zaikovskii, Y. Y. Tanashev, and V. N. Parmon, *J. Nucl. Mater.* **218**(2), 202–209 (1995).
142. J. W. Choi, R. J. McEachern, P. Taylor, and D. D. Wood, *J. Nucl. Mater.* **230**(3), 250–258 (1996).
143. G. S. You, K. S. Kim, D. K. Min, S. G. Ro, and E. K. Kim, *J. Korean Nucl. Soc.* **27**(1), 67–73 (1995).
144. B. G. Kim, K. W. Song, J. W. Lee, K. K. Bae, M. S. Yang, and H. S. Park, *Yoop Hakhoechi* **32**(4), 471–481 (1995).
145. K. Tokai and A. Ooe, *Jpn. Kokai Tokkyo Koho*.
146. G. L. Hofman and J. L. Snelgrove, *Mater. Sci. Technol.* (1994).
147. M. Handa, *Bull. Chem. Soc. Jpn.* **39**(10) (1966).
148. R. M. Dell, V. J. Wheeler, and E. J. McIver, *Trans. Faraday Soc.* **62**(12), 3591–3606 (1966).
149. E. H. Kim, C. S. Choi, J. H. Park, and I. S. Chang, *Yoop Hakhoechi* **30**(4), 279–288 (1993).
150. J. I. Kim, *Mat. Res. Soc. Symp. Proc.* **294**, 3 (1993).
151. Fr. Pat. 264447 A1 900921, H. R. Cartmell and J. F. Ellis.
152. B. S. Girgis and N. H. Rofail, *Radiochim. Acta* **57**(1), 41–44 (1992).
153. J. H. Pashley, *Radiochim. Acta* **25**(3–4), 135–138 (1978).
154. T. Ozawa, *Jpn. Kokai Tokkyo Koho, Japanese Patent, JP 63279195 A2 881116*.
155. A. F. Bishay, H. A. S. Abdel, F. H. Hammad, M. F. Abadir, and A. M. Elaslaby, *J. Therm. Anal.* **35**(5), 1405–1412 (1989).
156. A. F. Bishay, H. A. S. Abdel, F. H. Hammad, and A. M. Elaslaby, *J. Therm. Anal.* **32**(5), 1415–1420 (1987).
157. S. Yamagishi and Y. Takahashi, *J. Nucl. Sci. Technol.* **23**(8), 711–721 (1986).
158. C. V. Cortes, G. Kremenic, and T. L. Gonzalez, *React. Kinet. Catal. Lett.* **36**(1), 235–240 (1988).
159. S. Mori and M. Uchiyama, *Sekiyu Gakkai Shi* **19**(9), 758–762 (1976).
160. H. Serizawa, K. Fukuda, Y. Ishii, Y. Morii, and M. Katsura, *J. Nucl. Mater.* **208** (1–2), 128–134 (1994).
161. M. Miyake, M. Hirota, S. Matsuyama, and M. Katsura, *J. Alloys Compd.* **213**(214), 444–446 (1994).
162. H. Serizawa, K. Fukuda, and M. Katsura, *J. Alloys Compd.* **223**(1), 39–44 (1995).
163. M. Katsura, *Seisan to Gijutsu* **47**(2), 37–39 (1995).
164. M. Katsura, M. Hirota, and M. Miyake, *J. Alloys Compd.* **213**(214), 440–443 (1994).
165. K. Ananthasivan, S. Anthonysamy, V. Chandramouli, I. Kaliappan, and R. P. R. Vasudeva, *J. Nucl. Mater.* **228**(1), 18–23 (1996).
166. J. C. Fitzmaurice and I. P. Parkin, *New J. Chem.* **18**(7), 825–832 (1994).
167. I. P. Parkin and J. C. Fitzmaurice, *J. Mater. Sci. Lett.* **13**(16), 1185–1186 (1994).
168. A. Otsubo and K. Haga, *Emerging Nucl. Energy Syst., Int. Conf., 7th* (1994).
169. H. Sekimoto and Z. Su'ud, *Nucl. Technol.* **109**(3), 307–313 (1995).
170. Z. Su'ud and H. Sekimoto, *J. Nucl. Sci. Technol.* **32**(9), 834–845 (1995).
171. S. Zaki and H. Sekimoto, *Ann. Nucl. Energy* **22**(11), 711–722 (1995).
172. F. Ingold, S. Daumas, S. Pillon, M. Baumann, and G. Ledergerber, *Psi Proc.* (1995).
173. G. Ledergerber, Z. Kopajtic, F. Ingold, and R. W. Stratton, *J. Nucl. Mater.* **188**, 28–35 (1992).
174. d. R. S. M. Rizzo, d. A. A. Rodrigues, and A. Abrao, *An. Assoc. Bras. Quim.* **44**(2), 33–40 (1995).
175. R. S. Mehrotra, *Mater. Res. Bull.* **28**(11), 1193–1199 (1993).
176. L. L. Wang, H. G. Moore, and J. W. Gladson, *Aip Conf. Proc.* (1994).

177. A. S. Gontar, R. Y. Kucherov, N. V. Lapochkin, and Y. V. Nikolaev, *Aip Conf. Proc.* (1994).
178. A. G. Lanin, P. V. Zubarev, and K. P. Vlasov, *At. Energ.* **74**(1), 42–47 (1993).
179. S. Sahin and E. B. Kennel, *Nucl. Technol.* **107**(2), 155–184 (1994).
180. S. K. Mukerjee, J. V. Dehadraya, V. N. Vaidya, and D. D. Sood, *J. Nucl. Mater.* **210**(1–2), 107–114 (1994).
181. S. K. Mukerjee, G. A. R. Rao, J. V. Dehadraya, V. N. Vaidya, V. Venugopal, and D. D. Sood, *J. Nucl. Mater.* **199**(3), 247–257 (1993).
182. W. Runde, *Los Alamos Sci.* **26**(2), 392–411 (2000).
183. D. L. Clark, D. E. Hobart, and M. P. Neu, *Chem. Rev.* **95**, 25–48 (1995).
184. R. J. Silva and H. Nitsche, *Radiochim. Acta* **70/71**, 377 (1995).
185. I. Grenthe, J. Fuger, R. J. M. Konings, R. J. Lemire, A. B. Muller, Nguyen-Trung, C. Cregu, and H. Wanner, *1. Chemical Thermodynamics of Uranium*, Elsevier Science, New York, 1992.
186. R. Guillaumont, T. Fanghaenel, J. Fuger, I. Grenthe, V. Neck, D. A. Palmer, and M. H. Rand, *Update on the Chemical Thermodynamics of Uranium, Neptunium, Plutonium, Americium, and Technetium*, Elsevier, Amsterdam, The Netherlands, 2003.
187. J. H. Burns and P. L. Ritger, *Am. Cryst. Assoc. Ser. 2* **11**, 27 (1983).
188. A. Elbasyouny, H. J. Brugge, K. von Deuten, M. Dickel, A. Knochel, K. U. Koch, J. Kopf, D. Melzer, and G. Rudolph, *J. Am. Chem. Soc.* **105**, 6568 (1983).
189. I. Grenthe, J. Fuger, R. J. M. Konigs, R. J. Lemire, A. B. Muller, C. Nguyen-Trung, and H. Wanner, *Chemical Thermodynamics of Uranium*, Elsevier Science, New York, 1992.
190. J. Rebizant, C. Apostolidas, M. R. Spirlet, G. D. Andreeti, and B. Kanellakopulos, *Acta Cryst. C.* **44**, 2098 (1988).
191. J. L. M. Dillen, C. A. Strydom, C. P. J. van Vuuren, and P. H. van Rooyen, *Acta Cryst., C.* **44**, 1921 (1988).
192. R. C. Paul, S. Singh, and R. D. Verma, *J. Fluorine Chem.* **16**, 153 (1980).
193. L. Niinisto, J. Toivonen, and J. Valkonen, *J. Acta Chem. Scand., Ser. A* **33**, 621 (1977).
194. Y. N. Mikhailov, L. A. Kokh, V. G. Kutznetsov, T. G. Grevtseva, S. K. Sokol, and G. V. Ellert, *Sov. J. Coord. Chem.* (*Engl. Transl.*) **3**, 388 (1977).
195. P. Kierkegaard, *Acta Chem. Scand.* **10**, 599 (1956).
196. N. W. Alcock and S. Esperas, *J. Chem. Soc., Dalton Trans.* **9**, 893–896 (1977).
197. E. H. P. Cordfunke and P. Aling, *Rec. Trav. Chim. Pays-Bas.* **82**, 257 (1963).
198. N. W. Alcock, *J. Chem. Soc. (A)* **7**, 1588–1594 (1968).
199. P. C. Burns and K.-A. Hughes, *Am. Mineral.* **88**, 1165–1168 (2003).
200. T. Yajima, Y. Kawamura, and S. Ueta, *Mater. Res. Soc. Symp. Proc.* **353**, 1137–1142 (1995).
201. D. Rai, A. R. Felmy, and J. L. Ryan, *Inorg. Chem.* **29**, 260 (1990).
202. Y. Kato, G. Meinrath, T. Kimura, and A. Yoshida, *Radiochim. Acta* **64**(2), 107–111 (1994).
203. C. F. Baes and R. E. Mesmer, *The Hydrolysis of Cations*, John Wiley & Sons, New York, 1976.
204. C. M. King, R. B. King, and A. R. Garber, *Mater. Res. Soc. Symp. Proc.* **180**, 1083–1085 (1990).
205. C. M. King, R. B. King, A. R. Garber, M. C. Thompson, and B. R. Buchanan, *Mater. Res. Soc. Symp. Proc.* **180**, 1075–1082 (1990).
206. D. A. Palmer and C. Nguyen-Trung, *J. Solution Chem.* **24**(12), 1281–1291 (1995).
207. A. Navaza and F. Villain, *Polyhedron* **3**, 143 (1984).
208. M. Aberg, *Acta Chem. Scand., Ser. A* **A32**(2), 101–107 (1978).
209. I. Grenthe and B. Lagerman, *Acta Chem. Scand.* **45**, 122 (1991).

210. G. Bidoglio, P. Cavalli, I. Grenthe, N. Omenetto, P. Qi, and G. Tanet, *Talanta* **38**, 433 (1991).
211. M. Aberg, D. Ferri, J. Glaser, and I. Grenthe, *Inorg. Chem.* **22**, 3981 (1983).
212. P. G. Allen, J. J. Bucher, D. L. Clark, N. M. Edelstein, S. A. Ekberg, J. W. Gohdes, E. A. Hudson, N. Kaltsoyannis, W. W. Lukens, M. N. Neu, P. D. Palmer, T. Reich, D. K. Shuh, C. D. Tait, and B. D. Zwick, *Inorg. Chem.* **34**, 4797–4807 (1995).
213. I. Bányai, J. Glaser, K. Micskei, I. Tóth, and L. Zékány, *Inorg. Chem.* **34**, 3785–3796 (1995).
214. L. Ciavatta, D. Ferri, M. Grimaldi, R. Palombari, and F. Salvatore, *J. Inorg. Nucl. Chem.* **41**, 1175 (1979).
215. I. Grenthe, D. Ferri, F. Salvatore, and G. Riccio, *J. Chem. Soc. Dalton Trans.* 2439, (1984).
216. I. I. Chernyaev, V. A. Golovnya, and A. K. Molodkin, *Russ. J. Inorg. Chem.* **3**(12), 100 (1958).
217. K. W. Bagnall, in *Gmelin Handbook of Inorganic Chemistry, Supplement Volume C7*, 1988, p. 1.
218. J. Bruno, I. Grenthe, and P. Robouch, *Inorg. Chim. Acta* **158**, 221 (1989).
219. L. Ciavatta, D. Ferri, I. Grenthe, F. Salvatore, and K. Spahiu, *Inorg. Chem.* **22**, 2088 (1983).
220. V. A. Golovnya and G. T. Bolotova, *Russ. J. Inorg. Chem.* **6**(11), 1256 (1961).
221. J. Dervin and J. Faucherre, *Bull. Soc. Chim. France* **3**, 2930 (1973).
222. J. Dervin, J. Faucherre, and P. Herpin, *Bull. Soc. Chim. France* **7**, 2634 (1973).
223. Y. Dusausoy, N. E. Ghermani, R. Podor, and M. Cuney, *Eur. J. Mineral.* **8**(4), 667–673 (1996).
224. A. A. Burnaeva, Y. F. Volkov, A. I. Kryukova, O. V. Skiba, V. I. Spiryakov, I. A. Korshunov, and T. K. Samoilova, *Radiokhim* **29**(1), 3–7 (1987).
225. S. A. Linde, Y. E. Gorbunovaz, and A. V. Lavrov, *Zh. Neorg. Khim.* **28**(6), 1391–1395 (1983).
226. R. Masse and J. C. Grenier, *Fr. Bull. Soc. Fr. Mineral Cryst.* **95**(1), 136–142 (1972).
227. A. Cabeza, M. A. G. Aranda, F. M. Cantero, D. Lozano, M. Martinez-Lara, and S. Bruque, *J. Solid State Chem.* **121**(1), 181–189 (1996).
228. P. Benard, V. Brandel, N. Dacheux, S. Jaulmes, S. Launay, C. Lindecker, M. Genet, D. Louer, and M. Quarton, *Chem. Mater.* **8**(1), 181–188 (1996).
229. J. M. Schaekers and W. G. Greybe, *J. Appl. Cryst.* **6**(Pt. 3), 249–250 (1973).
230. N. Dacheux, V. Brandel, and M. Genet, *New J. Chem.* **19**(1), 15–25 (1995).
231. M. G. Shilton and A. T. Howe, *J. Solid State Chem.* **34**(2), 137–147 (1980).
232. S. A. Linde, Y. E. Gorbunova, and A. V. Lavrov, *Russ. J. Inorg. Chem.* (*Engl. Transl.*) **25**, 1105 (1980).
233. G. A. Sidorenko, I. G. Zhil'tsova, I. K. Moroz, and A. Valueva, *Dokl. Akad. Nauk SSSR* **222**(2), 444–447 (1975).
234. J. A. Danis, W. H. Runde, B. Scott, J. Fettinger, and B. Eichhorn, *Chem. Commun.* 2378–2379 (2001).
235. T. Y. Shvareva, T. A. Sullens, and A.-S. Shehee, *Inorg. Chem.* **44**, 300–305 (2005).
236. C. J. Burns and M. S. Eisen, in N. M. Edelstein, J. Fuger, and L. R. Morss, eds., *The Chemistry of the Actinide and Transactinide Elements*, 2006.
237. C. J. Burns, D. L. Clark, and A. P. Sattelberger, in R. B. King, ed., *Wiley Encyclopedia of Inorganic Chemistry*, Wiley Interscience, New York, 2005.
238. C. J. Burns, M. P. Neu, H. Boukhalfa, K. E. Gutowski, N. J. Bridges, and R. D. Rogers, *Comprehensive Coordination Chemistry II* **3**, 189–345 (2004).
239. R. McDonald, Y. Sun, J. Takats, V. W. Day, and T. A. Eberspracher, *J. Alloys Compd.* **213**(214), 8–10 (1994).
240. P. Scott and P. B. Hitchcock, *J. Chem. Soc., Dalton Trans.* **4**, 603–609 (1995).

241. K. M. Kadish, G. Moninot, Y. Hu, D. Dubois, A. Ibnlfassi, J. M. Barbe, and R. Guilard, *J. Am. Chem. Soc.* **115**(18), 8153–8166 (1993).
242. S. J. Coles, A. A. Danopoulos, P. G. Edwards, M. B. Hursthouse, and P. W. Read, *J. Chem. Soc., Dalton Trans.* **20**, 3401–3408 (1995).
243. S. J. Coles, P. G. Edwards, M. B. Hursthouse, and P. W. Read, *J. Chem. Soc., Chem. Commun.* **17**(8), 0022–4936 (1994).
244. P. G. Edwards, J. S. Parry, and P. W. Read, *Organometallics* **14**(8), 3649–3658 (1995).
245. R. D. Rogers, C. B. Bauer, and A. H. Bond, *J. Alloys Compds.* **213/214**, 305–312 (1994).
246. A. Aguiari, N. Brianese, S. Tamburini, and P. A. Vigato, *New J. Chem.* **19**(5–6), 627–639 (1995).
247. B. T. Thaker, A. Patel, J. Lekhadia, and P. Thaker, *Indian J. Chem., Sect. A: Inorg., Biol. Inorg., Phys., Theor. Anal. Chem.* **6**, 483–488 (1996).
248. P. Thuery, N. Keller, M. Lance, J. D. Vigner, and M. Nierlich, *New J. Chem.* **19**(5–6), 619–625 (1995).
249. D. W. Whisenhunt, Jr., M. P. Neu, Z. Hou, J. Xu, D. C. Hoffman, and K. N. Raymond, *Inorg. Chem.* **35**(14), 4128–4136 (1996).
250. A. P. Sattelberger and W. G. Van der Sluys, *Chem. Rev.* **90**, 1027 (1990).
251. J. M. Berg, D. L. Clark, J. C. Huffman, D. E. Morris, A. P. Sattelberger, W. E. Streib, W. G. Van der Sluys, and J. G. Watkin, *J. Am. Chem. Soc.* **114**(27), 10811–10821 (1992).
252. M. S. Eisen and T. J. Marks, *Organometallics* **11**(12), 3939–3941 (1992).
253. T. J. Marks, *Acc. Chem. Res.* **25**, 57 (1992).
254. J. Takats, in T. J. Marks and I. Fragala, eds., *Fundamental and Technological Aspects of Organo-f-Element Chemistry*, Reidel, Dordrecht, 1985.
255. I. Santos, P. D. Matos, and A. G. Maddock, *Adv. Organomet. Chem.* **34**, 65 (1989).
256. B. E. Bursten and R. J. Strittmatter, *Agnew. Chem. Int. Ed. Engl.* **30**, 1069 (1991).
257. M. Ephritikhine, *New J. Chem.* **16**(4), 451–469 (1992).
258. D. Baudry, A. Dormond, A. Hafid, and C. Raillard, *J. Organomet. Chem.* **511**(1–2), 37–45 (1996).
259. D. S. J. Arney and C. J. Burns, *J. Am. Chem. Soc.* **117**(37), 9448–9460 (1995).
260. P. C. Leverd, M. Ephritikhine, M. Lance, J. Vigner, and M. Nierlich, *J. Organomet. Chem.* **507**(1–2), 229–237 (1996).
261. J. C. Berthet, C. Boisson, M. Lance, J. Vigner, M. Nierlich, and M. Ephritikhine, *J. Chem. Soc., Dalton Trans.* **18**, 3019–3025 (1995).
262. A. R. Schake, L. R. Avens, C. J. Burns, D. L. Clark, A. P. Sattelberger, and W. H. Smith, *Organometallics* **12**, 1497 (1993).
263. M. Berlin and B. Rudell, in L. Friberg et al., eds., *Handbook on the Toxicology of Metals*, Elsevier Science, Amsterdam, 1979, pp. 647–658.
264. J. W. Howland, in C. Voegtlin and H. C. Hodge, eds., *Pharmacology and Toxicology of Uranium Compounds of Uranium Compounds*, McGraw-Hill, New York, 1949.
265. D. R. Fisher, M. J. Swint, and R. L. Kathre, Pacific Northwest National Laboratory, Report PNL-7328, 1990.
266. O. S. Andreyeva et al., in *Natural and Enriched Uranium*, Atomizdat, Moscow, 1979.
267. R. D. Carter, G. R. Kiel, and K. R. Ridgway, in *Criticality Handbook*, 1968, ARH-600.

GENERAL REFERENCES

I. Grenthe, J. Droz˙ dz˙ yn′ski, Takeo Fujino, E. Buck, T. E. Albrecht-Schmitt, and S. S. Wolfa, in N. M. Edelstein, J. Fuger, and L. R. Morss, eds., *The Chemistry of the Actinide and Transactinide Elements*, Vol. 1, Springer, New York, 2006.

C. J. Burns and M. S. Eisen, in N. M. Edelstein, J. Fuger, and L. R. Morss, eds., *The Chemistry of the Actinide and Transactinide Elements*, 2006.
C. J. Burns, D. L. Clark, and A. P. Sattelberger, in R. B. King, ed., *Wiley Encyclopedia of Inorganic Chemistry*, Wiley Interscience, New York, 2005.

DAVID L. CLARK
MARY P. NEU
WOLFGANG RUNDE
Los Alamos National Laboratory
D. WEBSTER KEOGH
Applied Marine Technology, Inc.